Proteasome subunit deficiency influences the innate immune response to *Streptococcus pneumoniae*

DISSERTATION

zur Erlangung des akademischen Grades

Doctor rerum naturalium

(Dr. rer. nat)

Im Fach Biologie

eingereicht an der

Lebenswissenschaftlichen Fakultät

der Humboldt-Universität zu Berlin

von

Felicia Claudia Kirschner, M.Sc.

Präsident der Humboldt-Universität zu Berlin

Prof. Dr. Jan-Hendrik Olbertz

Dekan der Lebenswissenschaftlichen Fakultät

Prof. Dr. Richard Lucius

Gutachter:

1. Prof. Dr. Peter-Michael Kloetzel
2. Prof. Dr. Emanuel Heitlinger
3. Prof. Dr. Bastian Opitz

Tag der mündlichen Prüfung: 29.10.2015

Table of contents

Abstract

The proteasome is an ATP-dependent multi-catalytic protease that is essential for degradation of intracellular short-lived and regulatory proteins. Thereby it influences various processes such as intracellular signaling and immune response. Following infection and subsequent IFN release, three proteolytically active subunits are replaced by three alternative subunits β5i/LMP7, β1i/LMP2, and β2i/MECL1, establishing the immunoproteasome. This proteasome sub-type is not only induced upon inflammation but is predominantly expressed in hematopoietic derived cells such as macrophages and granulocytes. These cells constitute the first line of defense against invading pathogens suggesting a potential role of immunoproteasomes in the initial phase of infection. Recent data provide evidence for crucial functions of immunoproteasomes for an efficient immune response against invasive microorganisms, including viral infections, parasitic infections, and intracellular bacterial infections. So far, no data exist discussing the influence of immunoproteasomes on the outcome of an extracellular bacterial infection. The extracellular bacterium *Streptococcus pneumoniae* is the leading causative pathogen in community acquired pneumonia which is still a major cause of morbidity and mortality. To clarify the impact of immunoproteasomes on the innate immune response against *S. pneumoniae*, we characterized the progression of disease and analyzed the local as well as systemic innate immune response in β5i/LMP7$^{-/-}$ mice by using a *S. pneumoniae* infection model. Data showed that β5i/LMP7$^{-/-}$ mice suffered from a more severe case of pneumonia which ended in a systemic inflammatory response syndrome indicated by aggravated clinical signs, diagnostic parameters, and immune suppression. The systemic inflammatory response probably established in consequence of an increased bacteremia and resulted in early mortality. Although, bacterial killing efficiency of β5i/LMP7$^{-/-}$ leukocytes was unaffected *ex vivo*, β5i/LMP7$^{-/-}$ mice exhibited a reduction in the expression of opsonizing molecules, facilitating bacterial uptake and intracellular elimination. Opsonin expression was only diminished in cells constitutively expressing immuno-subunits such as macrophages and liver cells. Proteasome expression was not influenced by *S. pneumoniae*, though it has changed due to β5i/LMP7 deficiency. WT macrophages mostly assembled 20S proteasomes containing immuno- and standard β–subunits, while β5i/LMP7$^{-/-}$ macrophages assembled 20S proteasomes mainly containing standard β–subunits. These proteasomal alterations were accompanied by changes in the pathogen induced activation of nuclear factors regulating gene transcription.

Taken together, β5i/LMP7 deficiency altered proteasome composition in macrophages and liver that remodeled pathogen induced intracellular signaling, which led to diminished opsonin expression and increased bacteremia. The high bacterial burden caused a more severe case of pneumonia with early mortality. These results highlight a yet unsuspected role for immuno-subunits in modulating the innate immune response to extracellular bacterial infections.

Zusammenfassung

Das Proteasom ist eine multikatalytische ATP-abhängige Protease, die kurzlebige und regulatorische Proteine abbaut und dabei verschiedene zelluläre Prozesse wie z.B. Signaltransduktion oder Immunreaktion beeinflusst. Während einer viralen Infektion oder Entzündungsreaktion, die mit einer IFN Freisetzung einhergeht, werden drei katalytischen Untereinheiten durch alternative Untereinheiten (β1i/LMP2, β2i/MECL-1, β5i/LMP7) ersetzt und so das Immunoproteasom assembliert. Dieser Proteasom Subtyp ist nicht nur induziert sondern auch konstitutiv exprimiert in Zellen hämatopoetischen Ursprungs, wie z.B. Makrophagen und Granulozyten. Diese Zellen gehören zum angeborenen Immunsystem und bilden die erste Angriffsfront gegen pathogene Mikroorganismen. Dies lässt auf eine wichtige Rolle des Immunoproteasoms in der Immunabwehr schließen, insbesondere in der Anfangsphase einer Infektion. Aktuelle Untersuchungen zeigen dessen Bedeutung für eine effiziente Immunantwort gegen Krankheitserreger, wie Viren, Parasiten und intrazelluläre Bakterien. Jedoch wurden bisher keine Daten veröffentlicht, die dessen Einfluss auf den Krankheitsverlauf einer extrazellulären bakteriellen Infektion diskutieren. Das extrazelluläre Bakterium *Streptococcus pneumoniae* ist der Hauptkrankheitserreger der Pneumonie, eine Infektionskrankheit mit hoher Krankheits- und Sterblichkeitsrate. Um die Bedeutung des Immunoproteasoms für die angeborene Immunantwort bei einer *S. pneumoniae* Infektion auf zu zeigen, charakterisierten wir den Krankheitsverlauf einer bakteriellen Pneumonie und analysierten lokale aber auch systemische Immunreaktionen in β5i/LMP7$^{-/-}$ Mäusen mit Hilfe eines *S. pneumoniae* Infektionsmodels. Die hier generierten Daten zeigten einen fortgeschrittenen Krankheitsverlauf in β5i/LMP7$^{-/-}$ Mäuse, der in einem systemischen inflammatorischen Response-Syndrom endete und sich in klinischen Parametern, wie physiologische Kondition, spezifische diagnostische Marker und Immunsuppression, andeutete. Der Zustand der Sepsis entwickelte sich aufgrund einer erhöhten bakteriellen Last im Blut und führte zu einer vorzeitigen Mortalität infizierter β5i/LMP7$^{-/-}$ Tiere. Obwohl die Fähigkeit von β5i/LMP7$^{-/-}$ Leukozyten *ex vivo* Bakterien zu eliminieren nicht beeinträchtigt war, zeigten β5i/LMP7$^{-/-}$ Mäuse *in vivo* eine verminderte Expression von opsonierenden Molekülen. Diese Moleküle fördern die Aufnahme, Elimination und Degradation pathogener Mikroorganismen. Deren Expression war ausschließlich in Gewebe und Zellen beeinträchtigt, die unter WT Bedingungen immunoproteasomale Untereinheiten konstitutive exprimieren, wie Makrophagen und Lebergewebe. Obwohl *S. pneumoniae* die proteasomale Zusammensetzung in Makrophagen und Lebergewebe nicht beeinflusst, gab es generelle Unterschiede zwischen WT und β5i/LMP7$^{-/-}$ Tieren. WT Makrophagen inkorporierten sowohl immuno- als auch standard- Untereinheiten, während β5i/LMP7$^{-/-}$ Makrophagen vor allem Standardproteasome assemblierten. Die Veränderung in der proteasomalen Zusammensetzung ging

mit einer modifizierten Pathogen-induzierten Aktivierung nuklearer Faktoren einher, die die Genexpression inflammatorischer Moleküle regulieren.

Zusammengefasst lässt sich sagen, dass das Fehlen der katalytischen immunoproteasomalen Untereinheit β5i/LMP7 die proteasomale Zusammensetzung in Makrophagen und Lebergewebe verändert, was mit einer Modulierung der Aktivität nuklearer Faktoren einhergeht. Dies führt zu einer verminderten Opsoninexpression und verstärkten Bakteriämie. Die erhöhte bakterielle Last führt zu einem schwereren Krankheitsverlauf der Pneumonie mit vorzeitiger Mortalität. Diese Ergebnisse unterstreichen eine bisher unbekannte Rolle immunoproteasomaler Untereinheiten bei der Regulierung der angeborenen Immunantwort während einer extrazellulären bakteriellen Infektion.

1. Introduction

1.1. Ubiquitin proteasome system

The ubiquitin proteasome system (UPS) is the primary non-lysosomal ATP-dependent protein degradation machinery in eukaryotic cells (Rock et al. 1994). By degrading short-lived poly-ubiquitin-tagged substrates it determines the availability of regulatory proteins and controls a large number of physiologically important cellular processes such as cell cycle progression, apoptosis, cell differentiation, gene regulation, inflammatory response, and antigen presentation (Ebstein et al. 2012). For example, cell cycle progression is controlled by selective degradation of cyclins (Hershko et al. 1991). The UPS preserves cell viability by preventing accumulation of irreversibly damaged and potentially toxic proteins (Seifert et al. 2010), and, by controlling levels of transcription factors, such as NFκB, the UPS influences gene transcription (Collins & Tansey 2006).

A chain of at least four ubiquitins (poly-ubiquitination), created by attaching additional ubiquitin moieties to one of the seven internal lysine residues at the position 48 (K48) of already attached ubiquitins, is the classical recognition motif for proteasomal degradation (Amm et al. 2014; Hershko & Ciechanover 1998). Also multi-ubiquitination, defined as addition of single ubiquitins to several different lysine residues of one target protein, is described to serve as signal for proteasomal degradation (Lu et al. 2015). The attachment of an ubiquitin moiety to a lysine residue is achieved via an ATP-dependent enzymatic cascade involving three classes of enzymes: Ubiquitin-activating enzymes (E1), ubiquitin-conjugating enzymes (E2), and ubiquitin ligases (E3) (Komander 2009). Whether a protein is degraded or otherwise modified depends on the structure of the ubiquitin chain. Modifications with a single ubiquitin molecule (mono-ubiquitination) or with chains of other linkage types (K6, K11, K27, K29, K33, K63, M1) are not degraded by the proteasome but are recognized as physiological target motifs, playing a role in cell regulation (Komander 2009). For example, mono-ubiquitin plays a role in histone regulation and DNA repair, K11-linked poly-ubiquitin is involved in cell-cycle regulation, K33-linked poly-ubiquitin is involved in kinase modification, and K63-linked poly-ubiquitin is involved in endocytosis, DNA-damage responses and in signaling processes (Pickart & Eddins 2004; Komander 2009; Hershko & Ciechanover 1998). Linear poly-ubiquitin, linked via an N-terminal methionine (M1) is supposed to play a role in cell signaling (Komander 2009).

1.1.1. 26S proteasome

The 26S proteasome (Figure 1.1) is the proteolytic enzyme of the UPS. It is structurally and functionally divided into two sub-complexes: The 20S proteasome core particle, where substrate

proteolysis occurs, and the 19S regulatory particle, which is involved in the recognition, unfolding, and translocation of ubiquitin-tagged substrates (Voges et al. 1999; Gallastegui & Groll 2010).

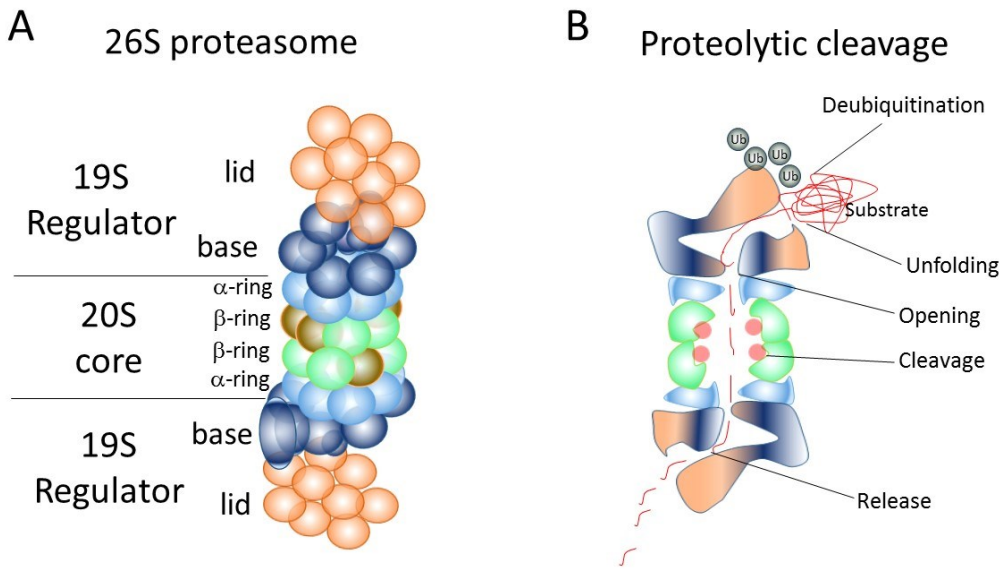

Figure 1.1: Structure of the 26S proteasome and proteolytic cleavage of ubiquitinated substrate. (A) The 26S proteasome consists of the 19S regulator particle and the 20S core complex. The 19S regulator is bound to either or both ends of the 20S core. The 19S particle consist of two sub-complexes, base and lid. The 20S core particle consist of two α- and two β-heptamic-rings, arranged in an αββα stoichiometry, forming a cylindrical barrel-like structure. The β-rings comprise the catalytic activity. **(B)** At the 19S proteasome the ubiquitin chain is disassembled and the substrate is unfolded before it can enter the cavity of the 20S core particle where proteolysis takes place (figure modified from Kaiser & Huang 2005).

The 20S proteasome core particle is a barrel-shaped complex that is composed of four stacked heptameric rings, enclosing a central cavity. It is formed by two outer α-rings and two inner β-rings, each made up of seven distinct α- and β-subunits displaying an $\alpha_{1-7}\beta_{1-7}\beta_{1-7}\alpha_{1-7}$ organization (Unno et al. 2002; Huber et al. 2012). The catalytic activity is restricted to three β-subunits (β1, β2, and β5) that expose N-terminal threonine residues, which display a nucleophile hydrolase activity for peptide bound cleavage. The catalytically active β1-, β2-, and β5-subunits account for the caspase-like, trypsin-like, and chymotrypsin-like activities of the proteasome reflecting cleavage specificities after acidic, basic, and hydrophobic amino acid residues, respectively (DeMartino & Slaughter 1999, Orlowski & Wilk 2000). Access to the active center of the 20S chamber is regulated by an adjustable gate that is formed by the N-termini of the α-subunits. When a regulator particle binds to the outer α-rings, it causes a structural rearrangement of the N-terminal portions of the α-subunits that opens

the central chamber and facilitates access of proteins to the catalytic core (Groll et al. 1997; Unno et al. 2002; Gallastegui & Groll 2010). In the absence of a regulator particle, the free 20S proteasomes show detectable but low activity towards small proteins with intrinsically unstructured regions in the absence of ubiquitin and ATP (Baugh et al. 2009).

The 19S regulator particle is formed by two sub-complexes, lid and base (Gallastegui & Groll 2010). The base is composed of six homologous ATPases (Rpt1-Rpt6) that form a hexameric ring. Additional four non-ATPases (Rpn1/2, Rpn10/13), including two ubiquitin receptors, Rpn10 and Rpn13, are associated to the hexameric ring. The lid consist of nine non-ATPase subunits including Rpn11, displaying deubiquitinating activity (Lander et al. 2012; Tanaka et al. 2012).

1.1.2. Proteasome sub-types

In response to IFNγ three alternative proteolytically active β-subunits, β1i/LMP2, β2i/MECL-1, and β5i/LMP7 are incorporated into a nascent 20S proteasome generating a new sub-type, named immunoproteasome (Aki et al. 1994). In the mouse, β1i/LMP2 and β5i/LMP7 are encoded within the major histocompatibility complex (MHC) class II region on chromosome 17, while β2i/MECL-1 is localized in a cluster of unrelated genes on chromosome 8 (Ferrington & Gregerson 2012).

The assembly of 20S proteasomes (Figure 1.2) is similar for all proteasome sub-types. It is guided by proteasome-assembling chaperones (PAC1/2, PAC3/4) which facilitate the formation of a closed heptameric α-ring. Subsequently, in case of the standard proteasome the β-ring formation starts with the incorporation of the first pro-β-subunit β2 assisted by the proteasome maturation protein (POMP). The remaining β-subunits (β3-β7) incorporate into the nascent complex and form an inactive half proteasome (Sahara et al. 2014). Finally, two half proteasome core particles are combined, assisted by POMP (Fricke et al. 2007; Krüger et al. 2001). This initiates maturation of the proteolytically active β-subunits (β1, β2, β5) by lysis of their pro-peptides. The last step is essential for activation of the catalytic threonine residues (Ditzel et al. 1998). The assembly of the immunoproteasome is favored over the standard proteasome, due to its cooperative manner (Griffin et al. 1998). In cells co-expressing both standard and immuno-subunits, β1i/LMP2 is the first incorporated β-subunit, while β1 is integrated later during the assembly process (De et al. 2003). The presence of β1i/LMP2 supports the incorporation of β2i/MECL-1 (Groettrup et al. 1997). Furthermore, POMP binds with high affinity to β5i/LMP7 and not to the β5 pro-peptide (Heink et al. 2005). The incorporation of β5i/LMP7 is required for the maturation of nascent immuno- 20S core particles by assisting the catalytic lysis of the pro-peptides of β1i/LMP2 and β2i/MECL-1 (Ferrington & Gregerson 2012).

Incorporation of immuno-subunits has been linked with altered chymotrypsin-like and caspase-like activities. β5i/LMP7 and β2i/MECL-1 display the same cleavage specificity as its homologous standard

subunit, but, in contrast to its standard caspase-like β1-subunit, the β1i/LMP2 subunit provides chymotrypsin-like activity (Gaczynska et al. 1994; Basler et al. 2013). The altered caspase-like activity of β1i/LMP2 is explained by an amino acid substitution in the β1i/LMP2 substrate binding pocket which changes the catalytic core more hydrophobic and constricted. Structural modifications in the substrate binding pocket result in altered cleavage preference and changes the quantity of peptides, generated and presented on MHC class I molecules (Huber et al. 2012; Mishto et al. 2014).

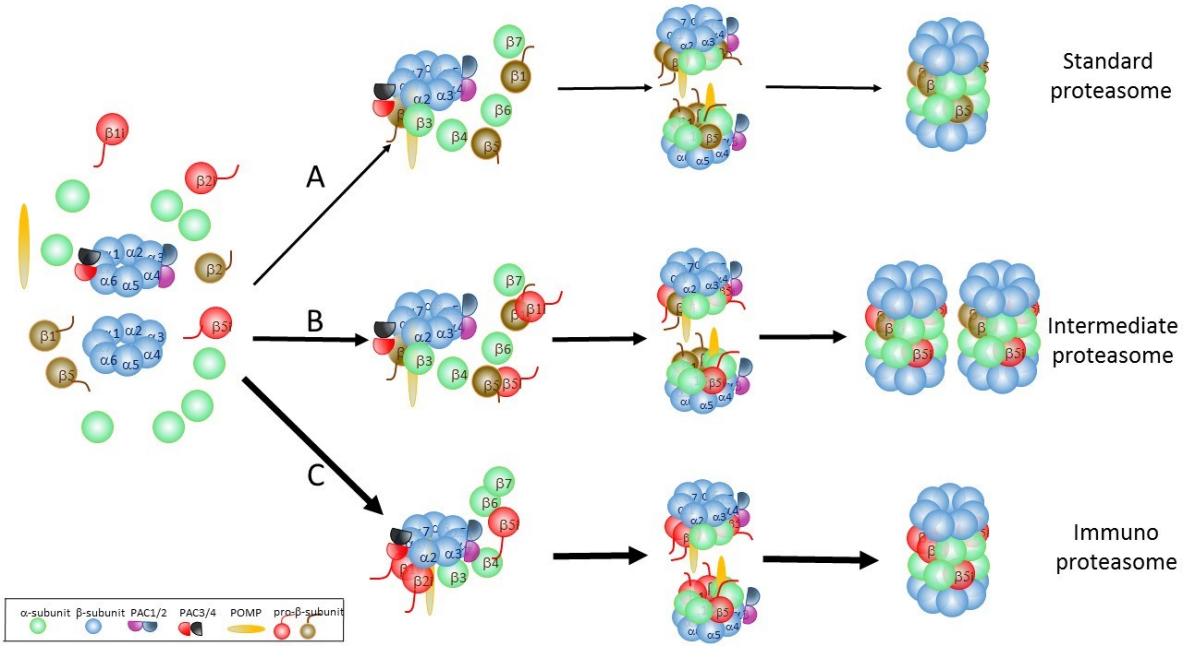

Figure 1.2: Assembly of 20S proteasome sub-types. The assembly of 28 α- and β-subunits into a 20S core particle begins with the formation of an α-ring which occurs with the aid of the chaperone heterodimer complexes PAC1/2 and PAC3/4. It is followed by the β-ring formation which, in case of the standard proteasome **(A)** starts with the association of the pro-β2-subunit on the α-ring facilitated by the chaperone POMP. The subsequent sequential incorporation of other β-subunits leads to the formation of half-proteasomes. Two half-proteasomes dimerize and form a 4-ring heptamer that, results in catalytic cleavage of the pro-β-subunits. **(B)** One (β5i/LMP7) or two (β2i/MECL-1 and β5i/LMP7) immuno-subunits can incorporated in nascent standard proteasomes forming intermediate proteasomes. **(C)** Immunoproteasome assembly occurs in a cooperative manner. β1i/LMP2 enters the assembly pathway earlier than the standard β1-subunit. The presence of β1i/LMP2 abets the incorporation of β2i/MECL-1 which abets the incorporation of β5i/LMP7. Incorporation of immuno-subunits is favored, indicated by the thickness of the arrows.

β5i/LMP7 is the only immuno-subunit that can be incorporated into proteasomes independent of the other subunits (Ferrington & Gregerson 2012). This allows the existence of intermediate proteasomes (Figure 1.2), which incorporate only one or two immuno-subunits (Gohlke et al. 2014;

Dahlmann et al. 2000). It is also possible that an asymmetric hybrid proteasome, consisting of immunoproteasome and constitutive proteasome, exists (Klare et al. 2007). Intermediate proteasomes are present in liver and colon, but not in heart and are mostly abundant in professional antigen presenting cells such as macrophages and DCs (Guillaume et al. 2010). Intermediate proteasomes have altered cleavage preferences in generating class I peptides (Guillaume et al. 2012).

Another protein complex induced by IFNγ is the proteasome regulator particle PA28. It is a large regulatory complex that binds the ends of the 20S proteasome in an ATP-independent manner, facilitating α-ring opening. (DeMartino & Slaughter 1999). PA28 is a hetero-heptameric ring made of two homologous subunits, PA28α and PA28β. A third PA28 family member, the PA28γ, is structurally related, forms homopolymeric complexes, and is associated with 20S proteasomes predominantly in the nucleus, but is not inducible by IFNγ (Tanahashi et al. 1997). PA28 can attach to both sides of the 20S core (PA28-20S-PA28) or it is found in complexes that also contain a 19S regulator, forming a so called hybrid proteasome (19S-20S-PA28) (Tanaka et al. 2012). Binding of PA28 to 20S cores increases substrate affinity and enhances either the uptake of substrates or release of products (Sijts et al. 2002).

1.1.3. Functions of immunoproteasomes during disease

Immunoproteasomes are involved in biological and pathological processes resulting in the development and aggravation of many diseases, including neurodegenerative diseases, inflammatory and autoimmune diseases, and viral and intracellular bacterial infections (Ferrington & Gregerson 2012). For example, the expression of immuno-subunits in non-lymphoid tissues is low but also strongly upregulated upon immunological and/or pathological challenge (Ebstein et al. 2012). Under healthy conditions immunoproteasomes are absent in neurons but are induced in animal models of neurodegenerative diseases such as Alzheimer´s disease (Mishto et al. 2006), Huntington´s disease (Díaz-Hernández et al. 2003), and amyotrophic lateral sclerosis (Puttaparthi et al. 2007). Elevated immunoproteasome levels have been reported in a number of autoimmune and inflammatory diseases, such as Crohn´s disease, ulcerative colitis, and hepatitis. A pronounced immunoproteasome expression was found in intestinal tissue of patients with Crohn´s disease (Visekruna et al. 2006), in liver of patients with cirrhosis (Vasuri et al. 2010), and in clinical samples of multiple sclerosis patients (Mishto et al. 2010). Furthermore, immunoproteasome formation was documented in microglia cells in response to infection with Lymphochoriomeningitis virus (LCMV) (Kremer et al. 2010), and in liver cells in response to infection with *Listeria monocytogenes* (Khan et al. 2001).

However, expression of immuno-subunits is not only induced upon inflammation (Aki et al. 1994) but is predominantly expressed in hematopoietic derived cells such as splenocytes, macrophages, and DCs (Ebstein et al. 2012). The constitutive expression of immuo-subunits is likely due to a permanent activation of intracellular signaling mechanisms. It has been shown that permanent unphosphorylated Stat1 binds IRF1 to form a complex which functions as transcription factor, constantly supporting β1i/LMP2 expression in hematopoietic derived cells (Ebstein et al. 2012; Chatterjee-Kishore et al. 2000).

Functions of immunoproteasomes have been investigated by studying animal infection or inflammation models using immunoproteasome deficient mice (reviewed in Ebstein et al. 2012; Ferrington & Gregerson 2012; Basler et al. 2013; Miller et al. 2013), and were complemented by descriptions of diseases in humans linked to mutations or single-nucleotide polymorphisms in genes encoding immuno-subunits (reviewed in McDermott et al. 2015). Furthermore, the use of selective immunoproteasome inhibitors helped to identify immunoproteasome involvement in a variety of immunological and physiological processes (reviewed in Kisselev & Groettrup 2014).

Proteasomes play a major role in generating peptides presented on MHC class I molecules that are recognized by $CD8^+$ cytotoxic T cell receptors (Rock et al. 1994). Immunoproteasome cleavage preferences alter the versatility of antigen processing and the possibility to generate and present immunogenic epitopes that contribute to an efficient anti-bacterial and anti-viral cellular immune response (reviewed in Ebstein et al. 2012; Groettrup, Kirk, and Basler 2010). For example, β5i/$LMP7^{-/-}$ mice exhibited a diminished generation of an epitope of the intracellular bacterium *Listeria monocytogenes* (Strehl et al. 2006), β1i/LMP2 deficiency resulted in a depressed response to a nucleoprotein epitope of influence A virus (IAV) (Van Kaer et al. 1994), and mice deficient in β1i/LMP2 or β2i/MECL-1 had a decreased $CD8^+$ cytotoxic T cell response to class I restricted epitopes of LCMV (Basler et al. 2006; Chen et al. 2001). In recent years it became apparent that immunoproteasomes not only function by generating MHC-I epitopes, but also possess additional immunological functions. However, whether immunoproteasome deficiency exerts a protective effect or exacerbates disease depends on the underlying pathology and/or inflamed tissue (reviewed in Ferrington and Gregerson 2012; Tanaka et al. 2012).

Immunoproteasome formation is essential for preservation of cell viability, as immunoproteasomes protect cells against harmful inflammation-induced accumulation of protein aggregates more efficiently than standard proteasomes (Seifert et al. 2010). For example, β5i/$LMP7^{-/-}$ mice failed to clear protein aggregates that accumulated in cardiomyocytes following Coxsackie virus B3 (CVB3) infection. Therefore, β5i/LMP7 deficient mice suffered from an aggravated myocarditis, which occurs in consequence of an impaired protection against virus-mediated protein damage (Opitz et al. 2011).

Immunoproteasomes are also crucial for the regulation of cell proliferation and differentiation. Mice deficient in β1i/LMP2 or β2i/MECL-1 exhibited significant reduced numbers of naive cytotoxic T cells (Van Kaer et al. 1994; Basler et al. 2006). Additionally, β1i/LMP2$^{-/-}$, β5i/LMP7$^{-/-}$, or β2i/MECL-1$^{-/-}$ T cells were unable to expand and survive when transferred into virus infected WT hosts (Moebius et al. 2010). The diminished proliferation of CD8^{+} cytotoxic T cells is assumed to be intrinsically regulated by the proteasome (Zaiss et al. 2008). Furthermore, β5i/LMP7 deficiency resulted in diminished CD4^{+} Th_1 and Th_{17} differentiation, and enhanced development of regulatory T cells, examined during the case of an experimental colitis (Kalim et al. 2012).

Pathophysiological functions of immunoproteasomes have been investigated in the context of auto-inflammatory diseases. For example, immunoproteasome deficiency is accompanied by an attenuation of pathological signs of experimental colitis. Deficient mice show no induction of pro-inflammatory cytokines such as TNFα, IL-6, IL-17, IL-23 and IL-1β and have less intestinal inflammation (Schmidt et al. 2010). The same positive effect on pathological signs of experimental colitis was documented in WT mice pretreated with a β5i/LMP7 specific inhibitor (Basler et al. 2010).

By using subunit-selective inhibitors it is possible to investigate how enzymatic activity, rather than absence of immuno-subunits, influences immunological and pathological functions. Treatment with a β5i/LMP7 specific inhibitor protected mice from several different auto-inflammatory diseases, showing reduced pathological signs and inflammation. It prevented the development or progression of experimental arthritis (Muchamuel et al. 2009), systemic lupus erythematosus (SLE) (Ichikawa et al. 2012), experimental colitis (Basler et al. 2010), and experimental auto-immune encephalomyelitis (EAE) (Basler et al. 2014). Interestingly, β5i/LMP7 inhibition did not consistently provoke the same effect on disease development as β5i/LMP7 deficiency. For example, β5i/LMP7 inhibition and not deficiency protected mice from disease in an experimental EAE model (Basler et al. 2014).

These studies underline the role of immunoproteasomes in specific signaling pathways, probably by elevating the protein turnover rate of critical signaling molecules (Ebstein et al. 2012). Some of this issue is described in more detail in section 1.2.3. (Figure 1.4).

A manifested expression of immunoproteasomes in intestine of patients with Crohn´s disease or ulcerative colitis was associated with an elevated activation of the NFκB signaling pathway (Visekruna et al. 2006). The NFκB pathway is one of the main signal transduction pathways for responding to various stressors such as cytokines and viral as well as bacterial products (Newton & Dixit 2012). Its dysregulation can lead to pathologies such as neurodegenerative and inflammatory diseases (Małek et al. 2007). NFκB is inhibited by forming a complex with IκB proteins that are degraded by the 26S proteasome upon stimulation. This results in NFκB activation and transduction into the nucleus (Newton & Dixit 2012). Immunoproteasomes enhance nuclear translocation by

degrading IκBα faster than standard proteasomes (Seifert et al. 2010; Visekruna et al. 2006). An impaired NFκB activation was observed in β5i/LMP7$^{-/-}$ mice upon CVB3 infection (Opitz et al. 2011), which was also documented in β1i/LMP2$^{-/-}$ B cells upon LPS stimulation (Hensley et al. 2010).
Reis et al. documented reduced levels of nitric oxide (NO), produced by LPS-stimulated β5i/LMP7$^{-/-}$ macrophages, as a consequence of a diminished activation of the TRIF/TRAM signaling cascade (Reis et al. 2011). TRIM/TRAF are adaptor molecules that are essential in the MyD88-independent signaling of TLR-4 (Newton & Dixit 2012).
Furthermore, it seems that immunoproteasomes are also involved in regulating the MAPK signaling pathway as increased phosphorylation of p38 with subsequent IL-6 production upon stimulation was documented in cells expressing a non-functional β5i/LMP7 mutant (Kitamura et al. 2011).
It is also proposed that immunoproteasomes influence the IFN signaling pathway. For example, PBMCs from patients with CANDLE syndrome (further explained below) exhibited a strong STAT1 phosphorylation in response to IFNγ which leads to an up-regulation of IP-10, MCP-1, and Rantes (Liu et al. 2012).

Several recent human genetics studies, identifying missense or nonsense mutations in the PSMB8 gene encoding β5i/LMP7, support the involvement of immunoproteasomes in inflammatory disorders. All patients carrying mutations in the PSMB8 gene have a decreased proteasome chymotrypsin-like activity and suffer from symptoms displaying recurrent fever, elevated levels of acute phase molecules, high levels of IL-6, and auto-immune abnormalities (McDermott et al. 2015). These disorders are called joint contractures, muscle atrophy, microcytic anaemia, and panniculitis-induced lipodystrophy syndrome (JMP) (Agarwal et al. 2010), chronic atrophical neutrophilic dermatosis with lipodystrophy and elevated temperature syndrome (CANDLE) (Liu et al. 2012), Nakajo–Nishimura syndrome (NNS) (Arima et al. 2011), and Japanese auto-inflammatory syndrome with lipodystrophy syndrome (JASL) (Kitamura et al. 2011).

1.2. Community acquired pneumonia

World health organization (WHO) statistics 2014 indicate that lower respiratory tract infections are the third leading cause of death globally and the number one cause of death in developing countries. (WHO 2014)

1.2.1. Pneumococcal pneumonia - Epidemiology and Disease

S. pneumoniae is estimated to cause 27 % of all cases of community acquired pneumonia, being the most frequent pathogen causing lower respiratory tract infections (Said et al. 2013). It is a common bacterium residing the upper respiratory tract, mainly as commensal flora. After colonization by one

of the 92 serotypes (Dockrell et al. 2012) it persists in adults for weeks and in children for months without any clinical signs (Dockrell et al. 2012). Airway colonization is detected in 10 % of healthy adults, in 20 - 40 % of healthy children and in more than 60 % of healthy infants in day-care settings (van der Poll & Opal 2009). Since it is easily transmitted by direct contact with contaminated respiratory secretions, this carrier state sustains the bacterium within human population (Bogaert et al. 2004).

Incidence of invasive pneumococcal disease varies substantially by age, with children younger than 5 years and adults older than 65 years being most at risk (Steel et al. 2013). Other risk factors comprise the socioeconomic status and immune status. They include decreased body weight, high alcohol consumption, smoking, immune compromised states such as HIV infection or asplenia, immunoglobulin and complement deficiencies, diabetes mellitus and other underlying co-morbidities (Torres et al. 2013).

Various pneumococcal vaccines are available for preventing pneumococcal disease. The most widely used 23-valent vaccine protects against only 23 out of over 92 serotypes worldwide and covers serotypes prevalent mostly in North America, Europe, and Australia (Kadioglu & Andrew 2004). Nevertheless, since the year 2000 there has been a dramatic decline in invasive pneumococcal disease in children as well as in adults in countries, where the vaccine has been used (Anon 2008).

S. pneumoniae infect humans, monkeys, rabbits, horses, and mice causing pneumonia, otitis media, meningitis, and bacteremia depending on the serotype (Henriques-Normark & Tuomanen 2013). It usually begins with mild upper-airway irritation, but when bacteria reach the lower respiratory tract systemic inflammation ensues with characteristic signs and symptoms. The onset of severe illness develops with fever, malaise, cough, and dyspnoea. Left untreated, this toxic illness can progress to acute respiratory failure, septic shock, multiorgan failure, and death within several days (Lynch & Zhanel 2009). Despite advances in medical care, mortality remains high. A recent cohort study estimated the 28-day mortality in patients, hospitalized due to community acquired pneumonia, to 13 % in South America, 9 % in Europe, and 7 % in North America (Arnold et al. 2013).

Multiple antibiotic resistance has rapidly increased in the last decade and covers the globe varying by geographic location. A recent US study demonstrated 21 % drug resistance to clindamycin, 39 % to erythromycin, and 21 % to oral penicillin (Pfaller et al. 2012). Since antibiotics are still the only choice of treatment and antibiotic resistance spreads *S. pneumoniae* remains a critical pathogen (Remington & Sligl 2014).

1.2.2. *Streptococcus pneumoniae* – Genetics and Virulence

Streptococcus pneumoniae are encapsulated Gram-positive diplococci that grow in pairs or chains and belong to the group of α-streptococci. They are α-hemolytic and live facultative anaerobe

(Watson et al. 1993). At least 92 different serotypes are known, which can be distinguished by their polysaccharide capsule and differ in virulence (Dockrell et al. 2012).

The pneumococcal genome is a covalently closed, circular DNA structure often accompanied by small cryptic plasmids. It contains a core set of more than 1500 genes that are essential for viability. Additional genes encode virulence factors and others maintain a non-invasive phenotype. Pneumococci cluster virulence genes into small defined sequences known as regions of diversity. These regions distinguish invasive from non-invasive strains (Tettelin et al. 2001). Pneumococci have a large number of insertion sequences and some strains contain transposons that mediate antibiotic resistance and are obtained by horizontal gene transfer (van der Poll & Opal 2009). Furthermore, the genome contains many copies of direct-repeat DNA elements that provide recombination hotspots for genetic variability. These spots are related to genes for example encoding capsular biosynthesis and adhesins (Dockrell et al. 2012).

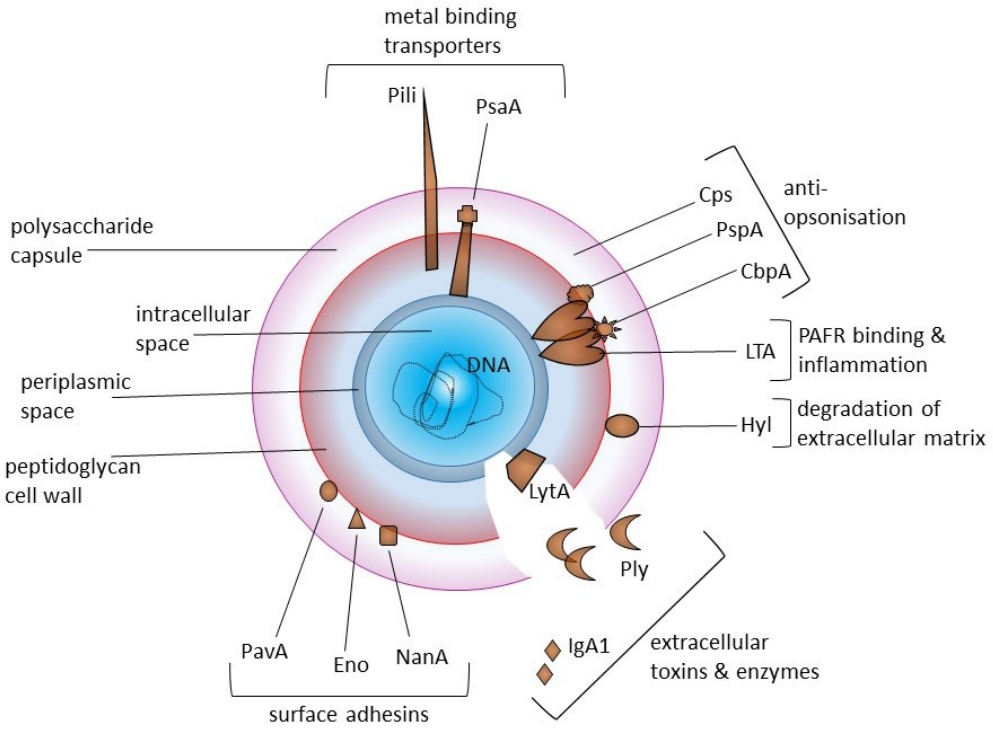

Figure 1.3: Selected virulence factors of *S. pneumoniae* and its main function. Polysaccharide capsule (**Cps**), pneumolysin (**Ply**), pneumococcal surface antigen A (**PsaA**), pneumococcal surface protein A (**PspA**), lipoteichonic acid (**LTA**), neuraminidases (**NanA**), enolase (**Eno**), pneumococcal adhesion and virulence (**pavA**), hyaluronidase (**Hyl**), autolysin (**LytA**), choline binding protein A (**CbpA**), IgA1 protease (**IgA1**), pili (figure modified from van der Poll & Opal 2009).

S. pneumoniae express various virulence factors determining its invasiveness (Figure 1.3). Among these factors the polysaccharide capsule and the pneumolysin are the most essential virulence

determinants (Kadioglu et al. 2008). The polysaccharide capsule is crucial during colonization, invasion, and dissemination from the respiratory tract. Its morphology alternates between two distinct phases known as the transparent (thin) and opaque (thick) phenotype. *S. pneumoniae* with a transparent phenotype express less pneumococcal surface protein (PspA) and more choline-binding protein A (CbpA), while pneumococci with an opaque phenotype express more PspA and less CbpA (Ogunniyi et al. 2002). Transparent capsules are favored in early colonization, in order to support adhesion, while opaque capsules are favored during invasion in order to resist complement-mediated opsonophagocytosis (Bogaert et al. 2004; Kadioglu et al. 2008; Henriques-Normark & Tuomanen 2013). Thick capsules reduce opsonisation by sterically inhibiting the interaction of C3b, fixed to pneumococci, and the CR3 receptor, expressed by phagocytes (Hammerschmidt et al. 2005).

Pneumolysin is an exotoxin, released during autolysis, facilitated by autolysin (LytA). It is expressed by almost all invasive strains since negative mutants are less likely to produce lethal pulmonary infections (Hirst et al. 2004; Kadioglu et al. 2008). This pore-forming toxin is a soluble monomer that intercalates and oligomerizes in host membranes and thereby lyses the cell. Beside its cytotoxicity, pneumolysin has many other pathological effects, including activation of $CD4^+$ T cells, decrease of respiratory burst of phagocytes, induction of chemokine and cytokine production, and activation of complement fixation (Mitchell & Mitchell 2010; Hirst et al. 2004; Kadioglu et al. 2008).

1.2.3. Immunology – Immune Recognition and Innate Immune Response

The immune system employs numerous mechanisms to protect the host from an invasive pneumococcal infection. Release of bacterial cell-wall particles, toxins, and DNA, facilitated by autolysis, initiates activation of these defense mechanisms (Koppe et al. 2012). These bacterial components contain conserved motifs that are referred to as pathogen-associated molecular patterns (PAMPs). This motifs are recognized by pattern-recognition receptors (PRRs) which are crucial components of the innate immune system (Newton & Dixit 2012).

PRRs belong to different protein families including Toll-like receptors (TLRs), nucleotide-binding oligomerization domain receptors (NOD-like receptors, NLRs and AIM2), and cytosolic DNA sensors (Koppe et al. 2012; Akira et al. 2006). TLRs can detect pneumococcal components at either the cell surface, in lysosomes, or endosomes. Lipoteichonic acid and proteoglycan is recognized by TLR-2 (Knapp et al. 2004), pneumolysin interacts with TLR-4 (Malley et al. 2003), and CpG-motif containing DNA is detected by TLR-9 (Newton & Dixit 2012). Receptors of the NLR family such as NOD2 recognize pneumococcal proteoglycans, while other members, such as NLRP3 or AIM2 bind pneumolysin or cytosolic DNA, respectively, and form protein complexes called inflammasomes, which mediate cleavage of pro-IL-1β into mature IL-1β (Koppe et al. 2012).

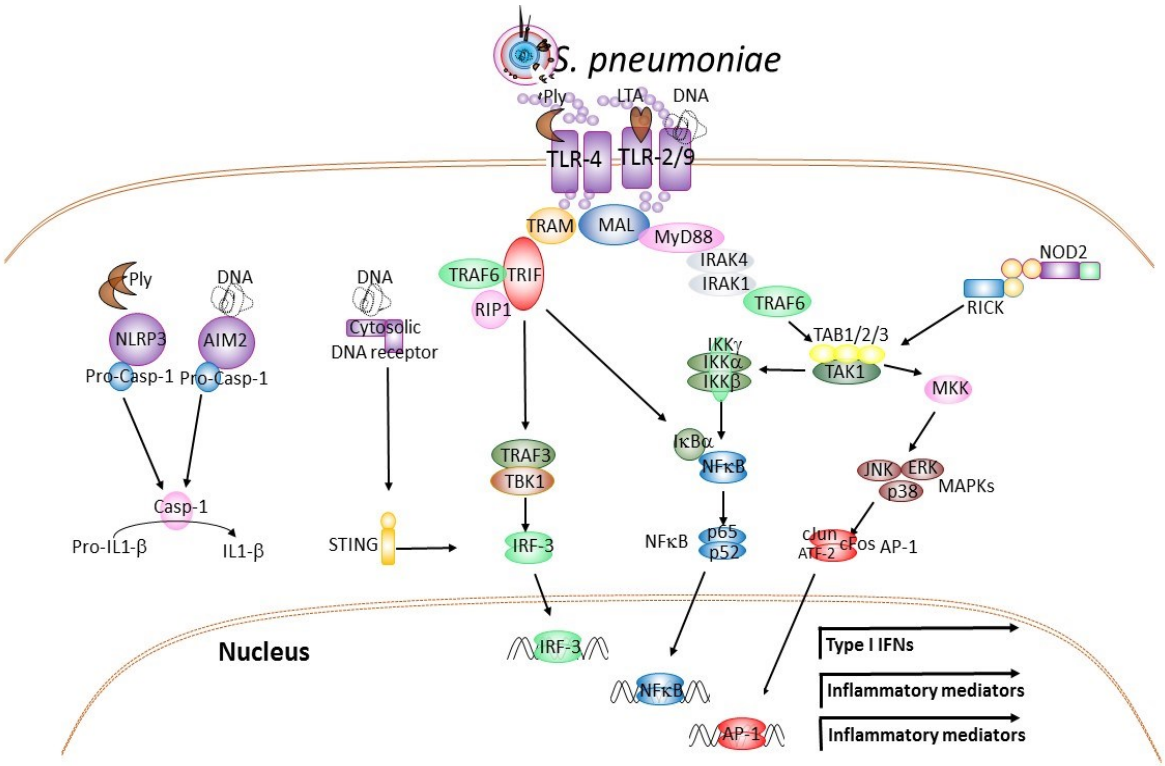

Figure 1.4: *S. pneumoniae* induces intracellular signaling. Binding of LTA, Ply, and CpG containing DNA on TLR-2, TLR-4, and TLR-9 triggers interactions between the cytosolic TIR domain of the TLRs and TIR-containing adaptor proteins (MAL and TRAM). MAL recruits the adaptor protein MyD88 that binds and activates IRAK4 which phosphorylates IRAK1, initiating auto-phosphorylation. Phosphorylated IRAK1 dissociates from the complex and activates TRAF6. Phosphorylated TRAF6 triggers the activation sequence TAB2 - TAK1 - IKK-complex. IκB phosphorylation and ubiquitination by the IKK-complex leads to its degradation by the proteasome and release and translocation of NF-κB (p65, p52) to the nucleus for gene regulation. Furthermore, TAK1 also activates MKKs for subsequent JNK, ERK, and p38 phosphorylation, leading to AP-1 (cJun, cFos, ATF-2) activation that triggers gene transcription of cytokines and inflammatory molecules. TLR-4 can also signal via the adaptor proteins TRAM and TRIF. TRAF6 and RIP1 interact with TRIF to signal NFκB activation, but also stimulate IRF3-dependent transcription via TBK1 and TRAF3. IRF3-dependent transcription can also be activated via STING by binding of CpG containing DNA to cytosolic DNA sensors. NOD2, activated by peptidoglycans, recruits and activates RICK that triggers the activation sequence TAB2 - TAK1 - IKK-complex which leads to ubiquintination and degradation of IκBα by the proteasome, resulting in production of NFκB dependent cytokines. The NLRP3 and AIM2 inflammasomes, activated by Ply and bacterial DNA, respectively, mediate cleavage of pro-IL-1β into mature IL-1β (figure modified from Qureshi et al. 2012; Koppe et al. 2012).

TLRs as well as NOD2 stimulate the production of NFκB and AP-1 dependent cytokines (Figure 1.4), including TNFα, IL-6, pro-IL-1β, as well as chemokines such as CXCL-1 and MIP-1β via the MyD88, TRIM/TRAF, and MAPK pathway (Koppe et al. 2012). Sensing of *S. pneumoniae* DNA by cytosolic DNA

receptors activate the transcription factor IRF3, and stimulate type I IFN responses (Koppe et al. 2012; Newton & Dixit 2012)

PRR signaling results in activation of innate immune defenses (Figure 1.5). The very first line of innate immune defense is the respiratory epithelium (Diamond et al. 2000). Beside its barrier function, alveolar epithelial cells help to clear *S. pneumoniae* by releasing protective inflammatory mediators including chemokines such as CXCL-1 and MIP-1β, opsonizing molecules such as pulmonary surfactants called surfactant protein A and D (SP-A and SP-D), and antimicrobial peptides such as lysosomes and defensins (Bals & Hiemstra 2004). SP-A and SP-D are collectins and play a role in the protection of the host by binding and opsonizing microbes (Hartshorn et al. 1998). SP-D deficient mice showed increased susceptibility to *S. pneumoniae* infection (Jounblat et al. 2005) while SP-A promoted phagocytosis in *in vitro* experiments (Kuronuma et al. 2004)

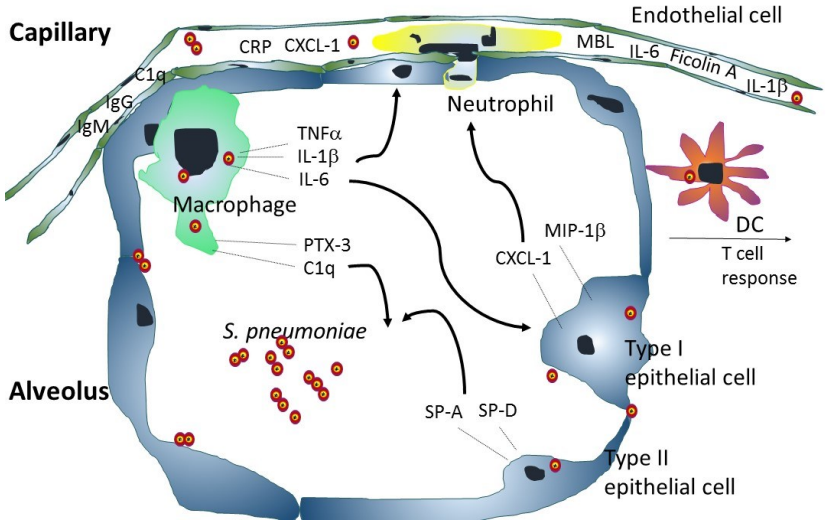

Figure 1.5: Inflammation in invasive pneumococcal pneumonia. Pathogen recognition by alveolar macrophages initiates production of inflammatory mediators including TNF-α, IL-1β, IL-6, and IFNβ, as well as opsonins such as PTX-3 and C1q. IL1-β and TNFα further stimulate alveolar epithelial cells to produce inflammatory mediators such as CXCL-1 and MIP-1β which stimulate recruitment of phagocytes. Alveolar epithelial cells also upregulate the synthesis of collectins (SP-A and SP-D), which sequester bacteria for opsonophagocytosis. DCs maturate and activate T cell responses. If alveolar defense mechanisms are overwhelmed by pneumococci replication, invasion of *S. pneumoniae* into the bloodstream takes place. In the bloodstream, bacteria have to combat various host proteins including natural IgG and IgM, CRP, and complement components such as MBL, Ficolin, and C1q (figure modified from Opitz et al. 2010).

Alveolar macrophages represent the first phagocytic defense and are essential in initiating and coordinating the innate immune response to infection (Cole et al. 2014). In addition to phagocytosis and endosomal clearance of *S. pneumoniae*, they rapidly produce large amounts of pro-inflammatory

cytokines such as TNFα, IL-1β, IL-6, and IFNβ as well as reactive oxygen species (ROS) and nitric oxide (NO). They are activated by PAMPs but also by cytokines, complement, and antibody complexes (Marriott & Dockrell 2007; Braun et al. 1999) and finally contribute to the resolution of inflammation in lung tissue by clearing apoptotic cells (Aberdein et al. 2013).

In established pneumonia neutrophils become the major cells eliminating bacteria. Chemokines such as CXCL-1, induced by TNFα and IL-1β, stimulate the chemotaxis of neutrophils, which are recruited to inflamed lung tissue (Kadioglu et al. 2000; Gauthier et al. 2007). Neutrophils recognize PAMPs on the surface of bacteria through PRRs and use surface Fc- and complement-receptors to bind bacteria opsonized by antibodies and complement components (Castellheim et al. 2009). The action of neutrophils is necessary to clear *S. pneumoniae*, achieved by phagocytosis and intracellular killing in phagosomes (Cohen 1994; Marriott & Dockrell 2007). This occurs via production of ROS, proteolytic enzymes, anti-microbial peptides, and acidification of the endosome (Castellheim et al. 2009). Neutrophils also bind and kill bacteria by neutrophil extracellular traps (NET), which consists of expelled histones, antimicrobial peptides, and enzymes bound to condensed DNA (Müller-Redetzky et al. 2014).

If alveolar defense mechanisms are overwhelmed, invasion of *S. pneumoniae* into the bloodstream takes place. In the blood, several host proteins contribute to host defense including natural IgM antibodies, complement products, and pentraxins (Kadioglu & Andrew 2004; Shishido et al. 2012). Clearance of pneumococci from circulation strongly depends on opsonization, which enhances bacterial phagocytosis by leukocytes (Watson et al. 1993; Bogaert et al. 2004).

Pentraxins are cytokine-inducible soluble pattern recognition receptors and part of the humoral innate immune system (Mantovani et al. 2008). They opsonize bacteria and promote phagocytosis by macrophages and neutrophils (Roy et al. 2002). They include the short pentraxins, C reactive protein (CRP) and serum amyloid P (SAP), as well as the long pentraxin PTX-3 (Doni et al. 2012). CRP is produced systemically in liver during the acute phase response, induced by IL-6 and IL-1β. It binds to phosphorylcholine in the pneumococcal cell-wall, but also to C1q and Ficolin, which are opsonizing molecules of the classical and lectin activation pathway of the complement system (Suresh et al. 2006). PTX-3 is produced locally in various cell types, with macrophages and neutrophils being the major sources. Like CRP, it interacts with components of the classical and lectin activation pathway of the complement system. PTX-3 recognizes and binds C1q, MBL, and Ficolin, and thereby amplifies effector functions of the complement system (Inforzato et al. 2013; Doni et al. 2012).

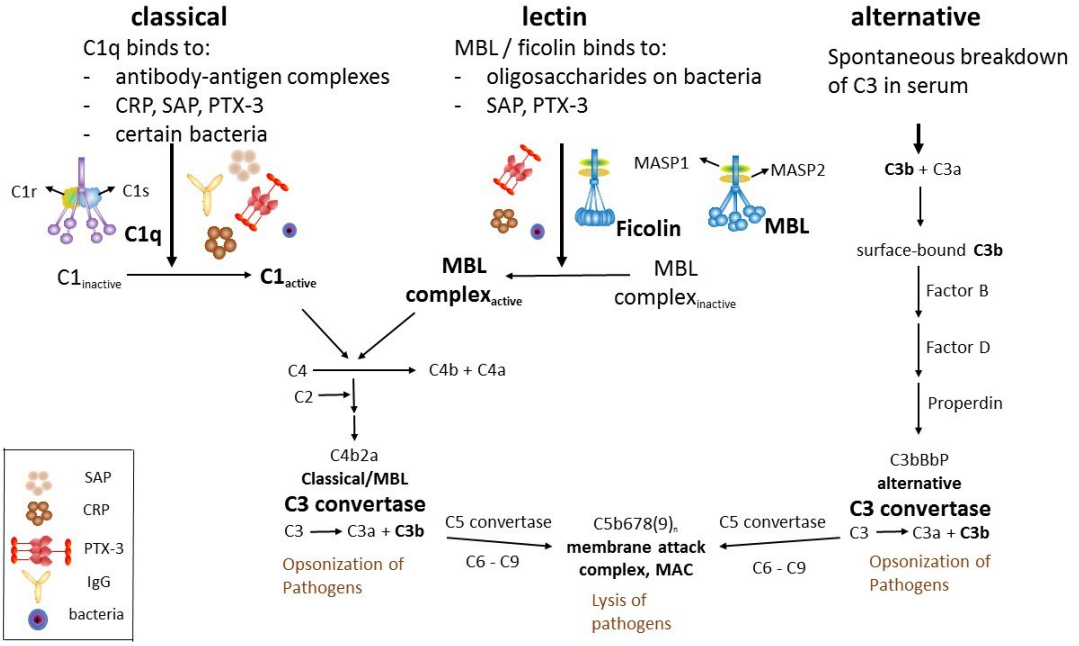

Figure 1.6: Complement cascades and their activators. The complement system is activated by three different pathways. The classical pathway is activated by IgM- or IgG-containing immune complexes, as well as CRP, SAP, and PTX-3 opsonized bacteria recognized by C1q, which activates C1s and C1r. The lectin pathway is activated by mannose-binding lectin motifs, exposed on bacteria, or by PTX-3 and CRP opsonized bacteria, recognized by MBL or Ficolin, which activates MASP2. The alternative pathway is activated by C3b-coated pathogens. The three pathways converge at the generation of the C3 convertase that cleaves C3 to C3a and C3b. C3b is an opsonizing protein that coats pathogen surfaces to facilitate their uptake and destruction by phagocytes. C3b associate to C3 convertase forming the C5 convertase that cleaves C5 to C5a and C5b. C5b forms with C6, C7, C8, and C9 the membrane-attack complex that destroys certain pathogens by disrupting their membrane integrity (figure modified from Doni et al. 2012; Sarma & Ward 2011).

The complement system is part of the humoral innate immune system and involves over 30 different membrane and serum proteins. It is initiated via three activation pathways (Figure 1.6). The classical pathway is activated by antibody binding to an antigen which is recognized by the collectin C1q. C1q is the opsonizing part of the C1 complex, which also comprises the proteases C1s and C1r. They are activated upon C1q binding and mediate complement activation. The lectin pathway is activated by the collectin mannose-binding lectin (MBL) or the Ficolin A or B, which recognize carbohydrates on microbial surfaces. Both MBL and Ficolin A circulate in serum as complex with MASP1/2. Binding of MBL or Ficolin A results in autoactivation of MASP2, which induces the complement activation cascade. The alternative complement pathway is continuously activated, but only amplified on foreign surfaces due to the absence of inhibitors such as factor B, factor D, and properdin, present on host cells (Gadjeva 2014; Sarma & Ward 2011). All the pathways converge at C3, which cleaves to C3a and C3b. The latter is an opsonizing protein that coats pathogen surfaces to facilitate their

uptake by phagocytosis. Moreover, C3 cleavage further results in the formation and activation of the membrane attack complex (C5b-9) (Gadjeva 2014; Sarma & Ward 2011).

Animal experiments suggest that among all complement activation pathways the classical pathway dominantly protects against *S. pneumoniae* infection (Brown et al. 2002). However, it is also published that patients, homozygotes for an MBL codon variant, are highly susceptible to invasive pneumococcal infections (Roy et al. 2002). Regardless of the activation pathway, the main function of complement is the opsonization of pathogen surface structures facilitating phagocytosis, the activation of neutrophil chemotaxis, and the direct killing of the pathogen via formation of the membrane attack complex (Gadjeva 2014).

1.3. Aim of the thesis

Recent data provide evidence for a crucial function of immunoproteasomes during an efficient immune response against invasive microorganisms. Numerous publications demonstrated the importance of immunoproteasomes for an effective immune reaction against viral infections for example Hepatitis B virus (HBV) (Robek et al. 2007), LCMV (Moebius et al. 2010), and IAV (Sibille et al. 1995). The role of immunoproteasomes in parasitic infections, including Toxoplasma gondii (Tu et al. 2009) and Trypanosoma cruzi (Chou et al. 2008), was discussed in several publications. A few studies investigated the function of immunoproteasomes in intracellular bacterial infections, including *Listeria monocytogenes* (Strehl et al. 2006) and *Mycobacterium tuberculosis* (Lv et al. 2011). So far, no data exists investigating the influence of immunoproteasomes on the progression of an extracellular bacterial infection.

In this context, this project has been created to study whether immunoproteasome deficiency influences the course of an *S. pneumoniae* infection. To clarify the impact of immunoproteasomes on the innate immune response against *S. pneumoniae*, many different immunological parameters were analyzed with the focus on *S. pneumoniae* elimination. Therefore, several key questions were raised, which have been studied in β5i/LMP7$^{-/-}$ mice.

- Does β5i/LMP7 deficiency influence the case and outcome of a pneumococcal pneumonia?
- Is β5i/LMP7 essential for bacterial clearance?
- Does β5i/LMP7 deficiency affect inflammation induced tissue damage?
- Does β5i/LMP7 deficiency alter the cellular and humoral innate immune response, locally as well as systemically?
- Is the composition of proteasomes changed during a *S. pneumoniae* infection?
- Is there a link between proteasome composition, anti-bacterial cellular immune function, and disease progression?

These questions were addressed *in vivo* by using a mouse *S. pneumoniae* infection model. Additionally, *ex vivo* co-culture experiments with *S. pneumoniae* and primary leukocytes were performed to examine distinctive immunological cell functions.

2. Material and Methods

2.1. Cell culture experiments

All cell culture experiments were performed under sterile conditions. Cells were incubated at 37 °C and 5 % CO_2. Primary cells were obtained from WT and β5i/LMP7$^{-/-}$ C57BL/6 (J) mice. The protocol was approved by the Committee on the Ethics of Animal Experiments of Berlin State authorities (Permit Numbers: T371/11).

Macrophage differentiation medium: RPMI, 10 % (v/v) FCS, P/S, 30 % (v/v) L929 supernatant

Stimulation medium: RPMI, 10 % (v/v) FCS, 30 % (v/v) L929 supernatant, various stimuli

Cultivation medium: RPMI, 10 % (v/v) FCS, P/S

PBS: 140 mM NaCl, 9 mM Na_2HPO_4, 2.7 mM KCl, 1.5 mM KH_2PO_4, pH 7.2

Detaching buffer: PBS, 5 mM EDTA

Digestion buffer: RPMI, 600 μg/ml collagenase A, 10 U/ml DNAse I

MACS buffer: PBS, 0.5 % (w/v) BSA, 2 mM EDTA

Chemicals, Reagents, Kits	Supplier
RPMI1640	Biochrom AG
Fetal calf serum (FCS)	Biochrom AG
L-glutamine	PAA Laboratories
Penicillin/Streptomycin	PAA Laboratories
Gentamicin	LONZA
Collagenase A	Roche
Lipopolysaccharide (LPS)	Sigma Aldrich
mIFNγ	Roche
MG132	VWR International

Chemicals, Reagents, Kits	Supplier
Griess reagent kit	Molecular Probes
Apo One	Promega
LDH Kit	Roche
CD45-MicroBeats	Miltenyi
MS-Columns	Miltenyi
EDTA	Applichem
Triton X	Sigma
Bovine serum albumin (BSA)	Applichem

Table 2.1: Chemicals, reagents and kits used in cell culture experiments

2.1.1. Cultivation of cell lines

Cell lines were provided by Prof. Bastian Opitz (Medical Clinics of Charité Berlin with focus on Infectiology and Pneumology, Berlin, Germany)

2.1.1.1. Cultivation of Raw264.7 cells

Raw264.7 cells were cultivated in cultivation medium and splitted 1:10 every third day. It is an adherent murine macrophage like cell line, immortalized with Ebstein Barr Virus (EBV).

2.1.1.2. Cultivation of L929 cells

L929 cells were cultivated in cultivation medium and split 1/10 every third day. It is an adherent murine fibroblast like cell line, constitutively expressing m-CSF. Its supernatant was used to generate bone marrow derived macrophages. Therefore, L929 cells were seeded on T175 cell culture flasks in 100 ml medium. After they reached confluence, cells were cultivated for additional 10 days. The conditioned supernatant was sterile filtered, aliquoted, and stored at -80 °C.

2.1.2. Generation and cultivation of bone marrow derived macrophages (BMM)

Mice were sacrificed by rapid cervical dislocation. The skin was peeled from each hind leg, which was cut off at the hip joint with scissors, leaving the femur and tibia intact. Excess muscles were removed and unopened bones sterilized with 70 % ethanol. Clean bones were opened on both ends and each bone cavity flushed with 5 ml cultivation medium. A single cell suspension was prepared by pushing the isolated bone marrow through a 70 μm mesh. This cell suspension was centrifuged at 500 g for 10 min at 4 °C, the pellet resuspended in 30 ml cultivation medium, and incubated over night by 37 °C and 5 % CO_2 in a cell culture dish. The next day, non-adherent cells, containing hematopoietic progenitor cells, were collected, centrifuged at 500 g and 4 °C for 10 min, and either processed further, or frozen in FCS with 10 % DMSO, and stored in liquid nitrogen.

Bone marrow progenitor cells of one mouse were resuspended in 100 ml macrophage differentiation medium, distributed to 10 uncoated sterile plastic petri dishes, and cultivated for 9 days at 37 °C and 5 % CO_2. On day 5, another 10 ml fresh macrophage differentiation medium was added to each dish. On day 9, macrophages were fully differentiated, culture supernatant was discarded, and remaining adherent cells (> 90 % macrophages) were washed with pre-warmed PBS. Finally, macrophages were harvested by incubating adherent cells with detaching buffer for 5 min at 37 °C. These cells were centrifuged for 10 min at 500 g and 4 °C, resuspended in macrophage differentiation medium, and seeded on target cell culture dishes in order to perform further experimental procedures.

2.1.3. Isolation of murine alveolar leukocytes

First, lungs were flushed with 20 ml PBS by puncturing the right cardiac ventricle to remove blood leukocytes from lung tissue. White flushed lungs were isolated, minced, and digested for 60 min at 37 °C in 5 ml digestion buffer. Later, a single cell suspension was prepared by pressing the lung homogenate through a 70 μm cell strainer. After two washing steps with 30 ml PBS and centrifugation for 10 min at 500 g and 4 °C, $CD45^+$ cells were enriched by magnetic isolation. This was performed according to the manufacturer's protocol (MACS, Miltenyi). Shortly, the cell pellet was resuspended in 90 μl MACS buffer and incubated with additional 10 μl CD45 MicroBeads for 15 min at 4 °C. Afterwards, cells were washed by adding 20 ml MACS buffer, centrifuged at 500 g and 4 °C

for 10 min, resuspended in 500 µl MACS buffer, and transferred to an MS column for positive isolation. Collected $CD45^+$ cells were finally centrifuged at 500 g and 4 °C for 10min, resuspended in PBS, and processed in various experimental procedures.

2.1.4. Stimulation of cells

For *ex vivo* maturation or cytotoxicity assays $1x10^5$, $3x10^5$, $6x10^5$, and $1x10^6$ cells were seeded on 96, 24, 12, and 6 well plate culture dishes on the eve of the experiment. The next day, cells were incubated with various stimuli in a total volume of 300 µl, 500 µl, 500 µl, and 1 ml stimulation medium, respectively, for maximal 48h.

Stimuli:

- LPS (1 µg/ml)
- D39Δcps (MOI 10)
- Heat inactivated D39Δcps (1/100)
- mIFNγ (200 U/ml); alone and in combination with LPS or heat inactivated D39Δcps
- Epoxomicin (250 nM): Cells were incubated with epoxomicin for 2h. Before additional stimulation, the inhibitor was removed and cells washed 3 times with PBS.

2.1.5. Phagocytosis assay

In order to characterize the phagocytosis efficiency of β5i/$LMP7^{-/-}$ phagocytes, alveolar leukocytes ($5x10^5$) were incubated with *E.coli* BioParticle-pHrodo (0.4 mg/ml) in 1 ml PBS and placed on ice for 15 min to synchronize phagocytosis. Phagocytosis by leukocytes was started by incubating them at 37 °C for 3h and stopped by cooling cells on ice. Negative control cells remained on ice. Subsequently, cells were stained with lineage antibodies and analyzed by flow cytometry (explained in section 2.4.1). Moreover, for a kinetic description $3x10^5$ BMM were seeded on a 24 well plate culture dish on the eve of the experiment. The following day, medium was aspirated, cells washed and covered with PBS. In order to synchronize phagocytosis, macrophages were placed on ice for 15 min. PBS was removed and cells covered with 100 µl ice-cold PBS containing D39Δcps-PKH67 (MOI 25). Except for the negative control cells, which remained on ice, macrophages were incubated at 37 °C for up to 120min. Finally, to stop phagocytosis, cells were placed on ice, D39Δcps-PKH67 were removed, cells washed 3 times with ice-cold PBS, and harvested by scraping. The fluorescent intensity of internalized D39Δcps-PKH67 was measured by flow cytometry.

2.1.6. Gentamicin protection assay

For the measurement of the intracellular early / late phase of killing, $6x10^5$ / $1x10^6$ BMMs were seeded on a 12 / 6 well plate culture dish. The following day, macrophages were co-cultivated with D39Δcps (MOI 10) in 500 µl macrophage differentiation medium without antibiotics. This co-culture was incubated at 37 °C for 30 min / 4h to allow bacterial internalization. In order to remove remaining extracellular bacteria, cells were washed 3 times with pre-warmed PBS and cultivated further with macrophage differentiation medium, containing gentamicin (300 µg/ml / 20 µg/ml). After an incubation period of several hours, cells were washed with PBS and lysed by adding PBS with 0.02 % Triton X. The supernatant, containing released bacteria, was diluted and plated on Columbia agar. Bacterial colonies were calculated after 9h incubation at 37 °C.

2.1.7. Phagosome acidification assay

For the determination of the phagolysosomal maturation efficiency, indicated by low pH values, macrophages were simultaneously incubated with *E.coli* BioParticles (0.4 mg/ml), which were labeled with a pH-sensitive fluorescent dye (pHrodo), and with heat inactivated D39Δcps (MOI 25), which were labeled with a pH-insensitive fluorescent dye (PKH67). The ratio of the fluorescent intensity of the pH-sensitive and the pH-insensitive reference dye is dependent on the pH and was determined by flow cytometry, and quantified by using a standard curve. On the eve of the experiment $3x10^5$ BMMs were seeded on a 24 well plate culture dish. The following day, cells were washed, covered with PBS, and placed on ice for 15 min, to synchronize phagocytosis. Subsequently, cells were covered with 100 µl ice-cold PBS, containing both types of fluorescent labeled particles. Except for negative control cells, which remained on ice, macrophages were incubated at 37 °C for up to 120 min. Acidification was stopped by placing cells on ice. Fluorescent labeled particles were removed and cells washed with ice-cold PBS. Concomitantly, a pH standard curve was created. Cells were incubated with *E.coli* BioParticles for 120 min and subsequently washed with ice-cold PBS to remove non-internalized BioParticles. Cells were incubated with pH-fixed PBS (2.5 to 8.1) for 10 min to allow permeabilization and equilibration of the phagosomal pH. Finally, cells were harvested by scraping and analyzed by flow cytometry.

2.1.8. Indirect measurement of nitric oxide

Nitrite (NO_2^-) is a stable oxidative end-product of the molecule nitric oxide (NO). Its measurement is a quantitative indicator of nitric oxide production. On the eve of the experiment $1x10^5$ BMM were seeded on a 96 well plate culture dish. The following day, macrophages were stimulated with LPS or heat inactivated D39Δcps. After an incubation period of maximal 48h, conditioned medium was

collected and its nitrite content determined, using the Griess Reagent kit for nitrite determination, according to the manufacturer's protocol (Molecular Probes).

2.1.9. Measurement of apoptosis and necrosis

Apoptosis was measured with an Apo-ONE Homogeneous Caspase 3/7 Assay, obtained by Promega. The amount of necrosis was determined by using the Cytotoxicity Detection Kit, provided by Roche. These assays were performed in 96 well plate dishes according to the manufacturer's instructions. Thereby, on the eve of the experiment $1x10^5$ BMM were seeded on a 96 well plate culture dish. The following day, macrophages were co-cultivated with D39Δcps for 4h. As positive control, cells were incubated with 10 μM MG132 for 24h.

2.2. Microbiological methods

All microbiological experiments were performed under sterile conditions (Gentechnik Sicherheitsstufe S2). Bacteria were incubated at 37 °C and 5 % CO_2.

THY medium: 30 % (w/v) Todd-Hewitt-Bouillion, 5 % (w/v) Yeast

PBS: 140 mM NaCl, 9 mM Na_2HPO_4, 2.7 mM KCl, 1.5 mM H_2PO_4, pH 7.2

Chemicals, Reagents	Supplier
Todd-Hewitt-Bouillion	BD
Columbia agar (5 % sheep blood)	BD
Yeast extract	BD
Canamycin	Calbiochem
Fetal calf serum (FCS)	Biochrom AG

Kits	Supplier
PKH67 linker kit	Sigma
pHrodo E.coli BioParticle	Molecular probes
Instruments	**Supplier**
Photometer Genesys 20	Thermo Scientific

Table 2.2: Chemicals, reagents, kits, and instruments used in microbiological experiments

2.2.1. Streptococcus pneumoniae

D39Δcps: This bacterium belongs to the bacterial strain *Streptococcus pneumoniae* serotype 2. It carries a deletion mutation in its capsule gene which was generated by homologous recombination with a canamycin cassette, performed by AG Hammerschmidt (University Greifswald, Department of Genetics of Microorganisms, Germany). The working glycerol stock was provided by Dr. Janine Zahlten; AG Hippenstiel (Medical Clinics of Charité Berlin, with focus on Infectiology and Pneumology, Berlin, Germany) and stored at -80°C. This strain was used in cell culture experiments.

PN36: This bacterium belongs to the bacterial strain *Streptococcus pneumoniae* serotype 3. It is a mouse adapted strain. The working glycerol stock was provided by Dr. Katrin Reppe; AG Witzenrath

(Medical Clinics of Charité Berlin, with focus on Infectiology and Pneumology, Berlin, Germany) and stored at -80°C. This strain was used to induce pneumonia in *in vivo* experiments.

2.2.2. Cultivation of D39Δcps for *in vitro* co-cultivation experiments

Bacteria, obtained from the glycerol stock with a sterile inoculating loop, were plated on Columbia agar and grown for 10h – 12h at 37 °C and 5 % CO_2. Single colonies were transferred to 20 ml THY with 10 % FCS. This suspension was incubated for 4h – 5h at 37 °C until it reached an OD_{600} of 0.2 – 0.4, which corresponds with the early middle log growth phase, containing bacteria being most vital. An adequate volume of this suspension was transferred to an eppendorf tube and centrifuged at 4000 g for 5 min. The THY with 10 % FCS was discarded and bacteria resuspended in an equal volume of RPMI with 10 % FCS. An OD_{600} of 0.1 corresponds with 10^8 cfu/ml.

2.2.3. Cultivation of PN36 for *in vivo* infection experiments

Bacteria, obtained from the glycerol stock with a sterile inoculating loop, were plated on Columbia agar and grown for 9h at 37 °C and 5 % CO_2. Single colonies were transferred with a cotton bud to 20 ml THY with 10 % FCS until reaching an initial OD_{600} of 0.03 – 0.04. This suspension was incubated for 2h at 37 °C until it grew to an OD_{600} of 0.3 – 0.4, which corresponds with the early middle log growth phase, containing bacteria being most vital. It was centrifuged at 4000 g for 10 min, without brake. The THY with 10 % FCS was discarded and bacteria resuspended in PBS ($1x10^9$ cfu/ml). This suspension was further diluted in PBS, depending on the experiment. An OD_{600} of 0.1 corresponds with 10^8 cfu/ml.

2.2.4. Generation of heat inactivated D39Δcps

Bacteria were grown in 50 ml THY with 10 % FCS to an OD_{600} of 0.6 – 0.7. This suspension was centrifuged at 4000 g for 10 min, THY medium discarded, and bacteria washed by adding 5 ml PBS. This bacterium solution was heat inactivated for 20 min at 60 °C. An OD_{600} of 0.1 is defined as 10^8 particles/ml. The heat inactivated D39Δcps solution was adjusted to an OD_{600} of 5.0, aliquoted, and stored at -20 °C.

2.2.5. Generation of fluorescent labeled D39Δcps

PKH67 is a fluorescent dye that intercalates in lipid double layer membranes. Heat inactivated D39Δcps were fluorescent labeled using the PKH67 green fluorescent cell linker mini kit according to manufacturer's (Sigma) protocol. Finally, the OD_{600} was determined, the lysate aliquoted, and stored at -20 °C. (An OD_{600} of 0.1 is defined as 10^8 particles/ml)

2.2.6. Generation of fluorescent labeled *E.coli* BioParticle conjugates

A solution of pHrodo *E.coli* BioParticle conjugates was prepared by resuspending an aliquot (2 mg) in PBS. This solution was strongly vortexed and sonicated for 5 min for proper homogenization (Molecular probes; Life technologies).

2.3. Animal infection experiments

All animal experimental protocols were approved by the Committee on the Ethics of Animal Experiments of Berlin State authorities (Permit Numbers: G0073/11). The *S. pneumoniae* mouse infection model was established by AG Witzenrath (Medical Clinics of Charité Berlin, with focus on Infectiology and Pneumology, Berlin, Germany). Experimental procedures were supervised by Dr. Katrin Reppe. All analyzed groups contained only female littermates with an age of 8-11 weeks.

Ulmer-Mix: 3 ml 100 mg/ml Ketamin, 2.4 ml Rompun 2 %, 3 ml NaCl 0.9 %

Narcosis-Mix: 2 ml 100 mg/ml Ketamin, 1 ml Rompun 2 %; 9 ml NaCl 0.9 %

Heparin-Mix: NaCl 0.9 % + Heparin (5000 IE/ml) in equal volumes

***S. peumoniae* solution:** Hyaluronidase + *S. pneumoniae* in PBS in equal volumes

Digestion buffer: RPMI + 2 mg/ml collagenase II + 0.3 mg/ml DNAse I

PBS: 140 mM NaCl, 9 mM Na_2HPO_4, 2.7 mM KCl, 1.5 mM KH_2PO_4, pH 7.2

BAL-Solution: PBS, Complete, 0.1 % (w/v) BSA

Chemicals, Reagents	Supplier
Ketamin	Cp pharma
Rompun	Cp pharma
NaCl solution 0.9 %	Braun
Hyaluronidase	Roche
Collagenase II	Roche
DNAse I	Roche

Reagents, Kits	Supplier
Anti-β5i/LMP7	abcam
BSA	Sigma
Heparin	Ratiopharm
EDTA Tubes	Sarstedt
Paraformaldehyd	Sigma
Erytrocyte. lysis b.	BD

Instruments	Supplier
Labor scale	G & G
Recal thermometer Bat12	Physitemp

Table 2.3: Reagents, kits, and instruments used in animal experiments

2.3.1. Mouse breeding

C57BL/6 (J) N6 β5i/LMP7$^{-/-}$ mice were generated by Ulrich Steinhoff and Hans Jörg Fehling (Fehling et al. 1994) and housed in FEM Bayer Unit 4. Mice were kept at the animal facilities of the Charité, University Medical Center, according to the European and Berlin State guidelines for animal welfare. Mice were bred in a heterozygous mating. Their genotype was determined by PCR analysis on genomic DNA, obtained from tail-biopsies.

2.3.2. Infection of mice

Animals were intranasally infected with PN36. Therefore, mice were anesthetized by a peritoneal application of 50 – 60 µl Ulmer-Mix. Animal's reflexes were tested and sedated mice hanged at their incisors. Subsequently, 10 µl of *S. pneumoniae* solution or PBS, as negative control, was applied on each nostril. Afterwards, sedated and infected mice were returned to their cages and exposed to red light for 1h. Mice, which inhaled the liquid, containing *S. pneumoniae*, established clinical signs of a pneumonia. Medical conditions of infected mice were monitored and documented every 12h. Thereby, the grade of activity, changes in breathing, in social behavior, and in drinking and food behavior was assessed. Furthermore, body temperature and body weight was determined, using a rectal thermometer and a labor scale. For every bacterial charge a dilution serious was plated on Columbia agar in order to control the amount of employed bacteria.

2.3.3. Preparation of mice

Mice were narcotized by a peritoneal application of 250 – 300 µl Narcosis-Mix. Animal's pain reflexes were tested, narcotized mice fixated, and dissected. Therefore, a median skin incision was performed from the abdomen to the mandibula. The muscle around the trachea was removed to get access to the trachea, which was ligated, if necessary. Afterwards, the peritoneum was opened till the Xyphoid. Heparin-Mix (50 µl) was applied through the diaphragm into the right cardiac ventricle. Blood was taken via the inferior vena cava by which mice bleed to death. Diaphragm was removed and the thorax disclosed. Lung was flushed with 20 ml PBS by puncturing the right cardiac ventricle. Lung tissue was dissected without bronchus and further processed. In some experiments other organs, such as liver, were removed and further analyzed.

2.3.4. Analysis of the cellular immune status

In order assess the amount of various different leukocytes upon infection in lung as well as in circulation, mice infected with $5x10^6$ cfu were sacrificed at 6h, 24h, and 48h of infection. Lungs were flushed and dissected without bronchus. Lungs were minced and digested in 6 ml digestion buffer for 30 min at 37 °C. A single cell suspension was prepared by pressing the lung homogenate through a 70 µm cell strainer. It was centrifuged for 10 min at 500 g and 4 °C. Lung cells were resuspended in 2 ml erythrocyte lysis buffer and incubated for 10 min at 4 °C. This reaction was stopped by adding 30 ml PBS. Cells were centrifuged for 10 min at 500 g and 4 °C, resuspended in 3 ml PBS, distributed to eppendorf tubes, and stained for flow cytometry. The total leukocyte amount per lung was determined by adding Trucount beads. FACS Calibur was used for the analysis of lungs obtained from mice infected for 48h. For the analysis of the cellular immune status of the lungs, obtained from mice at 6h and 24h of infection, the same lung preparation protocol was employed, but for the flow

cytometry a FACS Canton was used, kindly provided by AG Hackstein (Justus-Liebig-University Gießen; Centre of Transfusion Medicine and Hematotherapy).
Leukocyte distribution in venous EDTA blood, obtained from infected animals via the inferior vena cava, was assessed by flow cytometry, using Trucount beads and a FACS Calibur.

2.3.5. Determination of bacterial burden

Mice infected with $5x10^6$ cfu were sacrificed 24h and 48h post infection. Lungs were dissected without bronchus and minced by pressing the tissue through a 100 μm cell strainer. The lung homogenate was collected in a 50 ml Falcon tube, the cell strainer washed with PBS, and the volume of the tissue solution adjusted to 20 ml by adding PBS. An aliquot (10 μl) of this solution and of a dilution series (1/10 -> 1/10.000 in PBS) was plated on Columbia agar which was incubated at 37 °C for 9h. The quantity of bacteria was calculated by counting the cfu´s. Likewise, bacterial burden in blood was assessed by plating 10 μl venous EDTA blood (pure -> 1/10.000 in PBS) on Columbia agar which was incubated at 37 °C for 9h and quantified by counting cfu´s.

2.3.6. Study of the approximate survival rate

Mice were infected with $7.5x10^4$ cfu and monitored for 10 days. Their medical condition was documented every 12h. When the disease developed a severe state without possibility of physical recovery, and when it was conceivable that infected mice suffer sickness and pain which were not ethical, mice were euthanized by an intraperitoneal application of 300 μl Narcosis-Mix. The state of disease was measured by the means of a score sheet for “human endpoints”. This score sheet comprises guidelines for the clinical assessment of infected animals. These guidelines were provided by LAGESO. *(„Empfehlungen des Arbeitskreises Berliner Tierschutzbeauftragter für die vorzeitige Tötung erheblich leidender Versuchstiere“ [Stand 22.07.2009])*

2.3.7. Histological analysis of infected lung tissue

Mice were infected with $5x10^6$ and $1x10^6$ cfu and sacrificed at 24h and 48h, respectively, of infection. In order to remove the whole respiratory tract, the trachea was ligated and cut above the larynx. The trachea, bronchus, and lung were dissected in one piece and fixated in 3.7 % paraformaldehyd for 24h – 48h. Fixated tissue was further processed at the Institute of Animal Pathology, FU Berlin. Hematoxylineosin (HE) staining and immune detection of β5i/LMP7 expression was carried out by Dr. Olivia Kershaw (AG Gruber, FU Berlin, Department of Veterinary Pathology, Berlin, Germany).

2.3.8. Processing of a bronchial alveolar lavage (BAL)

Mice infected with $5x10^6$ cfu were sacrificed 48h post infection. After flushing the lung with 20 ml PBS by puncturing the right cardiac ventricle, the uncovered trachea was punctured with a cannula. The trachea and the cannula were ligated. BAL-solution (800 µl) was infused in and immediately aspirated off the lung. Recovered BAL fluid was centrifuged at 1200 g for 10 min, cell free liquid frozen in liquid nitrogen, and stored at -80 °C until it was analyzed using immunological methods.

2.4. Immunological methods

PBS: 140 mM NaCl, 9 mM Na_2HPO_4, 2.7 mM KCl, 1.5 mM KH_2PO_4, pH 7.2

FACS buffer: PBS, 0.05 % (v/v) FCS, 2 mM EDTA

Instruments	Supplier
FACS Calibur	BD
FACS Canton	BD
Photometer	SynergyHT
Bio-Plex working station	BioRad

Kits	Supplier
Trucount	BD
albumin ELISA	Bethyl
Bio-Plex Pro mouse Assay	BioRad

Software	Supplier
Cell Quest Pro	BD
FlowJo	FlowJo
BioPlex	BioRad

Table 2.4: Instruments, kits, and software used in immunological experiments

2.4.1. Flow cytometry

Antibody	Fluorochrom	Supplier
NK1.1	PE-CF594	BD
NK1.1	PE	BD
CD19	PerCP-Cy5.5	BD
CD19	APC	BD
CD3e	PE	BioLegend
CD3e	FITC	BD
TCR g/d	FITC	Biolegend
CD8a	APC	Biolegend
CD4	PE-Cy7	BD
Siglec-F	PE	BioLegend

Antibody	Fluorochrom	Supplier
CD86	PE	BioLegend
CD45	APC-Cy7	BD
CD45	PerCP-Cy5.5	BD
CD25	Pacific Blue	BD
F4/80	Pacific Blue	BD
F4/80	APC	BioLegend
Gr1	APC	BD
Gr1	PE	BD
CD11c	FITC	BD
CD11c	PE-Cy7	BD

Table 2.5: Antibodies used in flow cytometry

For flow cytometry $2.5x10^5$ cells were distributed to a 96 well plate in a total volume of 100 µl FACS buffer. Specific antibodies (1/100) were added and incubated in the dark at 4 °C for 30 min. Afterwards, cells were washed twice with 150 µl FACS buffer and centrifuged at 500 g and 4 °C for 5 min. Finally, cells were resuspended in 200 µl – 500 µl FACS buffer and analyzed.

Cell Type	Lineage marker
Leukocytes	$CD45^+$
Mph	$CD45^+$, Siglec F^+, $F4/80^+$
DC	$CD45^+$, Siglec F^-, $CD11c^+$
Granulocytes	$CD45^+$, $Gr1^+$
B-cells	$CD45^+$, $CD19^+$
NK-cells	$CD45^+$, $NK1.1^+$

Cell Type	Lineage marker
T-cells	$CD45^+$, $CD3^+$
T-helper	$CD45^+$, $CD3^+$, $CD4^+$
T-cytotox	$CD45^+$, $CD3^+$, $CD8^+$
T-reg	$CD45^+$, $CD3^+$, $CD25^+$
T-γδ	$CD45^+$, $CD3^+$, TCR g/d

Table 2.6: Antibody panels for cell discrimination by flow cytometry

2.4.2. Trucount

The cell number in 1 lung or 1 µl blood was assessed by spiking samples with Trucount beads. Therefore, 50 µl blood or 100 µl cell suspension, together with specific FACS antibodies, were added to a Trucount tube (BD), vortexed intensely, and incubated for 30 min at room temperature. Erythrocytes were lysed by adding 450 µl or 400 µl erythrocyte lysis buffer, respectively. Afterwards, without any further washing step, Trucount suspension was vortexed, transferred to a FACS tube, and analyzed by flow cytometry, using a FACS Calibur or FACS Canton.

Calculation - lung leukocytes:

(CD45+ cells x total beads in tube x total volume of cell suspension) / (beads x analyzed volume)

Calculation – blood leukocytes:

(CD45+ cells x total beads in tube) / (beads x volume of blood sample)

2.4.3. Elisa

The amount of serum albumin in plasma and in BAL fluid was measured by ELISA (Bethyl). Therefore, collected BAL fluid was diluted 1/10.000 and 1/20.000, plasma was diluted 1/750.000 in blocking buffer, and analyzed according to the manufacturer's instructions.

Coating buffer: 0.1 M sodium carbonate pH 9.5

Washing buffer: PBS, 0.05 % (v/v) Tween-20

Blocking buffer: PBS, 10 % (v/v) FCS

Stopping solution: 1 M H_3PO_4

2.4.4. Multi-plex analysis

Cytokine and chemokine concentrations in plasma and BAL fluids of infected mice were measured by using the Bio-Plex Pro Mouse Cytokine Group I Assay and the multiplex working station, provided by

the Deutsches Rheuma-Forschungszentrum (DRFZ) Berlin. Therefore, pure BAL fluid and plasma, diluted ¼, was processed according to manufacturer's protocol (BioRad).

2.4.5. Serological Analysis

The enzyme activity of ALAT and LDH in serum of ill animals was measured by the Institute of Veterinary Medicine and Diagnostics, Berlin.

2.5. Molecular methods

6 x DNA sample buffer: 50 % (v/v) glycerine, 50 mM EDTA, 0.25 % (w/v) bromophenol blue

TAE buffer: 40 mM Tris, 1 mM EDTA, 20 mM acetic acid

Tissue digestion buffer: 100 mM Tris, 200 mM NaCl, 5 mM EDTA, 0.2 % (w/v) SDS, 200 µg/ml proteinase K

Chemicals , Kits	Supplier
Taq Polymerase kit	Applichem
cDNA Synthesis kit	Roche
Real Time Mastermix	Applied Biosystems
Proteinase K	Sigma
PCR-Primer	Biotez
SYBR® safe DNA gel stain	Invitrogen
Agarose	Serva
Trizol	Invitrogen

Instruments	Supplier
Thermocycler Gradient	Eppendorf
Rotor Gene 3000	Corbett Research
MP-FastPrep24	MP-Biomedicals
NanoDrop 1000	Peqlab
Gel – Visualizer	Syngene
Software	**Supplier**
Rotor Gene Monitor 4.6	Corbett Research
PCR Visual	Gene Snap

Table 2.7: Reagents, kits, and instruments used in molecular biological assays

2.5.1. Isolation of genomic DNA

Tail biopsies were lysed with tissue digestion buffer over night at 55 °C. Undigested tissue was pelletized at 13000 g for 10 min and supernatant, containing genomic DNA, transferred to a new eppendorf tube. The DNA was precipitated by adding an equal volume of isopropanol. The eppendorf tube was inverted several times and centrifuged at 13000 g for 15 min. Supernatant was discarded and the DNA pellet washed with 70 % ethanol. This was centrifuged for 10 min at 13000 g, the supernatant discarded, and the remaining ethanol evaporated. The genomic DNA was dissolved in aqua bidest. and stored at 4 °C until analysis.

2.5.2. PCR and agarose gel electrophoresis

AppliTaq DNA PCR System together with primers was applied according to the manufacturer's instructions (Applied Biosystems). The PCR program was employed as described below. The PCR

products were supplemented with 10 x DNA-sample buffer and separated electrophoretically on 1 % agarose gels. Gels were stained with SYBR® safe DNA gel stain and visualized under UV light.

Primer sequence:

- LMP7 wild type allele (600 bp)
  LMP7 Fw: GGA CCA GGA CTT TAC TAC GTA GAT G
  LMP7 Rev: CTT GTA CAG CAG GTC ACT GAC ATC G
- LMP7 knock-out allele (700 bp)
  Neo Fw: CCG ACG GCG AGG ATC TCG TCG TGA
  LMP7 Rev: CTT GTA CAG CAG GTC ACT GAC ATC G

PCR Program:

	7 min 95 °C DNA denaturation
32 cycles	30 sec 94 °C
	30 sec 63 °C primer annealing
	45 sec 72 °C DNA polymerization
	7 min 72 °C
	∞ 4 °C

2.5.3. Isolation of RNA

Tissue or pelletized cells, incubated in 1 ml Trizol, was disintegrated using a shredding machine. After adding 200 µl chloroform, it was thoroughly mixed by shaking, incubated at room temperature for 3 min, and centrifuged at 13000 g for 20 min at 4°C. The upper liquid phase, containing the RNA, was transferred into a new eppendorf tube. After adding 500 µl isopropanol, RNA was precipitated at room temperature for 20 min and pelletized at 13000 g for 20 min at 4 °C. The supernatant was discarded, the RNA washed with 1 ml 70 % ethanol, and centrifuged at 13000 g for 10 min at 4 °C. The supernatant was removed, the RNA dissolved in 300 µl aqua bidest., and stored at -80 °C. RNA concentration was measured using the NanoDrop 1000.

2.5.4. cDNA synthesis

Transcription of mRNA into cDNA was performed by using the cDNA generation kit (Roche). Therefore, RNA (1 µg), Oligo-Td primer and aqua bidest. was added and annealed for 10 min at 70 °C. Afterwards reaction buffer, containing reverse transcriptase, was added and reverse transcription carried out at 37 °C for 60 min using a PCR cycler, according to the manufacturer's instructions.

2.5.5. Real Time PCR / TaqMan®

The reaction mix was prepared by adding 1 µl cDNA to 9 µl reaction buffer, containing 1 µl TaqMan primer, 3 µl aqua bidest. and 5 µl mastermix (2 x). The TaqMan® PCR was performed in duplicates,

using the Rotor gene 3000 cycler. Gene expression was analyzed with the Rotor Gene Monitor 4.6 software and normalized to the housekeeping gene HPRT1 by means of the ΔΔCt method.

Real-Time Primer	Supplier
Hprt (Mm01545399_m1)	Applied Biosystems
Saa1 (Mm00656927_g1)	Applied Biosystems
Mbl2 (Mm0087623_m1)	Applied Biosystems
Sfltpa (Mm00484287_m1)	Applied Biosystems
Sftpd (Mm00486060_m1)	Applied Biosystems
C1qa (Mm00432142)	Applied Biosystems
Ptx3 (Mm00477268_m1)	Applied Biosystems
Fcna (Mm00484287_m1)	Applied Biosystems
Il1b (Mm00434228_m1)	Applied Biosystems

Table 2.8: TaqMan primer

Real Time PCR Program:

	10 min 95 °C DNA denaturation
40 cycles	15 sec 94 °C
	30 sec 60 °C primer annealing
	60 sec 60 °C DNA polymerization

2.6. Biochemical methods

Chemicals, Reagents, Kits	Supplier
Prestained Protein Ladder	Fermentas
Nitrocellulose membrane	Immobilon Millipore
ECL Plus WB Detection Reagents	GE Healthcare
Film X-OMAT UV	Kodak
Complete Inhibitor Mix	Roche
RotiBlock	Roth
Coomassie	Serva
Fluorogenic substrates	Bachem
Epoxomicin	Calbiochem
BCA-protein Assay Kit	Thermo Fisher Scientific

Chemicals, Kits	Supplier
Acrylamide	Applichem
APS	Applichem
TEMED	Biomol

Instruments	Supplier
Electrophoresis chamber	BioRad
Blotting chamber	BioRad

Table 2.9: Chemicals, reagents, kits, and instruments used in biochemical experiments

RIPA buffer: 50 mM Tris-HCl, 150 mM NaCl, 1 % (v/v) Nonidet P40, 0.5 % Sodium-deoxycholate, 0.1 % (w/v) SDS and 1x Complete

TEAD buffer: 20 mM Tris-HCl, 1 mM EDTA, 1 mM NaN_3, 1 mM DTT, pH 7

10 x SDS-Running buffer: 250 mM Tris-HCl pH 8.8, 2 M glycine, 1 % (w/v) SDS

Blotting buffer: 25 mM Tris-HCl, 200 mM glycine, 25 % (v/v) methanol

Blocking solution: PBS, 0.5 % (v/v) Tween-20, 10 % (v/v) RotiBlock

Washing buffer: PBS, 0.5 % (v/v) Tween-20

4 x stacking gel buffer: 0.5 M Tris-HCl pH 6.8, 0.4 % (w/v) SDS

4 x separating gel buffer: 1.5 M Tris-HCl pH 6.8, 0.4 % (w/v) SDS

10 x SDS-sample buffer: 500 mM Tris-HCl pH 6.8, 60 % (v/v) glycerol, 20 % (w/v) SDS, 1 M DTT, 1% (w/v) bromophenol blue

Separating polyacrylamide gel (12.5 %): 15 ml 30 % acrylamide, 12 ml H_2O, 9 ml 4 x separating gel buffer, 25 µl TEMED, 300 µl 10 % (v/v) APS

Stacking polyacrylamide gel (5 %): 4.5 ml 30 % acrylamide, 10.5 ml H_2O, 7.5 ml 4 x stacking gel buffer, 30 µl TEMED, 300 µl 10 % (v/v) APS

Coomassie staining solution: 0.1 % (w/v) coomassie, 30 % (v/v) methanol, 10 % (v/v) acetic acid, 60 % (v/v) aqua bidest.

Coomassie destaining solution: 30 % (v/v) methanol, 10 % (v/v) acetic acid, 60 % (v/v) aqua bidest.

2.6.1. Protein isolation and quantification

Cells were harvested, washed with 1 ml PBS, and centrifuged at 8000 g for 2 min at 4 °C. Under denaturizing conditions, the cell pellet was lysed with 50 – 70 µl RIPA buffer, carried out for 1h on ice with occasional vortexing. Under native conditions, cell pellets were resuspended in 50 – 70 µl TEAD buffer, organs pestle in 200 µl TAED buffer and lysed by subsequent 3 cycles of freeze and thaw in liquid nitrogen. In order to separate lysate from cell debris, it was centrifuged at 13000 g for 15 min at 4 °C. The supernatant was collected and stored at -80 °C, or processed immediately. The protein concentration was determined with the BCA protein assay kit, according to manufacture´s instructions in 96 well plates.

2.6.2. SDS-PAGE, western blotting and immuno-detection

For separation of proteins under denaturating conditions, SDS-polyacrylamide gel electrophoresis was performed. Therefore, cell lysate was diluted in SDS-sample buffer to a final protein concentration of 1 µg/µl and denaturated at 95 °C for 5 min. Subsequently, 10 – 20 µg total lysate was loaded onto a 12.5 % SDS-polyacrylamide gel. The electrophoresis was performed at 120 V for 1 – 2h. The protein marker, PageRuler prestained protein ladder, was used as standard to estimate the molecular weight of separated protein bands. These proteins were transferred to a nitrocellulose membrane by using the Wet blot procedure and an appropriate blotting buffer. It was performed at a constant electric current of 4000 mA for 1h. Thereafter, free binding sites of the membrane were saturated with a blocking solution at room temperature for 1h. The incubation with the primary antibody against the antigen of interest was performed at 4 °C over night. The next day, the membrane was washed 3 times for 10 min in washing buffer, followed by incubation with the appropriate secondary antibody at room temperature for 1h. It targets an antigen from the first antibody and was diluted in blocking solution. Finally, the membrane was washed 3 times for 10 min in washing buffer. For visualization, horseradish peroxidase (HRP)-labeled secondary antibodies and ECL Plus™ Western Blotting Detection Reagent was used. The chemoluminescence signal was detected on autoradiography film X-OMAT UV.

Antibodies	Supplier
anti-β5i/LMP7	abcam
anti-β5	abcam
anti-β1i/LMP2	abcam
anti-β1	Self-made
anti-β2i/MECL-1	Self-made
anti-α4	Self-made
anti-IκBα	Santa Cruz
anti-βActin	Cell signaling

Antibodies	Supplier
anti-p-cFos	Cell signaling
anti-cFos	Cell signaling
anti-p-cJun	Cell signalling
anti-cJun	Santa Cruz
anti-p-ATF2	Cell signalling
anti-ATF2	Cell signalling
anti-rabbit-HRP	Dianova
anti-mouse-HRP	Seramun

Table 2.10: Antibodies used in western-blot

2.6.3. 20S purification

The 20S proteasome purification from differentiated BMM was performed by Alexander Kloß. Therefore, $1x10^9$ BMM were pestled in TEAD buffer, using a douncer, and centrifuged for 60 min at 13000 g and 4 °C. The resulting supernatant was used for the determination of the protein content, as well as for the purification of 20S proteasomes, as described in Schmidt et al. 2006. Briefly, this consists of the following steps: a fractionated protein precipitation with ammonium sulphate, chromatography on DEAE-Sephacel, gel filtration on Superose 6, and anion exchange chromatography on Mono Q. After purification of the 20S proteasome it was further processed for 2D gel electrophoresis.

2.6.4. 2D Gel analysis

The purified 20S proteasome (25 μg) was precipitated in ethanol (96 %) by incubating it in a 2.5 fold volume of ethanol over night at -20 °C. Precipitated 20S proteasomes were centrifuged for 60 min at 13000 g and 4°C, and its pellet washed (2 x) with 1 ml ethanol (70 %). The proteasomes were centrifuged again for 30 min at 13000 g and 4 °C, its pellet dried, and sent to Protalys GmbH, which performed the 2D electrophoresis.

2.7. Statistics

The statistical significance was determined by using the Mann-Whitney U Test for *in vivo* data and by using the Student t-test for *in vitro* generated data. All statistical analyses were performed using GraphPad Prism Software (version 4.03) (GraphPad, San Diego, CA, USA). Statistical significance was achieved when $p<0.05$; *$p<0.05$, **$p<0.01$, ***$p<0.001$.

3. Results

Since pathogenesis of pneumococcal pneumonia is a complex interplay between virulence and host immunity (van der Poll & Opal 2009), we analyzed the role of immunoproteasomes, contributed by the host, in preservation of immunological cell function and pathogen elimination during the innate immune response against *S. pneumoniae*.

Therefore, we investigated the involvement of the immuno-subunit β5i/LMP7 in antibacterial defense mechanisms of the innate immune system by using a murine infection model. In order to characterize microbiological, physiological, and immunological effects of pneumococcal pneumonia in β5i/LMP7$^{-/-}$ mice, we documented resulting histopathological tissue damage, leukocyte recruitment, leukocyte function, cytokine and chemokine release, expression of opsonizing molecules, bacterial clearance, and survival of infected animals. Furthermore, we analyzed immunoproteasome expression in pulmonary and peripheral tissue as well as leukocytes, and assessed its contribution towards an efficient immune reaction.

3.1. β5i/LMP7 deficiency aggravates the clinical signs of pneumococcal pneumonia

By illustrating the role of immunoproteasomes in the host defense during *S. pneumoniae* infection, we examined the impact of β5i/LMP7 deficiency on the clinical case of a pneumococcal pneumonia. Progression of pneumonia is manifested in a variety of clinical signs such as short breathing, scrubby fur, apathy but also loss in body weight and body temperature (Mizgerd & Skerrett 2008).

Infected animals seemed to recover for a while but then developed a gradually pronounced hypodynamic state which was associated with a gradual loss in body weight and body temperature from 24h to 48h of infection (Figure 3.1A). By applying an infectious dose of $5x10^6$ PN36/mouse, mice usually died short after 48h of infection and were therefore euthanized before reaching this endpoint. Nevertheless, the loss in body weight was significantly stronger in β5i/LMP7$^{-/-}$ compared to WT mice. While WT mice lost about 15.1 % of their initial body weight β5i/LMP7$^{-/-}$ mice lost about 18.7 % of their initial body weight 48h post infection. This effect was confirmed by documenting the drop in body temperature of ill animals. While the body temperature of β5i/LMP7$^{-/-}$ mice significantly decreased by a median of 2.1 °C, the body temperature of WT mice hardly fell between 24h und 48h of infection.

Clinical diagnostic parameters such as expression of acute phase proteins help to assess the severity of infection. Serum amyloid A (*saa1*) is an acute-phase protein which is expressed in liver in response to inflammation. It is used as marker of inflammation in clinical pathologies and correlates with the severity of infection (Yamada 1999). Therefore, its liver expression was determined 6h, 24h, and 48h post infection (Figure 3.1C). The expression of *saa1* started at 24h of infection and increased further

during the late phase of pneumonia, in both mouse strains, but significantly stronger and only significant in β5i/LMP7$^{-/-}$ mice. Between 24h und 48h of infection, the expression of *saa1* increased in β5i/LMP7$^{-/-}$ mice from about 1.8x10^5 to about 4.4x10^5 while in WT mice it elevated from about 1.2x10^5 to about 1.9x10^5.

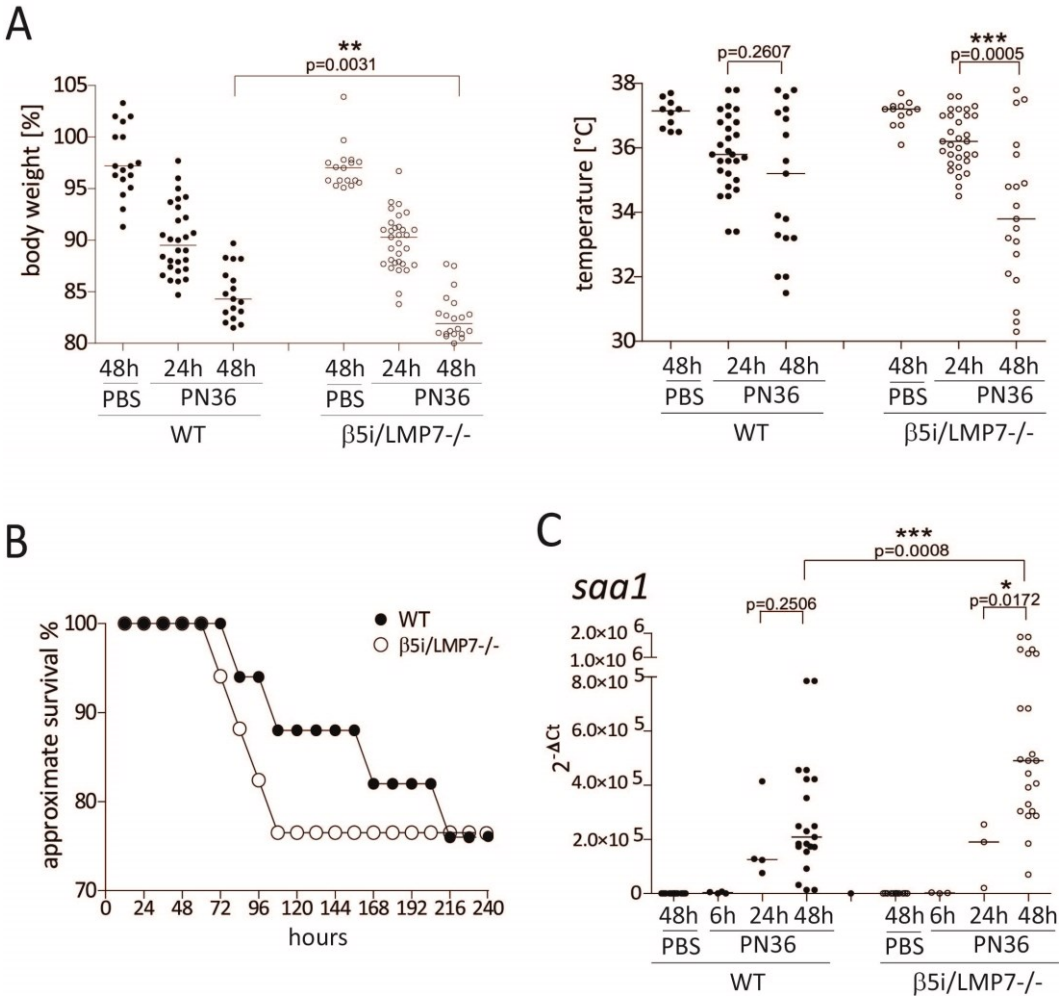

Figure 3.1: β5i/LMP7$^{-/-}$ mice suffer from a more severe case of pneumonia. (A) Monitoring of body weight and body temperature 24h and 48h after intranasal application of 5x10^6 PN36/mouse (each group with n= 12 – 29) **(B)** Assessment of the approximate survival rate for up to 10 days upon intranasal application of 7.5x10^4 PN36/mouse (each group with n= 17). **(C)** Analysis of mRNA expression of the acute phase protein SAA in liver after intranasal application of 5x10^6 PN36/mouse, performed by RT and Real Time PCR (each group with n= 3 - 14). In all experiments, 20 µl PBS/mouse was intranasally applied, as control (statistical analysis by Mann-Whitney U Test *p<0.05; **p<0.01; ***p<0.001).

In order to investigate whether β5i/LMP7 is required for survival of a pneumococcal pneumonia, β5i/LMP7$^{-/-}$ and WT mice were monitored for their ability to resist infection (Figure 3.1B). Clinical signs were noted in both mouse strains, 60h after intranasal application of 7.5x10^4 cfu/mouse. These signs started mildly and progressed through the clinics of a *S. pneumoniae* pneumonia. Although,

there was no difference in the overall approximate survival rate between WT and β5i/LMP7$^{-/-}$ mice, the latter died at earlier time points with an enhanced mortality during the first 108h of infection, showing an approximate death rate of about 12 % in WT and about 23.5 % in β5i/LMP7$^{-/-}$ mice.
The aggravated loss in body weight and drop in body temperature, the premature mortality, and the more pronounced expression of SAA suggest an advanced illness in β5i/LMP7$^{-/-}$ mice especially during the late phase of pneumonia.

3.2. WT and β5i/LMP7$^{-/-}$ mice react with an overwhelming local immune response

Physiological signs are associated with immunological observations. Recruitment of leukocytes and the local production of inflammatory molecules are central mediators of pathology during disease (van der Poll & Opal 2009). In this infection model, influx of immune cells towards lung tissue and release of pro-inflammatory cytokines were noted in β5i/LMP7$^{-/-}$ as well as WT mice. Both mouse strains established a local overwhelming immune response which increased in strength until death. Concerning the recruitment of leukocytes no significant difference was detected between WT and β5i/LMP7$^{-/-}$ mice. However, during the late phase of pneumonia, reduced levels of pro-inflammatory cytokines were recovered in BAL fluid of β5i/LMP7$^{-/-}$ animals.

3.2.1. Recruitment of inflammatory cells is not disturbed in β5i/LMP7$^{-/-}$ mice

By illustrating the influence of β5i/LMP7 deficiency on the inflammatory process in lung tissue we detected and distinguished levels of infiltrating immune cells at 6h, 24h, and 48h of infection. FACS analysis revealed variations in individual cell populations occurring over time.

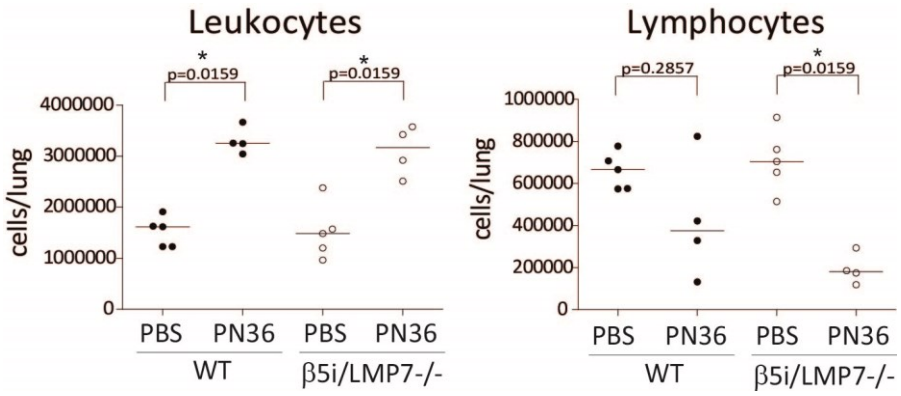

Figure 3.2: Recruitment of leukocytes and lymphocytes towards inflamed lung tissue is not influenced by β5i/LMP7 deficiency. Determination of leukocytes and lymphocytes in lung tissue analyzed by flow cytometry 48h after application of 5x10^6 PN36/mouse. As control, 20 µl PBS/mouse was applied intranasally (each group with n= 4 – 5; statistical analysis by Mann-Whitney Test *p<0.05).

While there was a strong recruitment of leukocytes towards lung tissue, the amount of lymphocytes dramatically decreased. These observations were determined for both, β5i/LMP7$^{-/-}$ and WT mice (Figure 3.2).

Especially during the late phase of pneumonia, leukocytes, mainly neutrophils, were recruited towards inflamed lung tissue (Figure 3.3).

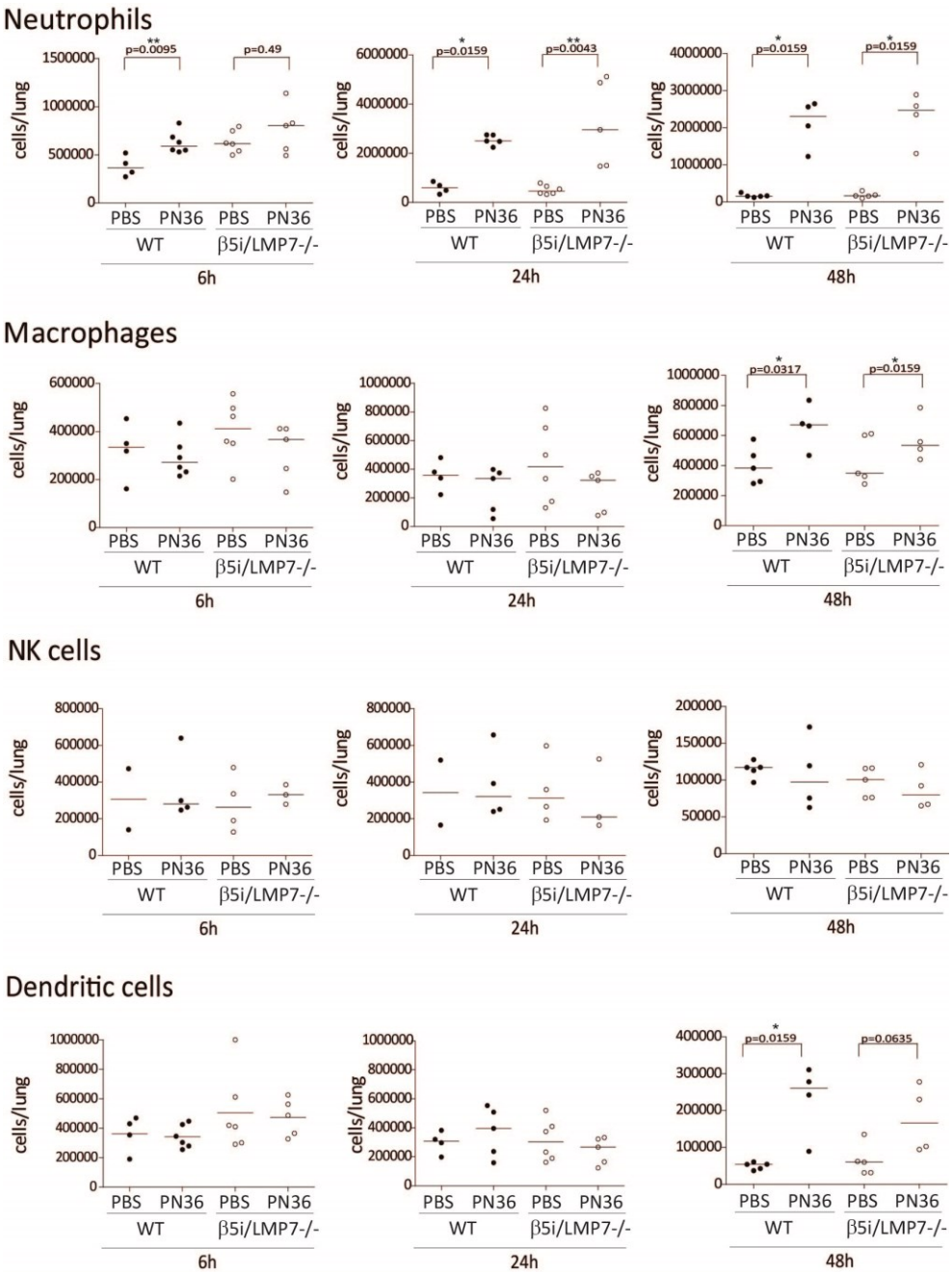

Figure 3.3: Recruitment of leukocytes towards inflamed lung tissue is not influenced by β5i/LMP7 deficiency. Discrimination of several types of leukocytes in lung tissue, analyzed by flow cytometry 6h, 24h, and 48h after application of 5x10^6 PN36/mouse. As control, 20 µl PBS/mouse was applied intranasally (each group with n= 4 – 6; statistical analysis by Mann-Whitney U Test *p<0.05; **p<0.01).

Its number increased dramatically by approximately 50-fold reaching statistical significance at 24h of infection with about 2.4x10^7 cells/lung. These levels persisted equally elevated at 48h of infection. The amount of NK cells remained constant at any time point. The total number of macrophages and DCs did not increase until 48h of infection, showing a maximum increase of about 2-fold to about 3-fold. This was detected in a similar extent for both mouse groups.

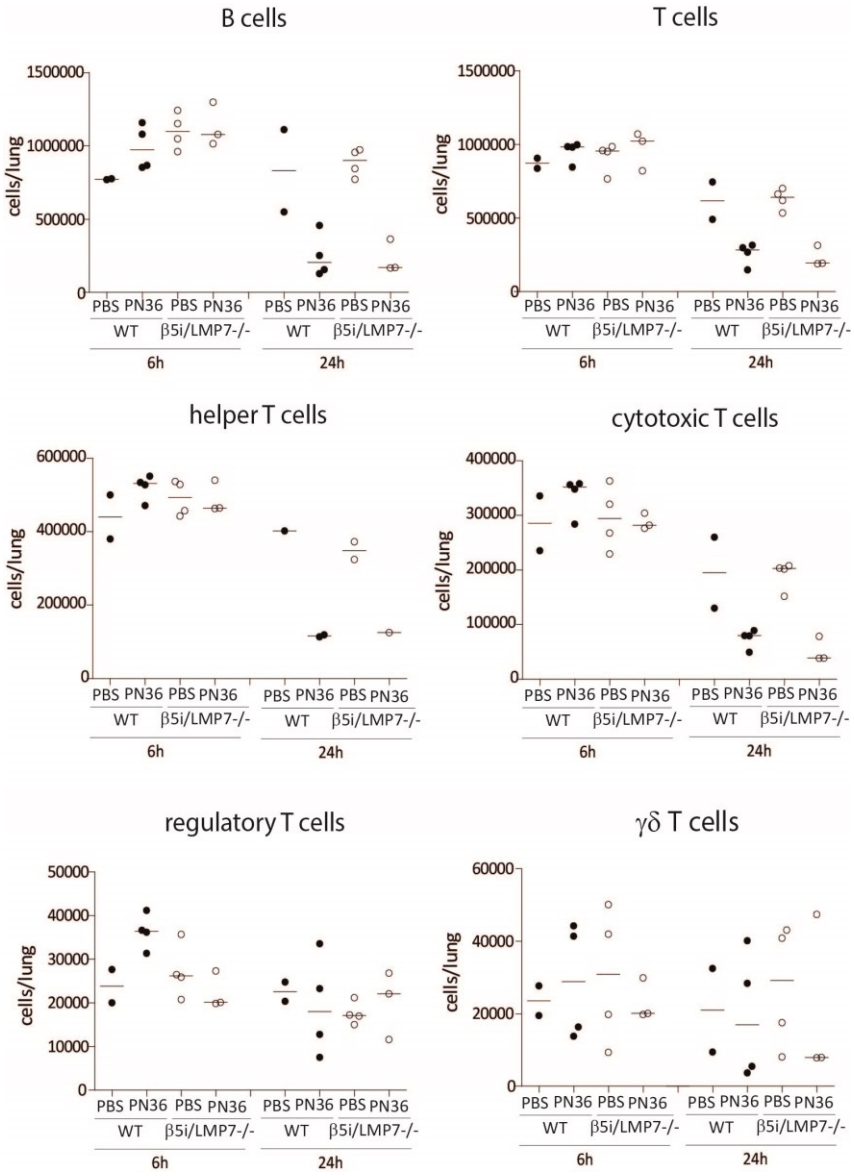

Figure 3.4: Recruitment of lymphocytes towards inflamed lung tissue is not influenced by β5i/LMP7 deficiency. Discrimination of several types of lymphocytes in lung tissue, analyzed by flow cytometry 6h and 24h after application of 5x10^6 PN36/mouse. As control, 20 µl PBS/mouse was applied intranasally (each group with n= 2 – 5).

During infection the number of lymphocytes diminished significantly (Figure 3.2). Initially approximately 7x10^6 cells/lung residual lymphocytes were measured in both mouse strains which declined to a median of 3.7x10^6 cells/lung in WT and to a median of 1.8x10^6 cells/lung in β5i/LMP7$^{-/-}$

mice. A combined reduction in the overall amount of B cells and T cells manifested this decrease, already detectable at 24h of infection (Figure 3.4). The numbers of B cells decreased approximately 5-fold to approximately 8-fold and the quantity of T cells fell about 3-fold to about 4-fold with infection. Thereby, all T cell populations were influenced differently. While the quantity of regulatory T cells and γδ T cells was unaffected throughout the whole experiment, the amount of cytotoxic T cells and helper T cells was decreased, resembling the range of the decline in the overall amount of T cells. This again was detected in a similar extent for both mouse strains.

Consequently, although, FACS analysis revealed variations in different leukocyte populations in lung tissue in response to a pneumococcal pneumonia, no differences in leukocyte recruitment towards inflamed lung tissue due to β5i/LMP7 deficiency was measured.

3.2.2. Lung pro-inflammatory cytokines are partially altered due to β5i/LMP7 deficiency

Cytokines play a critical role by protecting the host against bacterial infections. They modify various immune-modulatory mechanisms that trigger the inflammatory response. Consequently, levels of pro-inflammatory cytokines, released to the interstitial alveolar space, were determined in BAL fluids of *S. pneumoniae* infected WT and β5i/LMP7$^{-/-}$ mice (Figure 3.5). Measured cytokines were selected based on their known pro-inflammatory impact in host defense (van der Poll & Opal 2009; Koppe et al. 2012).

At 48h of infection, IL-6, TNFα, and IL-1β were recovered in BAL fluid with a significant increase in diseased animals when compared with uninfected control values. Among these cytokines variations were detected between β5i/LMP7$^{-/-}$ and WT BAL fluids.

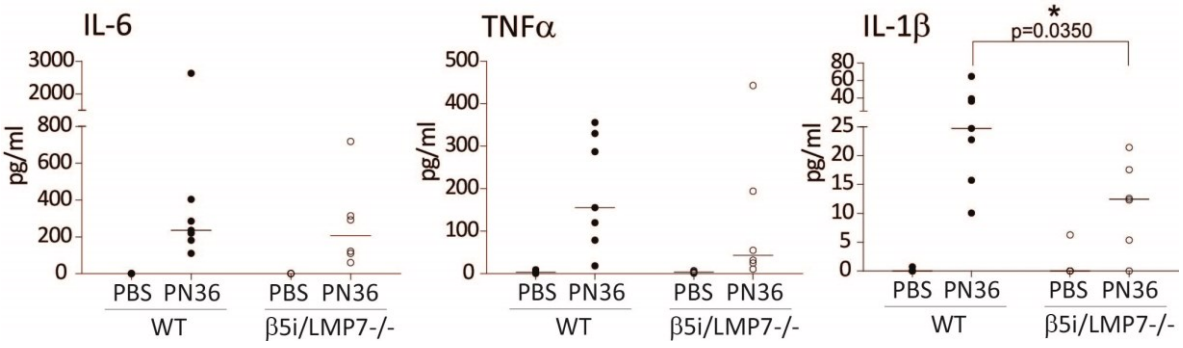

Figure 3.5: β5i/LMP7$^{-/-}$ mice show reduced levels of certain pro-inflammatory cytokines, measured in BAL fluid. Determination of pro-inflammatory cytokines in BAL fluid, obtained 48h after intranasal application of 5x10^6 PN36/mouse, and measured by multiplex analysis. As control, 20 µl PBS/mouse was applied intranasally (each group with n= 5 – 7; statistical analysis by Mann-Whitney U Test *p<0.05).

An elevated release of TNFα to the interstitial alveolar space was determined in both mouse groups. This increase was about 4-fold more pronounced in WT compared to β5i/LMP7$^{-/-}$ mice, though, by reason of high variances, this difference did not reach statistical significance. In contrast, IL-1β production revealed significant differences between infected WT and β5i/LMP7$^{-/-}$ animals. In BAL fluids of β5i/LMP7$^{-/-}$ mice significantly lower amounts of IL-1β (approximately 12.4 pg/ml) were measured compared to that recovered from BAL fluids of infected WT animals (approximately 24.7 pg/ml). By screening local levels of IL-6 no difference was detected between infected WT and β5i/LMP7$^{-/-}$ mice. During infection it increased equally high in both mouse strains with an approximated median of 200 pg/ml BAL fluid.

Taken together, β5i/LMP7$^{-/-}$ animals exhibited reduced pro-inflammatory cytokine levels in the alveolar space during the late phase of pneumonia.

3.3. β5i/LMP7$^{-/-}$ mice undergo an advanced case of pneumonia resulting in sepsis

During the late phase of pneumonia, mice not only suffered from pulmonary inflammation but developed signs of an overwhelming systemic immune response which led to sepsis and death. Sepsis is characterized by an extensive pro-inflammatory systemic immune reaction which coincides with organ damage (Castellheim et al. 2009). This overwhelming immune response often transits into a state of immune suppression (Markwart et al. 2014). By applying a lethal dose (LD_{100}) of *S. pneumoniae* to WT and β5i/LMP7$^{-/-}$ mice, prominent systemic immunological effects were documented in both mouse strains, though significantly more pronounced in β5i/LMP7$^{-/-}$ animals.

3.3.1. β5i/LMP7$^{-/-}$ mice suffer from a pronounced systemic inflammatory response

Challenged β5i/LMP7$^{-/-}$ and WT mice not only suffered from pneumonia but developed signs of a systemic inflammatory response syndrome (SIRS), indicated by a significant loss in body weight (Figure 3.1A) and enhanced expression of SAA (Figure 3.1C). By validating the effect of β5i/LMP7 deficiency on the severity of the systemic inflammatory response, we quantified and discriminated levels of circulating immune cells at 6h, 24h, and 48h of infection. FACS analysis of venous blood revealed variations in individual cell populations, especially during the late phase of pneumonia (Figure 3.6).

Although, levels of monocytes remained unaffected throughout the whole experiment the amount of granulocytes increased dramatically. Already at 24h of infection, a significant recruitment of granulocytes was detected, illustrated by an approximate 2-fold increase in both mouse groups. At 48h of infection, their total numbers increased further to an approximate 3.5-fold increase in WT

animals. This effect did not occur in β5i/LMP7$^{-/-}$ mice, whose granulocyte recruitment diminished to an approximate 1.3-fold difference.

Elevated levels of granulocytes did not automatically result in enhanced amounts of leukocytes. Throughout the whole experiment, levels of leukocytes remained unaffected in WT animals, while their numbers significantly declined in β5i/LMP7$^{-/-}$ mice (Figure 3.6). Already at 24h of infection, their amount of circulating leukocytes decreased by about 35 % lower the leukocyte amount determined in uninfected control littermates. This effect persisted significantly and equally high until 48h of infection. At this time point, β5i/LMP7$^{-/-}$ mice exhibited significantly less leukocytes compared to WT animals.

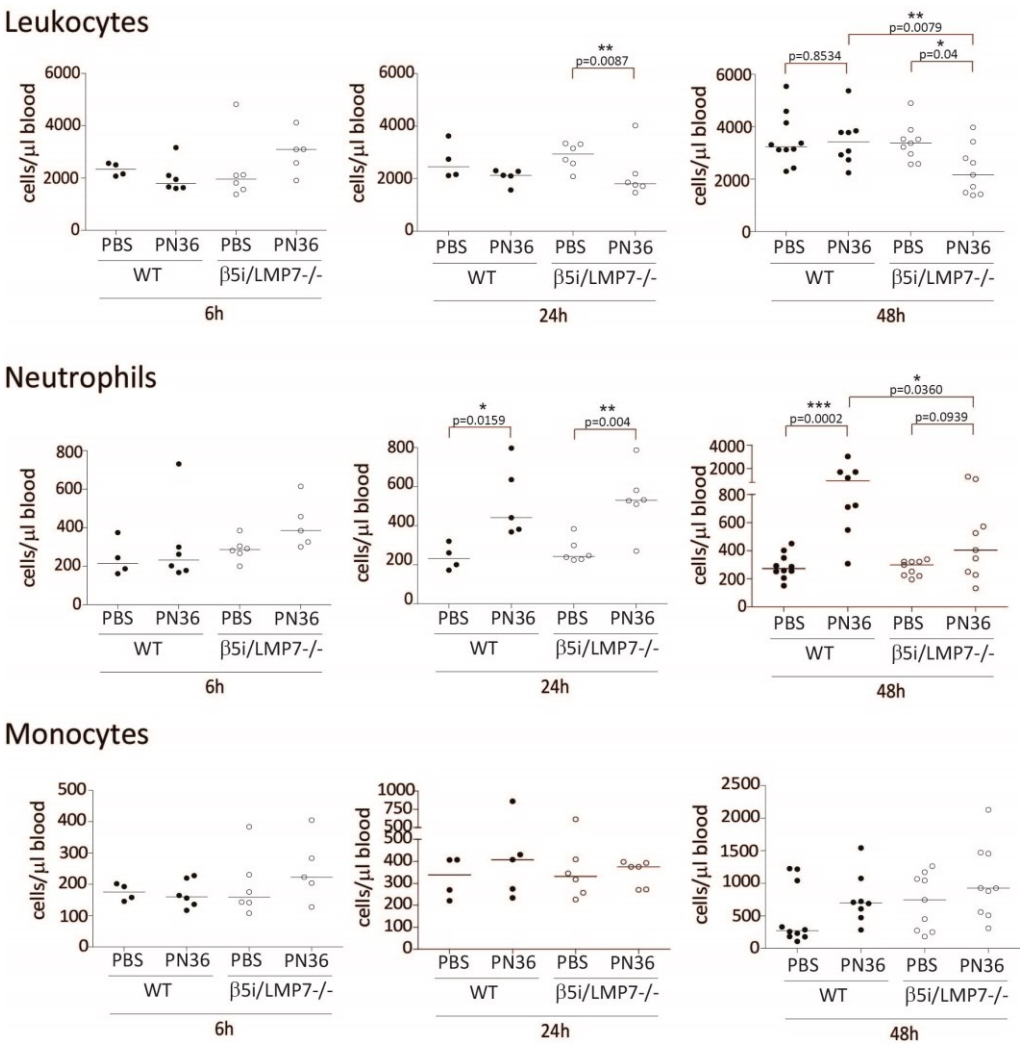

Figure 3.6: β5i/LMP7$^{-/-}$ mice suffer from a systemic inflammatory response syndrome. Determination of blood leukocytes, analyzed by flow cytometry 6h, 24h, and 48h after application of 5x10^6 PN36/mouse. As control, 20 µl PBS/mouse was applied intranasally (each group with n= 4 – 10; statistical analysis by Mann-Whitney U Test *p<0.05, **p<0.01; ***p<0.001).

The prominent leukopenia, measured in β5i/LMP7$^{-/-}$ mice, was established by a significant lymphopenia (Figure 3.7A). At 24h of infection a reduced level of circulating lymphocytes, which was reduced by half, was detected in WT as well as β5i/LMP7$^{-/-}$ mice. At 48h of infection, with an advanced state of disease, the total number of lymphocytes decreased further in β5i/LMP7$^{-/-}$ animals, establishing a significant difference of about 2-fold between infected WT and β5i/LMP7$^{-/-}$ animals. A correlation analysis between body weight, as indicator of health, and amount of lymphocytes proved an association of severity of disease and lymphopenia (Figure 3.7B).

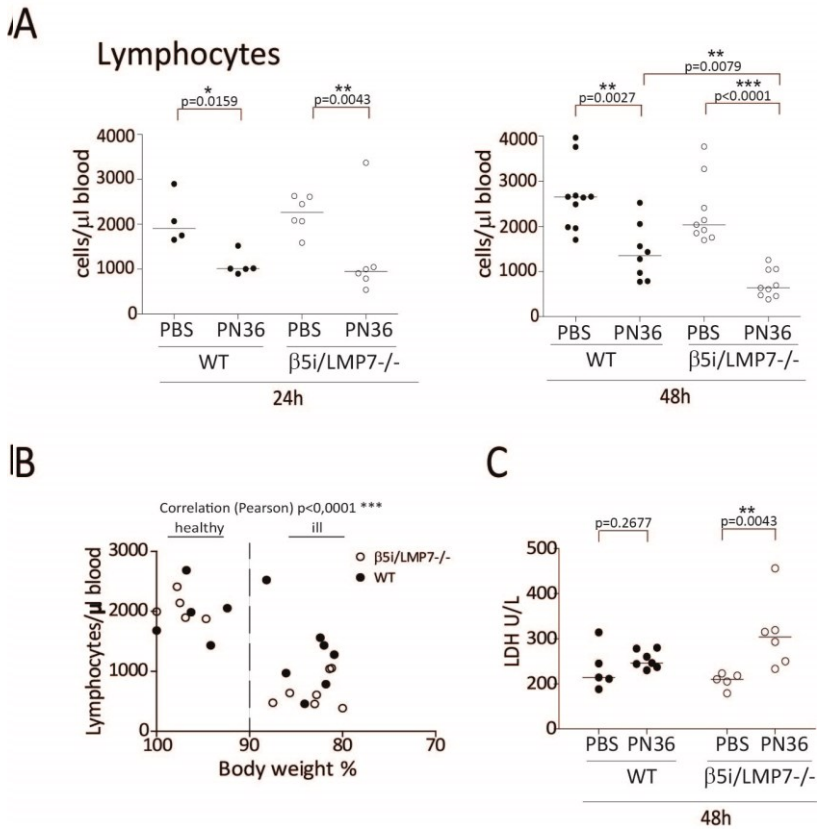

Figure 3.7: β5i/LMP7$^{-/-}$ mice develop lymphopenia that correlates with the severity of illness. **(A)** Determination of blood lymphocyte levels, analyzed by flow cytometry 24h and 48h after application of 5x10^6 PN36/mouse (each group with n= 4 – 10). **(B)** Illustration of correlation of lymphopenia and severity of infection, indicated by body weight. Amount of lymphocytes were determined by FACS analysis 48h after application of 5x10^6 PN36/mouse (each group with n= 9 – 10). **(C)** Documentation of tissue damage 48h post infection by measuring LDH activity in serum of mice, intranasally infected with 5x10^6 PN36/mouse (each group with n= 6 – 7). As control, 20 µl PBS/mouse was applied intranasally (statistical analysis by Mann-Whitney U Test *p<0.05; **p<0.01; ***p<0.001).

A pronounced systemic inflammatory response that causes and/or is accompanied by peripheral tissue injuries is defined as severe sepsis and leads to death of the organism (Castellheim et al. 2009). Therefore, in order to assess any kind of tissue damage, we evaluated serum levels of the enzyme lactate dehydrogenase (LDH), as it is generally released as a consequence of cell destruction

(Rotenberg et al. 1988). At 48h of infection, both, WT and β5i/LMP7$^{-/-}$ mice, showed elevated LDH serum levels which, however, were only significantly enhanced in β5i/LMP7$^{-/-}$ animals (Figure 3.7C). Conclusively, the strong recruitment of granulocytes at 24h of infection suggests a prominent systemic immune reaction which is later, at 48h of infection, accompanied by immunosuppression indicated by depletion of circulating leukocytes (lymphocytes, granulocytes).

These results in combination with the elevated serum levels of LDH indicate a progressed systemic inflammatory response which is more pronounced in β5i/LMP7$^{-/-}$ animals.

3.3.2. Pneumonia is accompanied by increased systemic levels of chemokines equally high in WT and β5i/LMP7$^{-/-}$ mice

Chemokines, which are released by various cell-types, are essential for the generation, mobilization, and navigation of leukocytes (Cruvinel et al. 2010). Since β5i/LMP7$^{-/-}$ but not WT mice suffered from leukopenia, at 48h of infection (Figure 3.6), we screened systemic levels of chemokines, selected based on their impact on granulocyte and macrophage recruitment. At 48h of infection, IL-6, CXCL-1, G-CSF, and MIP-1β were detected in plasma of both mouse groups with a significant increase in diseased animals compared to uninfected control values (Figure 3.8). No difference was detected between infected WT and β5i/LMP7$^{-/-}$ mice. All chemokines were synthesized at equal levels in both mouse strains demonstrating no dysregulation due to β5i/LMP7 deficiency.

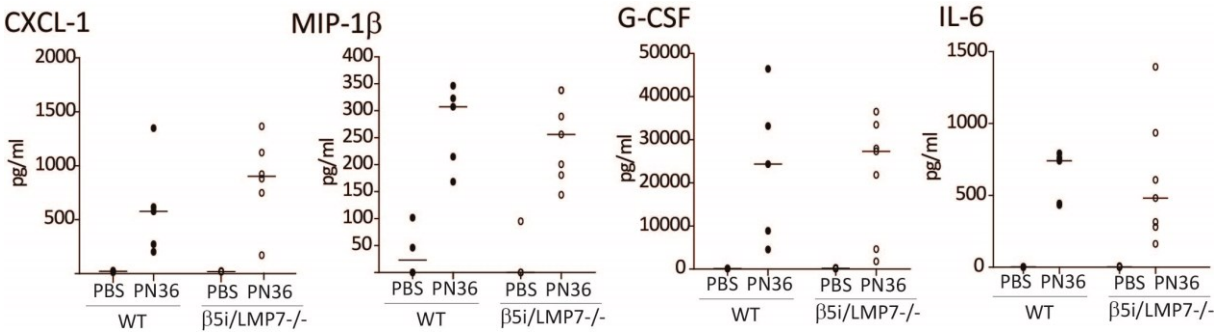

Figure 3.8: Systemic levels of chemokines increase with infection, but do not differ between WT and β5i/LMP7$^{-/-}$ mice. Determination of chemokines in plasma, obtained 48h after intranasal application of 5x10^6 PN36/mouse, and measured by multiplex analysis. As control, 20 µl PBS/mouse was applied intranasally (each group with n= 5 - 7).

3.4. β5i/LMP7 deficiency aggravates bacteremia during the late phase of pneumonia

When residual immune cells and waves of neutrophils fail to eradicate bacteria, sepsis is caused by high levels of bacteria in blood (Castellheim et al. 2009). Since this infection model leads to death rather by reason of sepsis than of the initial pulmonary infection (Ahl et al. 2013), we assessed the

extent of bacterial growth in lung and determined the magnitude of bacterial migration to bloodstream (Figure 3.9). Within the first 24h of infection proliferation of *S. pneumoniae* was documented in lungs of both mouse strains (Figure 3.9A), reaching extremely high numbers (about > $5.0x10^7$ cfu/lung). Between 24h and 48h of infection, proliferation continued with β5i/LMP7$^{-/-}$ mice showing a higher bacterial load compared to infected WT animals. However, due to high variances, this difference did not reach statistical significance (median of $4.3x10^8$ cfu/lung in WT and median of $8.0x10^8$ cfu/lung in β5i/LMP7$^{-/-}$ mice).

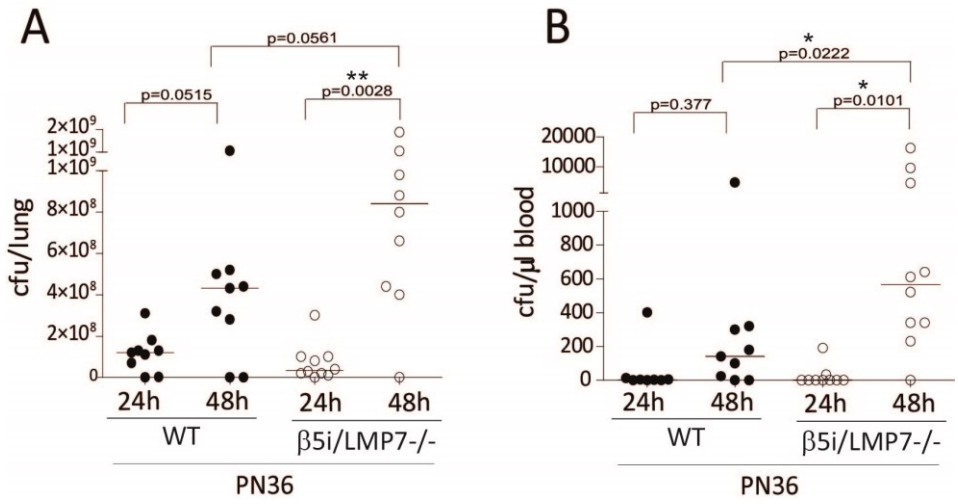

Figure 3.9: β5i/LMP7 deficiency is accompanied by an elevated bacterial load. Determination of bacterial load 24h and 48h post infection in **(A)** lung and **(B)** blood of mice, intranasally infected with $5x10^6$ PN36/mouse (each group with n= 9 - 10; statistical analysis by Mann-Whitney U Test *p<0.05, **p<0.01).

Moreover, hemocultures already became positive at 24h of infection, and at 48h of infection approximately 100 % of all β5i/LMP7$^{-/-}$ and WT animals established bacteremia (Figure 3.9B). At 48h of infection, β5i/LMP7$^{-/-}$ mice developed a manifested bacterial load, while WT animals cultivated significantly less bacteria. Having counted about $1.4x10^5$ cfu/ml in WT mice and about $5.6x10^5$ cfu/ml in β5i/LMP7$^{-/-}$ mice, they exposed approximately 4 times more bacteria in circulation.

Thus, during the late phase of pneumonia, β5i/LMP7$^{-/-}$ mice had an exacerbated bacterial dissemination manifested in a significantly higher bacterial burden in blood compared to WT animals.

3.5. β5i/LMP7 deficiency does not affect the integrity of the lung endo-epithelium

The main interface between the environment and the mammalian host is lined by continuous layers of specialized epithelial cells that serve many physiological functions including preventing the entry of microbes. Loss of integrity of these epithelial layers predisposes an individual to invasive infections (Bals & Hiemstra 2004). The key role of immunoproteasomes resides in the protection of cells against

harmful inflammation-induced formation of protein aggregates. This protective effect is ultimately essential for the preservation of cell viability (Seifert et al. 2010). Therefore, we examined lung tissue damage histopathologically and measured the integrity of the lung endo-epithelium by evaluating oedema formation.

In order to investigate pneumonia induced tissue damage, lesions were qualitatively and quantitatively characterized by histopathological examinations of lung tissue obtained from WT and β5i/LMP7$^{-/-}$ mice at 24h / 48h of infection (Figure 3.10).

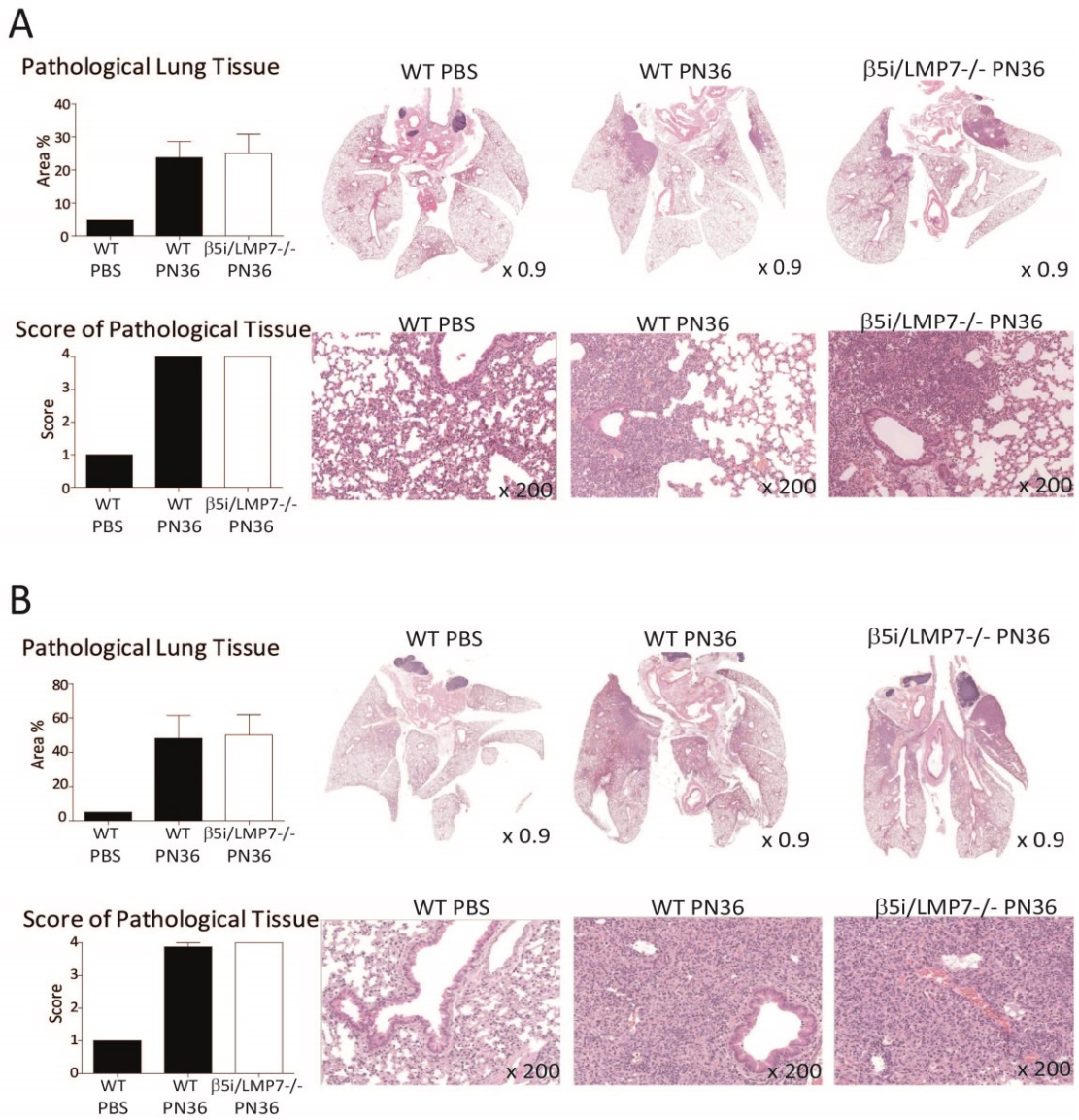

Figure 3.10: Pneumococcal pneumonia induces lung tissue damage, equally severe in β5i/LMP7$^{-/-}$ and WT mice. Assessment of lung tissue damage by H&E stain. **(A)** Lungs were analysed 24h after intranasal application of 5x10^6 PN36/mouse (each group with n= 4) and **(B)** 48h after intranasal application of 1x10^6 PN36/mouse (each group with n= 8). As control, 20 µl PBS/mouse was applied intranasally to WT C57BL/6J mice (each group with n= 4).

Morphological examinations revealed approximately 23 % / 48 % pathological tissue in WT mice and about 25% / 50% pathological tissue in β5i/LMP7$^{-/-}$ mice. Both, WT and β5i/LMP7$^{-/-}$ mice, suffered from progressive oedema and hepatisation of tissue. These modifications were associated with an intense inflammatory response, with an excessive infiltration of neutrophils and tissue injury. This damage was documented in both mouse strains with a pathological score of the 4th grade. There was no difference detectable between WT and β5i/LMP7$^{-/-}$ mice in inflammation induced tissue damage in lung caused by *S. pneumoniae*, neither at 24h nor at 48h of infection.

Leakage of the endo-epithelial barrier leads to vascular permeability that results in pulmonary oedema (Mizgerd & Skerrett 2008). Therefore, air space filling with protein-rich plasma exudates was measured by quantifying concentrations of total protein and serum albumin in BAL fluids (Figure 3.11). Both parameters increased significantly in diseased animals compared to uninfected control values. However, no difference was documented between WT and β5i/LMP7$^{-/-}$ animals. Protein concentrations, which increased to a median of 0.78 mg/ml in WT and to a median of 0.89 mg/ml in β5i/LMP7$^{-/-}$ mice, as well as serum albumin levels, which increased to a median of 0.19 in WT and to a median of 0.22 in β5i/LMP7$^{-/-}$ animals, demonstrated no enhanced aggravation of endo-epithelium destruction by reason of β5i/LMP7 deficiency.

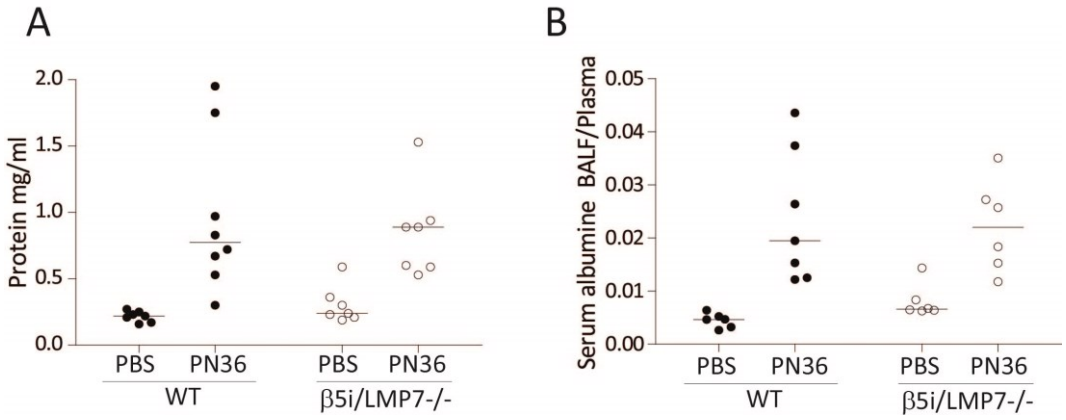

Figure 3.11: Pulmonary infection provokes oedema formation in lungs of β5i/LMP7$^{-/-}$ and WT mice. **(A)** Detection of cell damage, assessed by determining protein concentration in BAL fluid, obtained 48h after intranasal application of 5x10^6 PN36/mouse, performed by BCA (each group with n= 7 - 8). **(B)** Evaluation of leakage the of endo-epithelial barrier by measuring concentrations of serum albumin in BAL fluid, obtained 48h after intranasal application of 5x10^6 PN36/mouse, performed by ELISA (each group with n= 7 - 8).

3.6. β5i/LMP7 deficiency affects bacterial elimination

Considering that elimination of pathogens is a crucial step in host defense during pneumonia, we investigated the anti-bacterial properties of WT and β5i/LMP7$^{-/-}$ leukocytes, by studying their ability

to phagocytose and eliminate pneumococci. Additionally, since opsonization of bacteria results in facilitated pathogen recognition, enhanced phagocytosis, and elimination, we analysed the expression of various opsonizing molecules in lung and liver of WT and β5i/LMP7$^{-/-}$ mice. Although, no dysregulation of the anti-bacterial leukocyte function due to β5i/LMP7 deficiency was documented *ex vivo*, the *in vivo* expression of especially systemically located opsonins was affected in β5i/LMP7$^{-/-}$ mice.

3.6.1. The efficacy to kill *S. pneumoniae* is unaffected in β5i/LMP7$^{-/-}$ leukocytes

Leukocytes, including macrophages and granulocytes, play a central role in the innate immune response against extracellular pathogens. One of the main characteristics of these cells is their ability to internalize, kill, and degrade microbes (Underhill & Ozinsky 2002). Since β5i/LMP7$^{-/-}$ mice had a higher bacterial load in blood during the late phase of pneumonia (Figure 3.9), we investigated the impact of β5i/LMP7 deficiency on leukocyte function and their ability to kill bacteria.

Granulocytes and macrophages are critical in phagocytosis of *S. pneumoniae* (van der Poll & Opal 2009). Consequently, we assessed the effect of β5i/LMP7 deficiency on their ability to internalize pneumococci. For this purpose, lung leukocytes were isolated from WT and β5i/LMP7$^{-/-}$ mice and incubated with fluorochrome-labeled particles. FACS analysis revealed no difference in the amount of WT and β5i/LMP7$^{-/-}$ lung macrophages, granulocytes, and dendritic cells, having incorporated this particle (Figure 3.12A).

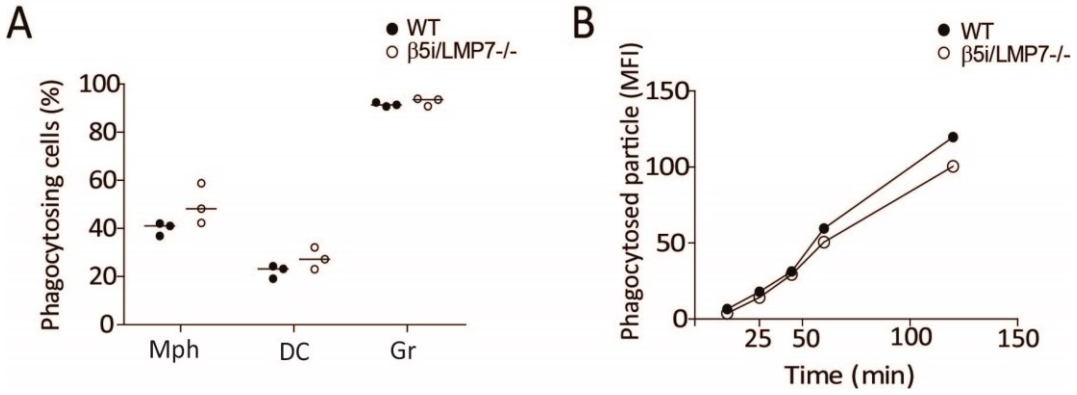

Figure 3.12: Phagocytosis of bacteria by leukocytes is not altered due to β5i/LMP7 deficiency. (A) Analysis of phagocytosis of fluorochrome-labeled particles by alveolar leukocytes, determined by flow cytometry (each group with n= 3). **(B)** Measurement of the phagocytosis rate of fluorochrome-labeled heat inactivated D39Δcps by BMM at different time points, determined by flow cytometry (each group with n= 3).

To confirm this result with pneumococcal protein, bone marrow derived macrophages (BMM) were incubated with fluorochrome-labeled heat inactivated D39Δcps. By assessing the amount of

incorporated *S. pneumoniae* by FACS analysis no difference between β5i/LMP7$^{-/-}$ and WT BMM was determined (Figure 3.12B). Deficiency of β5i/LMP7 did not influence phagocytosis of *S. pneumoniae*.

After internalization, microbes are degraded in mature phagolysosomes. The maturation status, which is reflected by the phagolysosomal pH milieu, is an indicator of successful intracellular killing (Nüsse 2011). Therefore, we investigated the impact of β5i/LMP7 deficiency on phagolysosomal maturation by incubating BMM with pH-dependent-fluorochrome-labeled particles. Subsequent FACS analysis revealed changes in the phagolysosomal pH value, decreasing from neutral (approximately pH 6.7) to acid (about pH < 4.0) (Figure 3.13A). Acidification was similar in WT and β5i/LMP7$^{-/-}$ BMM, indicating no effect of β5i/LMP7 deficiency on phagolysosomal maturation and intracellular killing competence.

This result was confirmed by directly determining the amount of internalized vivid *S. pneumoniae*. We investigated the success of β5i/LMP7$^{-/-}$ macrophages to intracellularly kill *S. pneumoniae* by co-cultivating them with active D39Δcps. Macrophages effectively eliminated *S. pneumoniae* in the early phase of intracellular killing (Figure 3.13B), however, no difference was detected between WT and β5i/LMP7$^{-/-}$ macrophages. Furthermore, it is reported that intracellular bacterial elimination is enhanced by apoptosis resulting in an improved late phase of intracellular killing (Ali et al. 2003), which is induced by phagocytosis of *S. pneumoniae* itself. We analyzed the efficiency of β5i/LMP7$^{-/-}$ BMM to eliminate internalized bacteria in the late phase of killing by co-cultivating them with active D39Δcps for longer periods (Figure 3.13C). The success to eliminate bacteria after 12h of infection was equally high in β5i/LMP7$^{-/-}$ and WT BMM. Consequently, β5i/LMP7 deficiency had no impact on intracellular killing efficiency.

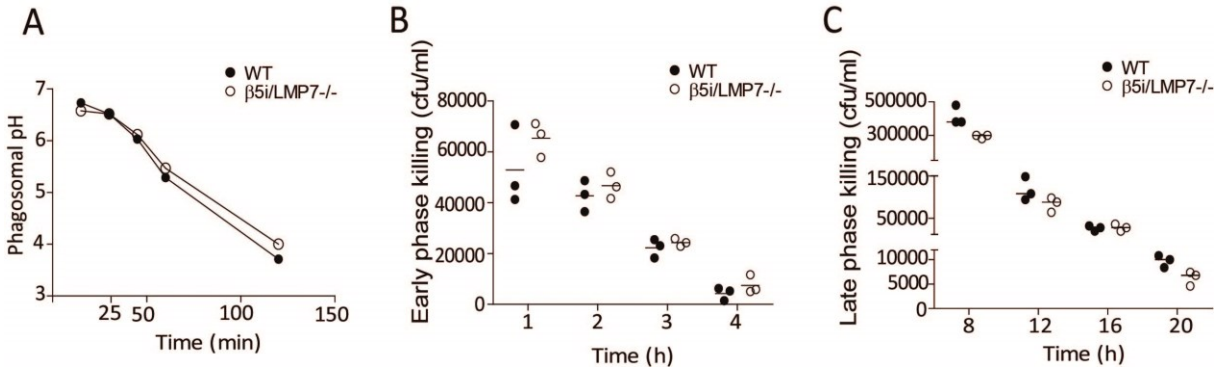

Figure 3.13: Bacterial elimination by leukocytes is not altered due to β5i/LMP7 deficiency. (A) Measurement of the pH value in the surrounding of phagocytosed particles, which reflects the efficiency of phagolysosomal maturation. This was investigated by flow cytometry (each group with n= 3). **(B)** The intracellular early phase of killing and **(C)** late phase of killing of D39Δcps by BMM was assessed after indicated time points. Therefore BMM were co-cultivated with D39Δcps MOI 10, cells lysed, and plated on blood agar plates. Finally, cfu/ml was determined (each group with n= 3).

Extracellular killing is facilitated by reactive nitrogen species, mainly nitric oxide (NO), which is for example produced by macrophages expressing iNOS (Burgner et al. 1999; Cole et al. 2014). Mice deficient for iNOS are highly susceptible to systemic infections and suffer from increased bacteraemia (Kerr et al. 2004; MacMicking et al. 1995). In order to investigate the competence of WT and β5i/LMP7$^{-/-}$ BMM to produce NO, we stimulated BMM with either LPS or heat inactivated D39Δcps, and determined the production of reactive nitrogen species indirectly by measuring NO_2^- levels in the supernatant using Griess reagent.

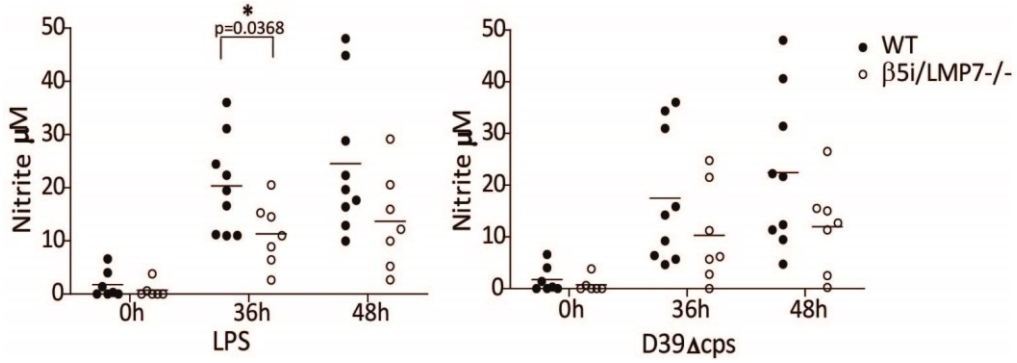

Figure 3.14: β5i/LMP7$^{-/-}$ BMM produce NO less efficiently. Analysis of NO secretion by WT and β5i/LMP7$^{-/-}$ BMM, stimulated either with LPS (1 µg/ml) or heat inactivated D39Δcps lysate (1/100) for up to 48h. NO concentrations in the supernatant were photometrically determined by Griess-Reagent (each group with n= 7; statistical analysis by student´s t-test. * p<0.05)

At 36h and 48h of stimulation, elevated NO_2^- levels were detected in both mouse groups. However, β5i/LMP7$^{-/-}$ BMM accumulated less NO_2^- compared to WT BMM, upon stimulation with LPS or pneumococcal protein (Figure 3.14). This result is depicting that β5i/LMP7 deficiency influences NO production.

Unfortunately, it was not possible to demonstrate a link between affected NO release and bacterial counts in tissue or blood, since no NO_2^- level above the background value was detected in BAL fluid of WT or β5i/LMP7$^{-/-}$ mice. This suggests a limited role for reactive nitrogen species on bacterial clearance and pneumonia, at least in this infection model.

3.6.2. β5i/LMP7 deficiency diminishes expression of opsonizing molecules

The on-site as well as systemic expression of various types of opsonizing molecules is an important early defense mechanism and its impairment increases the susceptibility to pneumococcal infection (van der Poll & Opal 2009).

As the synthesis of opsonizing molecules in lung directly facilitates termination of the pulmonary bacterial growth at the site of infection (Ariki et al. 2012; Shishido et al. 2012), we examined mRNA expression of collectins and pentraxins, including surfactant protein A (*sftpa*), surfactant protein D (*sftpd*), C1q (*c1qa*), and PTX-3 (*ptx3*), in lungs of diseased WT and β5i/LMP7$^{-/-}$ mice (Figure 3.15). At 48h of infection, gene expression analysis revealed a significant increase in the expression of *sftpa* and *sftpd*, which improved by approximately 1.5-fold and approximately 4.5-fold, respectively. However, no difference was detected between infected WT and β5i/LMP7$^{-/-}$ animals. The amount of PTX-3 mRNA significantly increased upon infection in both mouse strains, though significantly less pronounced in β5i/LMP7$^{-/-}$ mice, which was reduced by about 55 % compared to WT animals (Figure 3.15). Furthermore, expression of *c1qa* was only significantly induced in WT animals (about 1.7-fold), β5i/LMP7$^{-/-}$ mice hardly exhibited any up-regulation.

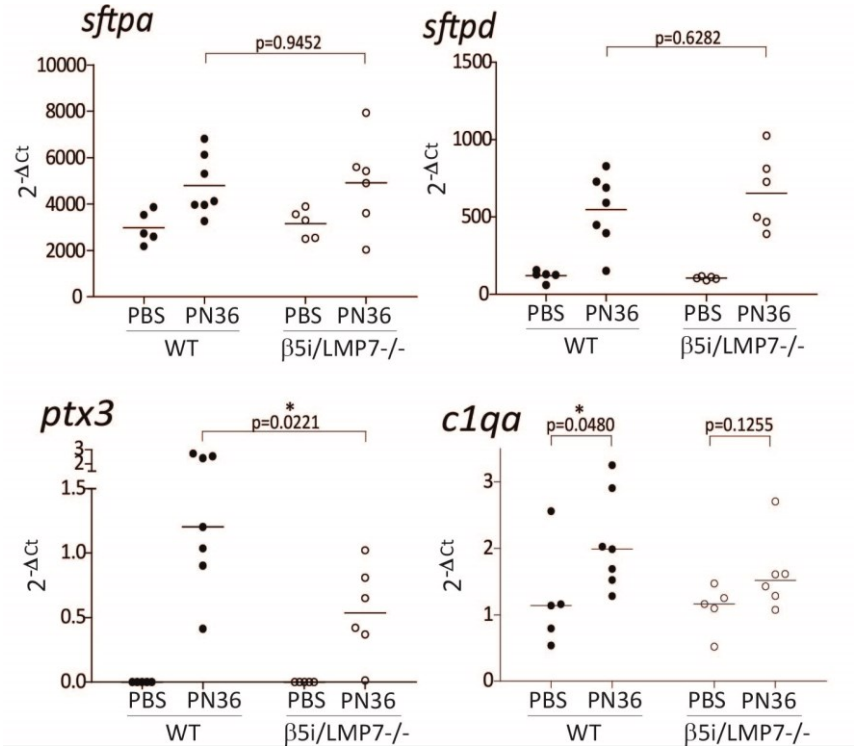

Figure 3.15: β5i/LMP7$^{-/-}$ mice exhibit a diminished expression of opsonizing molecules in lung tissue. (A) Gene expression analysis of lungs, 48h after intranasal application of 5x10^6 PN36/mouse, performed by RT and Real Time PCR. As control, 20 µl PBS/mouse was applied intranasally (each group with n= 5 – 6; statistical analysis by Mann-Whitney U Test *p<0.05).

PTX-3 is expressed by various different cell-types with macrophages being a major source (He et al. 2007). In order to confirm the *in vivo* obtained data with *in vitro* experiments, we assessed PTX-3 mRNA expression in WT and β5i/LMP7$^{-/-}$ macrophages, co-cultivated with *S. pneumoniae* (Figure 3.16). Thereby it was documented that *ptx3* expression was induced upon infection in both mouse

groups. However, β5i/LMP7$^{-/-}$ macrophages expressed significantly less PTX-3 mRNA compared to WT macrophages.

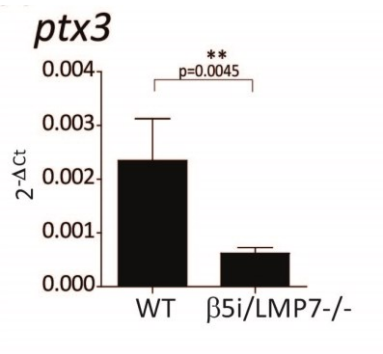

Figure 3.16: β5i/LMP7 deficiency affects PTX-3 expression in macrophages. Gene expression analysis of BMM, co-cultivated with D39Δcps lysate (MOI 10) for 4h, performed by RT and Real Time PCR (each group with n= 4, illustrated experiment is representative for 4 individual replicates; showing mean+- SD; statistical analysis by student's t-test **p<0.01).

Serum opsonizing molecules facilitate elimination of bacteria in bloodstream (Shishido et al. 2012). Because β5i/LMP7$^{-/-}$ mice suffered from a pronounced bacterial growth in blood (Figure 3.9B), we investigated mRNA expression of circulating collectins, ficolins, and pentraxins, including mannose binding lectin MBL (*mbl2*), c-reactive protein CRP (*crp*), C1q (*c1qa*), and Ficolin A (*fcna*), in liver of infected WT and β5i/LMP7$^{-/-}$ mice. It was demonstrated that, upon infection, expression of all analyzed opsonins was diminished in β5i/LMP7$^{-/-}$ compared to WT animals (Figure 3.17).

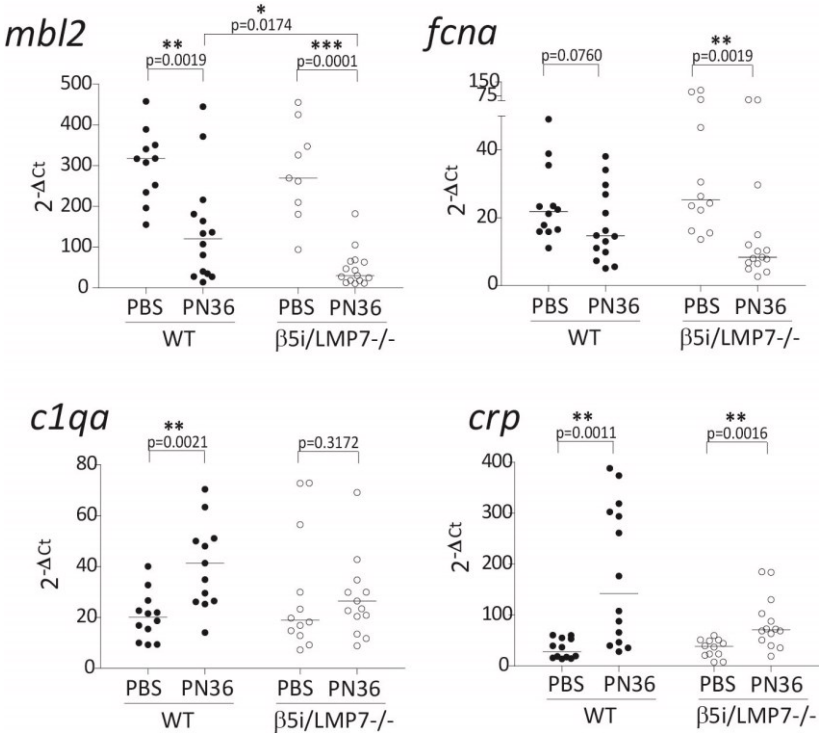

Figure 3.17: β5i/LMP7$^{-/-}$ mice exhibit diminished expression of opsonizing molecules in liver. Gene expression analysis of liver 48h after intranasal application of 5x10^6 PN36/mouse, performed by RT and Real Time PCR. As control, 20 µl PBS/mouse was applied intranasally (each group with n= 5 – 14; statistical analysis by Mann-Whitney U Test *p<0.05; **p<0.01).

At 48h of infection, gene expression analysis revealed a significant decline in MBL mRNA levels in both mouse groups, though significantly more prominent in β5i/LMP7$^{-/-}$ mice (about 89 %), reaching a difference of about 3.4-fold compared to WT animals (about 62 %). *Fcna* expression also was down regulated upon infection, but only significantly in β5i/LMP7$^{-/-}$ animals. While WT mice showed approximately 32.8 % less Ficolin A expression, β5i/LMP7$^{-/-}$ mice expressed approximately 66.9 % less Ficolin A. In contrast, expression of C1q mRNA was significantly upregulated in WT animals compared to uninfected control mice, though it hardly increased in β5i/LMP7$^{-/-}$ mice. At 48h of infection, expression of *crp* was significantly increased in both mouse strains, though less pronounced in β5i/LMP7$^{-/-}$ animals. In β5i/LMP7$^{-/-}$ mice it improved by approximately 1.8-fold, in WT mice by about 5.0-fold.

The diminished expression of various different opsonizing molecules in liver, lung, and macrophages of β5i/LMP7$^{-/-}$ mice upon *S. pneumoniae* infection or co-cultivation suggest a functional important role of immunoproteasomes in the regulation of genes involved in the anti-bacterial innate immune response against *S. pneumoniae*.

3.6.3. Affected opsonin expression is not the consequence of impaired macrophage maturation or cytotoxicity

Macrophages initiate and coordinate the innate immune response by secreting various pro- and anti-inflammatory immune-modulating molecules, including pentraxins, NO, but also cytokines, and chemokines (Marriott & Dockrell 2007).

Since only fully activated macrophages secrete immune modulators, we analyzed the maturation efficiency of stimulated β5i/LMP7$^{-/-}$ BMM by determining their CD86 surface expression, a co-stimulatory molecule and activation marker (Cole et al. 2014). After treatment with several different stimuli and their combination, an enhanced CD86 surface expression was documented, though at equal levels in WT and β5i/LMP7$^{-/-}$ macrophages (Figure 3.18A). Activation is accompanied by cytokine secretion (Cole et al. 2014). We therefore investigated induction of IL-1β gene expression in stimulated β5i/LMP7$^{-/-}$ BMM. Upon co-cultivation with *S. pneumoniae* enhanced IL-1β mRNA levels were detected but without a significant difference between WT and β5i/LMP7$^{-/-}$ macrophages (Figure 3.18B).

These results suggest that β5i/LMP7 deficiency did not influence production of immune-modulating molecules by affecting macrophage activation.

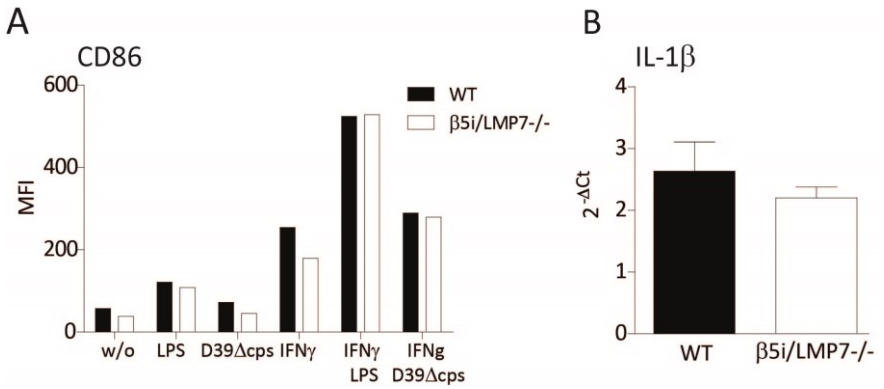

Figure 3.18: Macrophage activation is not affected by β5i/LMP7 deficiency. (A) WT and β5i/LMP7$^{-/-}$ BMM were stimulated either with LPS (1 μg/ml), heat inactivated D39Δcps lysate (1/100) and/or IFNγ 100 U/ml for up to 24h, in order to analysis the surface expression of the activation marker CD86 (illustrated experiment is representative for 3 individual replicates). **(B)** Gene expression analysis of BMM, stimulated for 4h with heat inactivated D39Δcps lysate (1/100), performed by RT and Real Time PCR (each group with n= 4, illustrated experiment is representative for 4 individual replicates; showing mean+- SD; statistical analysis by student's t-test).

Immunoproteasomes are critical for preservation of cell viability by preventing inflammation-induced formation of harmful protein aggregates (Seifert et al. 2010). To confirm that the reduction in expression of opsonins or decline in secretion of NO is not a consequence of cell death, we performed cytotoxicity assays on *S. pneumoniae* co-cultivated WT and β5i/LMP7$^{-/-}$ macrophages, and assessed the grade of liver damage by examining clinical parameters in serum of infected WT and β5i/LMP7$^{-/-}$ mice.

Caspase 3/7 activity, used as indicator for apoptosis, increased by maximal 5-fold in *S. pneumoniae* co-cultivated macrophages. This induction was about 2.5-fold below the caspase activity of MG132 treated cells, which were used as positive control (Figure 3.19A). LDH activity in the supernatant of stimulated WT and β5i/LMP7$^{-/-}$ macrophages, which was used as indicator for necrosis, was only determined in positive control cells, treated with MG132 (Figure 3.19A). No necrotic effect could be detected in *S. pneumoniae* co-cultivated macrophages. Generally, no difference was documented between stimulated WT and β5i/LMP7$^{-/-}$ BMM.

Additionally, serum levels of alanine-aminotransferase (ALAT), used as indicator for liver damage, was not elevated at 48h of infection, neither in WT nor in β5i/LMP7$^{-/-}$ animals (Figure 3.19B). Deficiency in β5i/LMP7 did not provoke excessive inflammation-induced damage of hepatocytes.

Overall, β5i/LMP7 deficiency did not exacerbate inflammation-induced apoptosis or cytotoxicity in macrophages or liver. The diminished expression of opsonizing molecules is not the consequence of cytotoxic effects, but presumably the result of gene dysregulation.

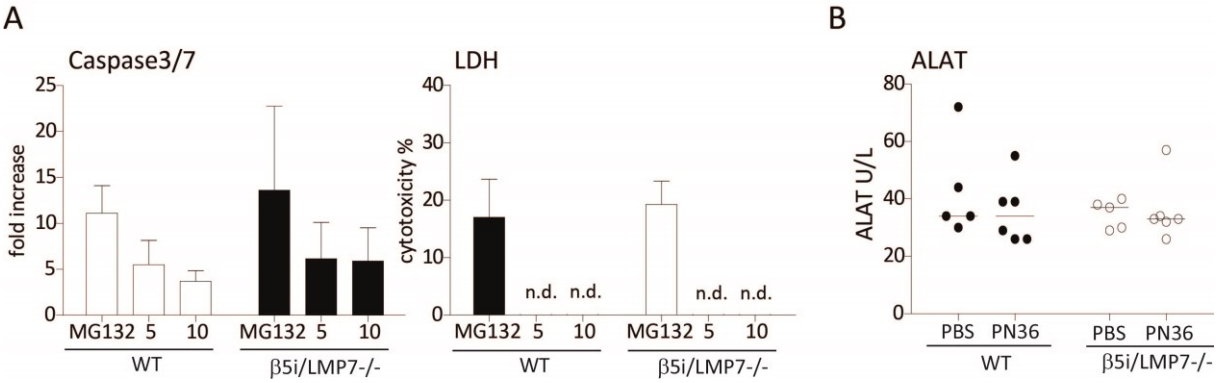

Figure 3.19: β5i/LMP7 deficiency has no apoptotic or cytotoxic effect upon infection. (A) Analysis of the activity of caspase 3/7 in cell lysate and of LDH in supernatant of stimulated BMM. They were co-cultivated with D39Δcps (MOI 10) for 4h, or treated with 10 μM MG132 for 24h, used as positive control (each group with n= 4). **(B)** Documentation of liver damage, 48h post infection, by measuring ALAT activity in serum of mice intranasally infected with $5x10^6$ PN36/mouse. As control, 20 μl PBS/mouse was applied intranasally (each group with n= 5 – 6).

3.7. β5i/LMP7 deficiency influences intracellular signaling in consequence of changes in proteasome composition in macrophages and liver

Assuming that diminished expression of opsonizing molecules in β5i/LMP7$^{-/-}$ liver (Figure 3.17), lung (Figure 3.15), and macrophages (Figure 3.16) upon *S. pneumoniae* infection and co-cultivation, respectively, might be due to altered proteasome function in consequence of changes in proteasome content and composition, we determined proteasome protein expression in different cell-types, without and upon *S. pneumoniae* infection. We also analyzed the impact of β5i/LMP7 deficiency on intracellular signaling transduction pathways resulting in gene transcription of inflammatory mediators. Certainly, due to the absence of the β5i/LMP7 subunit, the composition of proteasomes has been altered. Upon stimulation, these modifications were accompanied by alterations in transcription factor activation.

3.7.1. β5i/LMP7 deficiency alters proteasome subunit composition in liver and in macrophages independent of infection

In liver, CRP, MBL, and Ficolin A are expressed in hepatocytes but C1q is mainly secreted by Kupffer cells (macrophages) (Eisen et al. 2006; He et al. 2007; Mold et al. 2002; Lu et al. 2008). It has been reported that both cell-types constitutively express immuno-subunits (Vasuri et al. 2010). We confirmed this by immuno-blot (Figure 3.20A), showing a positive signal for all three immuno-subunits in WT liver. Also standard β-subunits were expressed, showing a signal for the β1- and β5-protein. Liver of β5i/LMP7$^{-/-}$ mice had no β5i/LMP7 protein and less intensive signals for β1i/LMP2

and β2i/MECL-1. The protein amount of the β1-subunit remained unchanged but the signal for the β5-subunit was enhanced. The overall amount of proteasome did not change due to β5i/LMP7 deficiency, indicated by equal levels of α4 protein in WT and β5i/LMP7$^{-/-}$ mice. Upon infection subunit composition did not change, neither in WT nor in β5i/LMP7$^{-/-}$ liver, indicated by unaltered signals for all analyzed β-subunits.

In lungs, SP-A and SP-D are expressed in alveolar epithelial cells (Bals & Hiemstra 2004), and PTX-3 as well as C1q expression is mostly regulated in macrophages (He et al. 2007; Lu et al. 2008). In order to assess β5i/LMP7 protein expression in distinct lung cell populations we scrutinized β5i/LMP7 protein expression in uninfected WT lung tissues but also upon *S. pneumoniae* infection using immune precipitation (Figure 3.20B). Infiltrating lymphocytes and granulocytes, but also residual macrophages exposed a positive signal for the β5i/LMP7 protein with and without infection. However, no β5i/LMP7 protein was detected in alveolar epithelial or endothelial cells. Expression of the β5i/LMP7 protein in these cells was not induced upon *S. pneumoniae* infection.

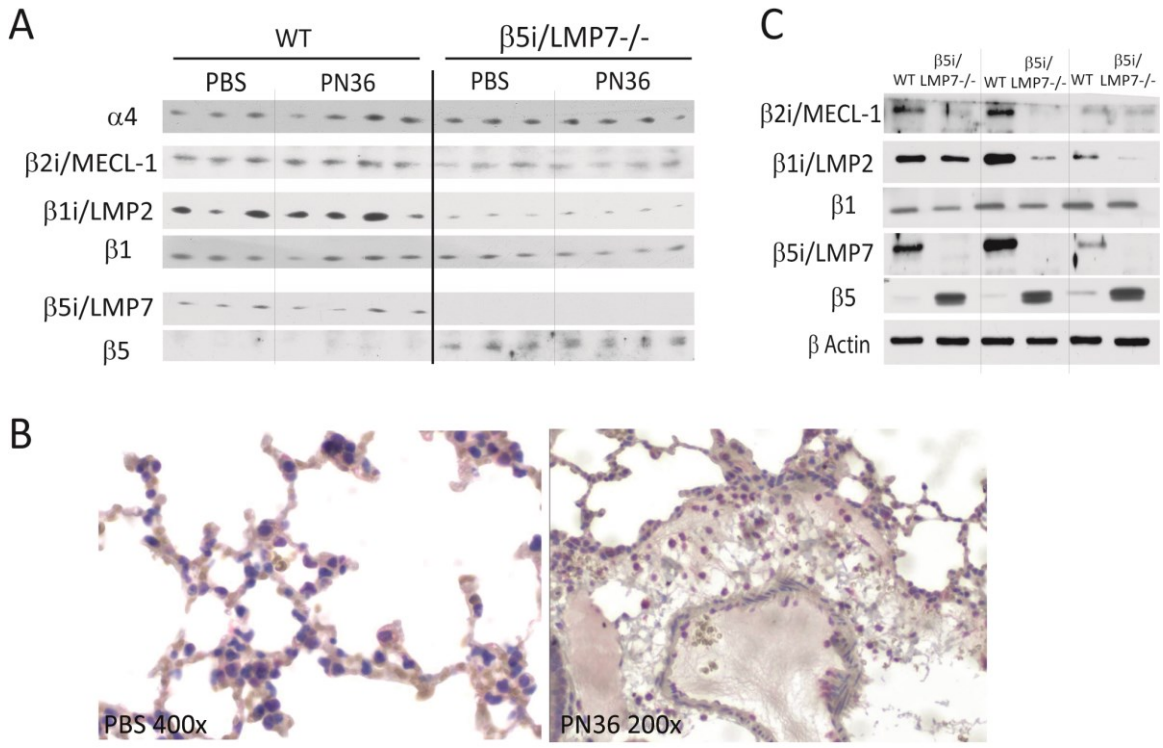

Figure 3.20: Immuno- and standard subunits are constitutively expressed in leukocytes and liver cells. (A) Analysis of expression of proteasome catalytic β-subunits on protein level in liver lysate, 48h after intranasal application of 5x10^6 PN36/mouse, performed by immuno-blot. **(B)** Visualization of β5i/LMP7 expression in inflamed lungs by immune precipitation. Lungs were analyzed 24h after intranasal application of 5x10^6 PN36/mouse. As control, 20 µl PBS/mouse was intranasally applied to WT C57BL/6J mice (each group with n= 4, showing representative pictures). **(C)** Analysis of expression of proteasome catalytic β-subunits on protein level in BMM lysate performed by immuno-blot (each group with n= 3).

Likewise alveolar macrophages, BMM constitutively express immuno-subunits (Figure 3.20C). Macrophages deficient in β5i/LMP7 did not only lack β5i/LMP7 protein but also showed reduced amounts of β1i/LMP2 and β2i/MECL-1. The overall amount of proteasomes did not change, indicated by equal amounts of α4 protein in WT and β5i/LMP7$^{-/-}$ macrophages.
These results suggest that in cells constitutively expressing β5i/LMP7 such as macrophages or hepatocytes the absence of β5i/LMP7 is associated with diminished expression of immune modulators.

Hypothesizing that the absence of β5i/LMP7 alters proteasome function in consequence of changes in proteasome composition, we determined the impact of β5i/LMP7 deficiency on proteasome composition by 2D gel electrophoresis of purified β5i/LMP7$^{-/-}$ and WT BMM 20S proteasomes.

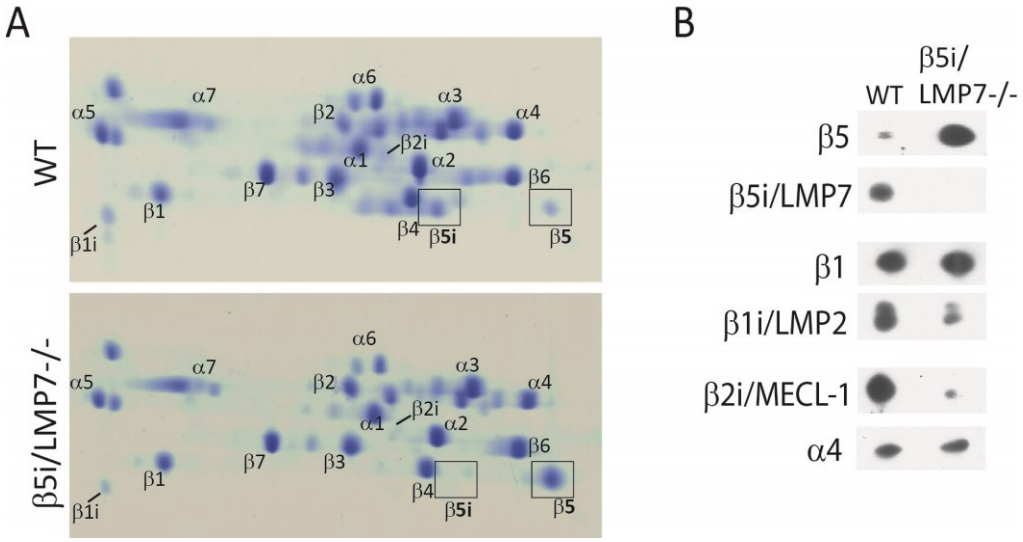

Figure 3.21: WT macrophages assemble immuno and standard β-subunits and β5i/LMP7$^{-/-}$ macrophages standard β-subunits. (A) 2D gel electrophoresis of purified 20S proteasomes, isolated from WT and β5i/LMP7$^{-/-}$ BMM. Proteasome subunits were visualized by coomassie staining. **(B)** Determination of β-subunits, incorporated in BMM 20S, detected by immuno-blot.

WT macrophages assembled immuno- and standard subunits, whereas β5i/LMP7$^{-/-}$ macrophages mainly exhibited standard proteasomes (Figure 3.21A). Densitometrical analysis of β5 and β5i/LMP7 spots proved that macrophages expressed approximately 40 % β5 and approximately 60 % β5i/LMP7. In β5i/LMP7$^{-/-}$ 20S proteasomes, the disappearance of the β5i/LMP7 protein was accompanied by an increased incorporation of the standard β5-subunit. The absence of β5i/LMP7 had a negative influence on the protein amount of β1i/LMP2 and β2i/MECL-1 that was markedly less incorporated in 20S proteasomes (Figure 3.20B).

These results indicate that β5i/LMP7 deficiency alters proteasome subunit composition independent of stimulation.

3.7.2. Deficiency in β5i/LMP7 is accompanied by a modified intracellular signaling in stimulated macrophages

Recognition of pathogens by TLRs initiates induction of several intracellular signaling cascades resulting in transcription factor activation including NFκB and AP-1. Activation of these nuclear factors is crucial for the transcriptional regulation of various different inflammatory mediators (Newton & Dixit 2012). Assuming that altered proteasome composition or proteasome inhibition might have an influence on proteasome function for modulating intracellular signaling cascades and thereby influences gene transcription, we assessed the pathogen induced activation of AP-1 and NFκB in β5i/LMP7$^{-/-}$ or epoxomicin pretreated macrophages.

Pathogen recognition results in NFκB activation via IκBα degradation by the proteasome (Cuschieri et al. 2004). In order to investigate the impact of β5i/LMP7 deficiency on proteasomal IκBα degradation following LPS stimulation or D39Δcps co-cultivation, we performed immuno-blot analyses on *in vitro* stimulated BMM (Figure 3.22A/B). At 30min of stimulation and co-cultivation, respectively, the IκBα protein disappeared in both, WT and β5i/LMP7$^{-/-}$ macrophages. There was no impaired IκBα degradation, and presumably no weakened NFκB activation, following pathogen stimulation due to β5i/LMP7 deficiency.

Unlike NFκB, AP-1 activation and nuclear translocation is not the consequence of the degradation of an inhibitor protein but the result of phosphorylation of its components, mediated by MAPKs (Newton & Dixit 2012; Cuschieri et al. 2004). In order to study the influence of β5i/LMP7 deficiency on AP-1 activation we detected its components, cJun, cFos, and ATF-2, together with their phosphorylated forms in LPS stimulated or D39Δcps co-cultivated BMM by immuno-blot (Figure 3.22A/B). LPS stimulation or *S. pneumoniae* co-cultivation resulted in AP-1 activation indicated by a robust phosphorylation of cJun, cFos, and ATF-2, which was more pronounced in β5i/LMP7$^{-/-}$ compared to WT macrophages. Phosphorylation was already detected after 30min of stimulation for cJun and ATF-2, and after 2h of stimulation for cFos. Protein expression of all three AP-1 components was only minimally up-regulated in WT and β5i/LMP7$^{-/-}$ macrophages upon pathogen recognition. However, β5i/LMP7$^{-/-}$ macrophages expressed higher levels of cJun, cFos, and ATF-2, which exhibited enhanced phosphorylated statuses, even in the absence of stimulation.

Enhanced AP-1 activation following stimulation due to impaired proteasome function was confirmed in macrophages pretreated with the proteasome inhibitor epoxomicin (Figure 3.22C). Depending on its concentration, this inhibitor covalently binds and thereby inhibits certain proteolytically active β-

subunits of the proteasome. In this experiment, epoxomicin mainly inhibited the chymotrypsin-like activity of the protreasome by binding at β5, β5i/LMP7, and β1i/LMP2, but not at β1 and β2i/MECL-1, indicated by a molecular shift in immuno-blot (Figure 3.22D).

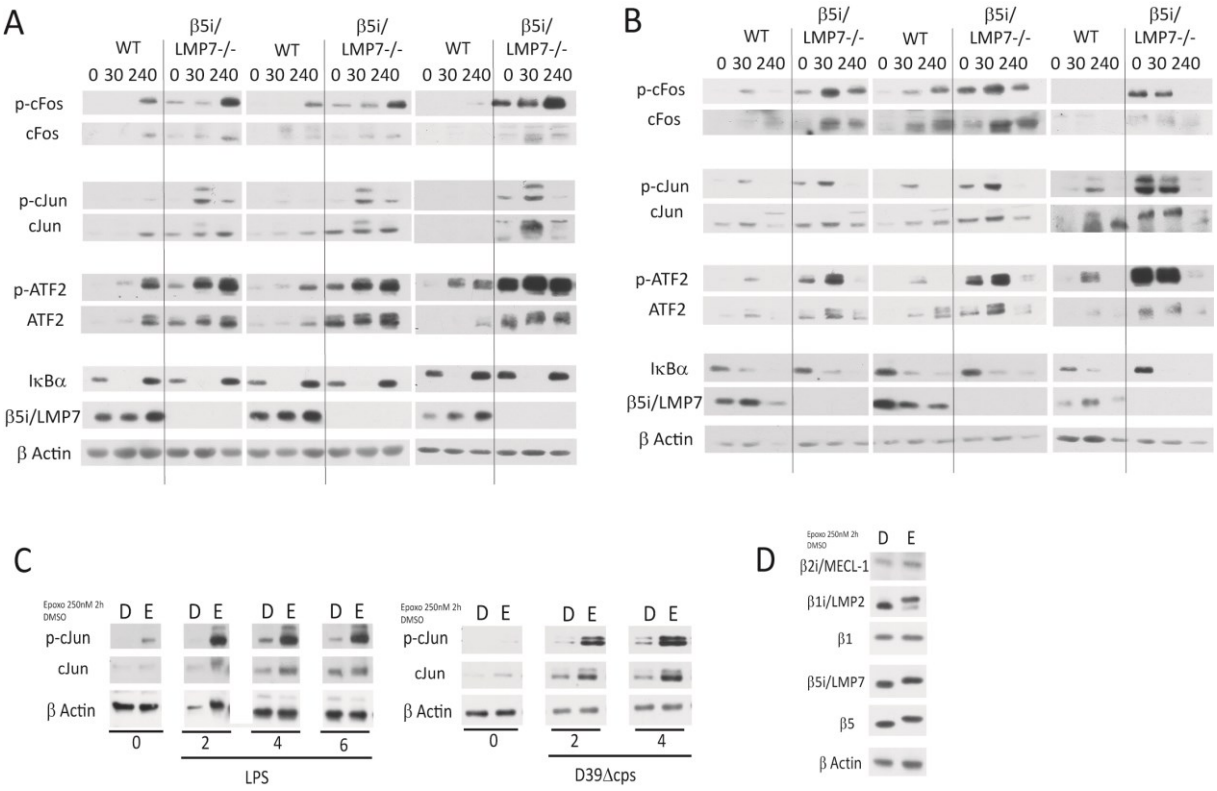

Figure 3.22: β5i/LMP7 deficiency as well as proteasome inhibition enhances AP-1 activation in stimulated macrophages. (A-B) Immuno-blot on phosphorylated and non-phosphorylated members of AP-1 and the NFκB activating pathway in WT and β5i/LMP7$^{-/-}$ BMM, stimulated *in vitro* for 0h, 30min, and 240min with **(A)** LPS (1 μg/ml) or **(B)** D39Δcps (MOI 10) (each group with n= 3). **(C)** Immuno-blot on phosphorylated and non-phosphorylated cJun in RAW264.7 cells, pretreated with DMSO or epoxomicin (250 nM) for 2h, and subsequently stimulated with LPS (1 μg/ml) or D39Δcps (MOI 10) for 0h, 2h, 4h, and 6h. **(D)** Immuno-blot on catalytic β-subunits of the proteasome in RAW264.7 cells incubated for 2h with DMSO or epoxomicin (250 nM). Molecular shift indicates inhibitor binding.

Macrophages, pretreated with epoxomicin, exhibited an enhanced protein level of cJun exposing a stronger phosphorylation signal without further stimulation. Following LPS stimulation or D39Δcps co-cultivation cJun protein expression and phosphorylation was induced, though, more pronounced in epoxomicin pretreated cells.

These results suggest that changes in proteasome composition or inhibition have a selective effect on transcription factor activation, which presumably influence gene transcription upon *S. pneumoniae* co-cultivation.

4. Discussion

Since there is a strong need to improve the understanding of host defense mechanisms influencing progression of pneumococcal infection we investigated the involvement of the immuno-subunit β5i/LMP7 in antibacterial defense mechanisms of the innate immune system, by using a murine infection model. This *S. pneumoniae* infection model is a model of untreated fatal pneumonia. Macrophages, neutrophils, and lymphocytes failed to clear pneumococci which proliferated and induced bacteremia in addition to the initial pulmonary infection. All mice, developed a sequential pathogenesis with a lethal outcome. Thereby, β5i/LMP7$^{-/-}$ mice developed critical illness resulting in an aggravated systemic inflammatory response with enhanced bacteremia likely due to a diminished expression of opsonizing molecules.

4.1. β5i/LMP7$^{-/-}$ mice suffered from critical illness

The body weight is a common noninvasive diagnostic parameter, employed in animal infection studies, predicting infection, inflammation, and physiological sequelae (Olfert & Godson 2000). Decreased body weight indicates the severity of disease. *S. pneumoniae* infected animals developed a gradual loss in body weight which was significantly stronger in β5i/LMP7$^{-/-}$ compared to WT animals (see figure 3.1A). The decrease in body weight is likely due to changes in behavior and metabolism, because cytokines, released upon infection, affect production of appetence and anorexia (Mizgerd & Skerrett 2008). The loss in body weight was accompanied by a significant drop in body temperature in β5i/LMP7$^{-/-}$ mice but not in WT animals (see figure 3.1A). It is known that animals in a septic state lose their ability to maintain their body temperature. A decrease beyond a certain point has been correlated with a lethal outcome in several infectious diseases (Olfert & Godson 2000). Kerr et al. suggested that a drop in body temperature in mice infected with pneumococci accurately mirrors the health of animals as it preceded with a fundamental pulmonary inflammation. The decrease might be induced by a strong cytokine production, which stimulates prostaglandin release and temperature change (Kerr et al. 2002). A severe state of illness during the late phase of pneumonia was confirmed by a prominent acute phase response which was significantly more pronounced in β5i/LMP7$^{-/-}$ animals (see figure 3.1C). Acute phase proteins are synthesized in hepatocytes after cytokine stimulation in response to infection, inflammation, and trauma (Yamada 1999). The major acute phase protein, synthesized in mice, is serum amyloid A (Olfert & Godson 2000). High levels of SAA accurately correlate with the presence and severity of infection, and thus, are commonly used as diagnostic marker for the extent and outcome of infection (Yamada 1999). These clinical signs suggest a higher morbidity and a more severe course of pneumococcal disease with critical illness in β5i/LMP7$^{-/-}$ mice, especially during the late phase of pneumonia.

Critical illness ensues premature mortality. Although, there was no difference in the overall approximate survival rate between infected WT and β5i/LMP7$^{-/-}$ mice, the latter reached the predetermined human endpoint at earlier time points (see figure 3.1B), indicating a more progressive case of pneumococcal pneumonia with an advanced chronology of microbiological and immunological procedures. Survival studies predict resistance to infection and validate the clinical relevance of medical treatments or genetic deficiencies.

By determining immunological events at certain time points of infection, it was possible to classify the status of disease in WT as well as β5i/LMP7$^{-/-}$ mice. Both, WT as well as β5i/LMP7$^{-/-}$ mice underwent characteristic pathogenesis steps, described by Bergeron at al., who characterized the chronology of events associated with fatal pneumococcal pneumonia by determining and correlating levels of cytokines as well as leukocyte in BAL fluid and blood with the time course and outcome of pneumonia. Thereby they identified the major pathogenesis steps from the initial infection to death. The first steps (0h - 24h) involved a local pulmonary infection, with partial but ineffective bacterial clearance by alveolar macrophages, bacterial growth, and recruitment of neutrophils in blood and lung. The next step (24h - 48h) was described by a transition from pulmonary to systemic infection, with high amounts of leukocytes in lung and blood and bacterial dissemination (Bergeron et al. 1998). During the first steps of infection, WT as well as β5i/LMP7$^{-/-}$ mice developed similar immunological statuses. Amounts of lung and circulating granulocytes increased dramatically while levels of lymphocytes, both B and T cells, declined (see figure 3.3, 3.4, 3.6). Bergeron et al described the last pathogenesis step (> 48h) with a systemic inflammatory response syndrome that led to severe tissue injuries and death. The overall inflammation during the late phase of pneumonia was characterized by immune suppression, defined by decreased levels of circulating leukocytes including neutrophils and lymphocytes (Bergeron et al. 1998). During the late phase of pneumonia, WT mice exhibited a highly activated immune system, while, despite progression of disease, β5i/LMP7$^{-/-}$ mice transited to a state of immune suppression. At 48h of infection, the amount of circulating granulocytes peaked in WT mice and diminished in β5i/LMP7$^{-/-}$ animals (see figure 3.6). This was not a consequence of reduced neutrophil enrolment due to missing chemokines, because CXCL-1 and G-CSF plasma levels, promoting development and recruitment of granulocytes, were at equal levels in both mouse strains (see figure 3.8).

Although, amounts of leukocytes remained unaffected in WT animals they significantly declined in β5i/LMP7$^{-/-}$ mice resulting in a prominent leukopenia (see figure 3.6). This was established by a significant lymphopenia and correlated with the magnitude of illness (see figure 3.7). Immune suppression, signified by lymphopenia, is a common event of a systemic infection leading to critical illness and death (Hotchkiss et al. 2009; Drewry et al. 2014). *S. pneumoniae* is an important cause of sepsis in humans, generally occurring as a form of an advanced stage of pneumonia (Garcia-Vidal et

al. 2010; Chiou & Yu 2006). Sepsis is defined as a systemic inflammatory response syndrome (SIRS) that occurs during severe microbial infection and is diagnosed by clinical parameters such as blood leukocyte counts, body temperature, and release of acute phase proteins (Lever & Mackenzie 2007). It is characterized by a massive activation of the immune system with leukocyte recruitment and activation but also with an excessive production of inflammatory mediators, such as cytokines and ROS. In the acute phase of fatal sepsis, the overwhelming immune reaction transits into a state of immune depression, provoked by an anti-inflammatory response and manifested as lymphopenia, affecting both B cells and T cells (Castellheim et al. 2009; Drewry et al. 2014). There are multiple cellular mechanisms which might trigger immune suppression. One explanation for sepsis-associated immune suppression appears to be apoptosis of cells of the innate and adaptive immune system due to TNFα release or due to direct effects of bacterial toxins or bacteria themselves (Hotchkiss et al. 1999). Depletion of white pulpa and bone marrow also could cause an immune compromised state, resulting in leukopenia.

Although there was no difference in the cellular composition in lung tissue between both mice strains, cytokine levels, recovered from BAL fluid, varied. Reduced TNFα and significantly less IL-1β levels were recovered in BAL fluid of β5i/LMP7$^{-/-}$ mice compared to WT animals (see figure 3.5). Alveolar levels of IL-6 were equally elevated in infected WT and β5i/LMP7$^{-/-}$ mice. Bergeron et al. documented a transient appearance of TNFα and IL-1β in BAL fluid of lethally infected animals which peaked within the first 12h of infection and dropped to basal level during the late phase of pneumonia, whereas IL-6 levels in BAL fluid peaked early after infection and persisted increased. While IL-6 probably reflects the severity of stress rather than severity of infection (Bergeron et al. 1998), the transient appearance and especially the drop in TNFα and IL-1β in BAL fluid of β5i/LMP7$^{-/-}$ animals indicates a progressed step in the pathogenesis of infection and thus a state towards a more profound illness.

Critical illness, coinciding with organ dysfunction and peripheral tissue damage, is defined as severe sepsis (Castellheim et al. 2009). Elevated LDH serum levels, which indicate general cell destruction, is a clinical diagnostic marker, predicting tissue damage (Rotenberg et al. 1988). Only β5i/LMP7$^{-/-}$ animals exhibited significantly enhanced LDH serum levels (see figure 3.7C). This supports the phenotype of β5i/LMP7$^{-/-}$ mice of a more pronounced critical illness during the late phase of pneumonia.

4.2. Neither leukocyte function nor endo-epithelial leakage but diminished opsonin expression coincided with enhanced bacteremia in β5i/LMP7$^{-/-}$ mice

Leukopenia often coincides with bacteremia, which is defined as case of systemic infection with bacteria present in blood (Castellheim et al. 2009). When residual immune cells and infiltrating granulocytes fail to eliminate *S. pneumoniae*, bacteria proliferate, disseminate, and provoke peripheral tissue damage leading to death of the organism. During the late phase of pneumonia, β5i/LMP7$^{-/-}$ mice developed a significantly stronger pneumococcal dissemination compared to WT animals, manifested in an enhanced bacterial burden in blood (see figure 3.9B).

Pneumococcal dissemination is facilitated by serious damage of the alveolar endo-epithelium, provoked by for example TNFα release, granulocyte activity, and pneumococcal virulence factors such as LTA and Ply (Bergeron et al. 1998; Cundell et al. 1995). Leakage of the endo-epithelial barrier leads to vascular permeability that results in pulmonary oedema (Mizgerd & Skerrett 2008). Exudates, consisting of inner cell contents and serum proteins, serve as a source of nutrients, support bacterial growth, and predispose individuals to systemic infection (Bals & Hiemstra 2004). Although, previous data discussed the importance of immunoproteasome formation during inflammation for preservation of cell viability by protecting cells against harmful formation of protein aggregates (Seifert et al. 2010; Opitz et al. 2011) we could not prove aggravated endo-epithelium destruction by reason of β5i/LMP7 deficiency (see figure 3.11, 3.10).

Leukocytes, including macrophages and granulocytes, are central for eradication of *S. pneumoniae*. One of the main characteristics of these cells is their ability to internalize and kill bacteria (Underhill & Ozinsky 2002). However, the intracellular killing properties were not affected in β5i/LMP7$^{-/-}$ leukocytes. Deficiency in β5i/LMP7 did not influence the ability of lung macrophages, granulocytes, and dendritic cells to phagocytose bacteria (see figure 3.12). It neither affected phagolysosomal maturation, nor the intracellular early and late phase killing competence of BMM (see figure 3.13), nor influenced their activation efficiency (see figure 3.18). Interestingly, *S. pneumoniae* stimulated β5i/LMP7$^{-/-}$ macrophages released reduced levels of nitric oxide (NO) (see figure 3.14), which is shown to control pneumococcal viability (Kerr et al. 2004). These results are in accordance with recently published data by Reis et al., who reported diminished NO production in β5i/LMP7$^{-/-}$ macrophages stimulated with LPS (Reis et al. 2011). Although Bergeron et al. documented a sustained release of NO in BAL fluid during the late phase of pneumonia (Bergeron et al. 1998), we were not able to detect NO release in BAL fluid of either WT or β5i/LMP7$^{-/-}$ mice, and thus were not able to demonstrate a link between NO release and bacterial burden. These results suggest an impact of β5i/LMP7 deficiency on the synthesis of NO, which may only have a limited impact on the magnitude of bacterial load in tissue or blood, at least in this infection model.

Despite an efficient leukocyte effector function, bacterial clearance can be affected by impaired bacterial opsonophagocytosis. Opsonization is a crucial step during pathogen elimination that enables bacterial recognition, enhances bacterial internalization, and facilitates bacterial degradation (Ariki et al. 2012; Shishido et al. 2012).

The on-site expression of opsonizing molecules directly facilitates termination of pulmonary bacterial growth in lung tissue. SP-A, SP-D, and C1q as well as PTX-3, whose synthesis increased during *S. pneumoniae* infection, are locally expressed by various different alveolar cell types (Bottazzi et al. 2010; Ariki et al. 2012). Although PTX-3 mRNA expression increased in lungs of both mouse strains, β5i/LMP7$^{-/-}$ mice exhibited significantly less PTX-3 mRNA levels (see figure 3.15). The influence of β5i/LMP7 deficiency on PTX-3 expression was reproduced *ex vivo* with *S. pneumoniae* co-cultivated β5i/LMP7$^{-/-}$ macrophages that exhibited significantly less PTX-3 mRNA compared to WT macrophages upon *S. pneumoniae* co-cultivation (see figure 3.16). Its protective role during lung infections was observed by Moalli et al. who showed that PTX-3$^{-/-}$ mice were highly susceptible towards infection with *Pseudomonas aeruginosa*. They also reported that recombinant PTX-3 facilitated pathogen clearance by promoting an appropriate immune response in the lungs of PTX3$^{-/-}$ mice (Moalli et al. 2011). PTX-3 is produced in lung mainly in macrophages and binds to microbial surface structures and complement components including C1q, MBL, and Ficolin and thereby amplifies the effector functions of the complement system (Inforzato et al. 2013; Doni et al. 2012). The similar expression of surfactant proteins in WT and β5i/LMP7$^{-/-}$ lungs, which are produced by type II alveolar epithelial cells upon cytokine stimulation (Crouch & Wright 2001), may explain the remote effect of β5i/LMP7 deficiency on bacterial replication in lungs (see figure 3.9A). Although, SP-A and SP-D expression increased significantly at the late phase of infection, no difference was detected between WT and β5i/LMP7$^{-/-}$ animals (see figure 3.15). *In vivo* studies revealed that SP-A and SP-D are involved in bacterial clearance by directly interacting with *S. pneumoniae* and stimulating pneumococcal uptake by phagocytes (Crouch & Wright 2001; Hartshorn et al. 1998).

Systemic opsonizing molecules such as the pentraxin CRP and the complement components C1q, MBL, and Ficolin A promote elimination of invading *S. pneumoniae* (Bottazzi et al. 2010; Shishido et al. 2012). In animal models, human CRP protects against a lethal infection with *S. pneumoniae,* and in humans, it contributes to host defense during a bacteremic pneumonia (Suresh et al. 2007). In this mouse model, CRP expression was significantly increased in both, WT and β5i/LMP7$^{-/-}$ animals, though less pronounced in β5i/LMP7$^{-/-}$ mice. CRP binds to phosphorylcholine in pneumococcal cell-wall, C1q, as well as Ficolin, and thereby facilitates complement activation via the classical and lectin pathway (Suresh et al. 2006). It is produced in liver in response to cytokine stimulation, mostly contributed by IL-6, and to a lesser degree by IL-1β (Cha-Molstad et al. 2000). The reduced CRP expression is not in consequence of low cytokine stimulation because IL-6 levels were at equal levels

in WT and β5i/LMP7$^{-/-}$ mice (see figure 3.8). In addition to CRP, liver expression of other opsonizing molecules, initiating complement activation, was diminished due to β5i/LMP7 deficiency. Likewise lung expression, liver expression of C1q was only significantly induced in WT but not in β5i/LMP7$^{-/-}$ animals, MBL mRNA levels significantly declined in both mouse groups, though significantly more prominent in β5i/LMP7$^{-/-}$ mice, and Ficolin A expression was only significantly down regulated in β5i/LMP7$^{-/-}$ animals. C1q, MBL, and Ficolin A either directly opsonize bacteria or promote complement mediated opsonization (Bottazzi et al. 2010). The complement-mediated opsonophagoytosis is critical in competing with *S. pneumoniae*. C1q activates the classical complement pathway upon interaction with immunoglobulin or pentraxin containing immune complexes (Bottazzi et al. 2010). The lectin pathway is initiated by the binding of MBL or Ficolin at carbohydrate structures on the surface of pathogens or bound pentraxins (Bottazzi et al. 2010). Complement activation leads to C3b deposition on the bacterial surface which is further processed to C3b, also acting as opsonin for phagocytosis (Sarma & Ward 2011). The C1q mediated complement activation pathway is supposed to be the dominant complement pathway which is required for an effective innate immune reaction against *S. pneumoniae.* C1q deficiency results in an impaired C3b deposition and increased systemic replication of pneumococci, leading to an enhanced susceptibility to *S. pneumoniae* infection (Brown et al. 2002). However, recently published data also demonstrate the importance of the lectin complement pathway for resistance against *S. pneumoniae.* Ali et al. reported that the complete absence of the lectin cascade, achieved by MASP-2 deficiency, led to a total loss of C3b deposition, Ficolin A deficiency resulted in impaired C3b deposition, and MBL deficiency had no influence on C3b deposition. These results promoted Ficolin A as the key recognition component of the lectin activation pathway, which is essential for an effective host defense against pneumococcal infection (Ali et al. 2012). Nevertheless, it is also reported that patients, homozygotes for an MBL codon variant exhibited reduced MBL serum levels and were highly susceptible to invasive pneumococcal infections (Roy et al. 2002).

Deficiency in β5i/LMP7 did not exacerbate inflammation-induced apoptosis or cytotoxicity in liver or macrophages (see figure 3.19). The diminished expression of opsonizing molecules is not the consequence of cytotoxic effects, but may be the result of affected gene regulation provoked by altered proteasome function in consequence of changes in proteasome composition.

4.3. Altered proteasome composition is accompanied by affected gene transcription of immune modulating molecules in liver and macrophages

Proteasome composition differs among cell types and tissues, adapted to their individual functional needs. For example, spleen mainly contains immunoproteasomes, heart expresses standard proteasomes, and liver assembles intermediate proteasomes (Guillaume et al. 2010; Ebstein et al. 2012; Gohlke et al. 2014). The absence of the β5i/LMP7 subunit has a substantial impact on the assembly and composition of proteasomes in cells constitutively expressing or upregulating immuno-subunits. Changes in the cellular pool of proteasomes lead to altered proteasome activities and/or cleavage preferences that effect cell and tissue function during infection and inflammation (Joeris et al. 2012). The impact of proteasome composition and function on pathogen elimination and inflammation varies between pathological challenges but also inflamed tissue.

For example, by analyzing the importance of immunoproteasome activity for an efficient antiviral immune response in mice, Basler et al. reported that LPS or anti-CD3/CD28 stimulated splenocytes, devoid of immunoproteasome activity, secreted reduced levels of IL-6, TNFα, and IFNγ, but equal amounts of IL-10 (Basler et al. 2011). Kremer et al. described a less pronounced LCMV-induced meningitis in β5i/LMP7$^{-/-}$ mice and suggested that β5i/LMP7$^{-/-}$ microglia cells, which express β5i/LMP7, and not astrocytes, which lack β5i/LMP7, prevent immunopathological damage by exhibiting a lower pro-inflammatory status (Kremer et al. 2010). Infection with *L. monocytogenes* rapidly enhances β5i/LMP7 expression in liver which is essential to exceed the quantity of immunogenic peptides presented on MHC class I molecules. Antigen presentation in infected β5i/LMP7$^{-/-}$ hepatocytes was insufficient resulting in an impaired bacterial clearance due to a weak CTL response in liver (Strehl et al. 2006). Modulation of the proteasome activity, either by β5i/LMP7$^{-/-}$ or proteasome inhibition, attenuated experimental colitis, by limiting the secretion of pro-inflammatory mediators, such as IL-1β, IL-6, TNFα, IFNγ, and IL-17, determined in colon of inflamed animals. By using bone marrow chimeras it was confirmed that β5i/LMP7$^{-/-}$ predominantly affected the induction of the pro-inflammatory program within leukocytes, constitutively expressing β5i/LMP7, but not in intestinal epithelial cells (Schmidt et al. 2010). In the here described *S. pneumoniae* infection model, affected gene transcription of immune modulating molecules coincided with an altered proteasome composition and presumably function in macrophages and liver. A correlation between cell specific expression of immune modulating molecules and β5i/LMP7 expression was documented by scrutinizing β5i/LMP7 protein expression in lung and liver tissue. Alveolar macrophages as well as infiltrating granulocytes exhibited β5i/LMP7 protein in WT mice with and without infection, however, β5i/LMP7 protein was not expressed and neither induced in alveolar epithelial cells upon infection (see figure 3.20). This is in accordance with recently reported data by Keller et al., who detected only very low amounts of immuno-subunits in alveolar epithelial cells, but

highly positive signals for β1i/LMP2 in alveolar macrophages (Keller et al. 2015). Vasuri et al. documented the presence of immuno-subunits, in different cell-types of healthy human liver tissue including hepatocytes and Kupffer cells (Vasuri et al. 2010). Guillaume et al. characterized 20S proteasomes, isolated from human monocytes as well as liver, and found proteasomes comprising 54 % intermediate proteasomes in both isolates. Furthermore, monocytes assembled 15 % standard and 31 % immunoproteasomes, and liver consisted of 31 % standard and 15 % immunoproteasomes (Guillaume et al. 2010). Moreover, Gohlke et al. documented that rat liver exclusively assembled intermediate proteasomes, mainly incorporating both the β1i/LMP2 and β5i/LMP7 immuno-subunit (Gohlke et al. 2014). Intermediate proteasomes assemble in the absence of and remain unchanged following stimulation or inflammation (Guillaume et al. 2010). The same was documented in liver of *S. pneumoniae* challenged mice. Under healthy conditions liver proteasomes incorporated both, standard and immuno-subunits, and were unchanged during pneumococcal pneumonia, in WT but also β5i/LMP7$^{-/-}$ animals (see figure 3.20). The appearance of the β5i/LMP7 protein in macrophages and hepatocytes and its absence in alveolar epithelial cells suggest a link between β5i/LMP7 deficiency and reduced expression of PTX3, C1q, MBL, Ficolin A, and unaffected expression of SP-A and SP-D (Eisen et al. 2006; He et al. 2007; Mold et al. 2002; Lu et al. 2008).

By investigating the composition of purified 20S proteasomes, isolated from β5i/LMP7$^{-/-}$ and WT BMM, it became apparent that WT macrophages assembled immuno- and standard β-subunits, presumably forming immuno- and intermediate proteasomes, while β5i/LMP7$^{-/-}$ macrophages mainly incorporated standard β-subunits, forming standard proteasomes (see figure 3.21). De et al. documented that, in the absence of β5i/LMP7, the constitutive counterpart is incorporated into 20S immunoproteasomes (De et al. 2003). In addition, the remaining immuno-subunits, β1i/LMP2 and β2i/MECL-1, exhibit an affected incorporation due to their cooperative assembly (Griffin et al. 1998; Groettrup et al. 1997).

4.4. Proteasomes fine-tune pathogen mediated cell signaling and gene transcription

Different proteasome sub-types exhibit different enzymatic properties, first reported by Dahlmann et al., who isolated and characterized a pool of rat muscle 20S proteasomes. They reported that different proteasome sub-types differ in their degradation rate and quality of generated products (Dahlmann et al. 2000). Since the crystal structure of the active site of immunoproteasomes differ from that of standard proteasomes (Huber et al. 2012), the presence or absence of a catalytic subunit could structurally change the conformation of the catalytic chamber, altering its specificity for substrates. Therefore, it may be conceivable that different proteasome sub-types influence gene transcription by differential degrading specific proteins of intracellular signaling cascades or by degrading regulatory molecules that either inhibit or activate gene transcription.

It has been reported that proteasomes play a regulatory role in inflammatory-mediated intracellular signaling pathways resulting in NFκB and AP-1 activation and thus modulate gene transcription (Gerber et al. 2004; Cuschieri et al. 2004). Considering iNOS expression NFκB activation has a master regulating role since microbial compounds induce but antioxidants reduce iNOS expression by directly targeting NFκB nuclear translocation (Pautz et al. 2010). In case of CRP expression NFκB functions as a synergistic modulator, via enhancing the inducing effect of other nuclear factors such as C/EBPβ and STAT3, (Cha-Molstad et al. 2000). NFκB activation is mediated by the proteasome through degradation of the inhibitor protein IκBα and the NFκB precursor protein p105 (Visekruna et al. 2006). The role of especially immunoproteasomes, in case of NFκB activation, has been controversially discussed. Following LPS or *S. pneumoniae* stimulation IκBα degradation was not impaired in β5i/LMP7$^{-/-}$ macrophages (see figure 3.22A/B). However, to clarify the impact of β5i/LMP7 deficiency on NFκB activation upon *S. pneumoniae* co-cultivation more sensitive readout systems, such as ELISA against p65 on nuclear extracts, are necessary. The multiplicity of studies discussing the impact of immunoproteasomes on NFκB activation provides evidence for its involvement. T2 cells deficient in β1i/LMP2 and β5i/LMP7 have substantial defects in NFκB activation upon TNFα stimulation compared to the parental T1 cell line. They exhibited reduced nuclear levels of p50 and p52 as well as showed a defective IκBα degradation (Hayashi & Faustman 2000). Schmidt et al., reported that β5i/LMP7$^{-/-}$ mice developed attenuated DSS induced colitis in consequence of reduced NFκB signaling due to a diminished nuclear translocation of p65. This resulted in a limited secretion of pro-inflammatory mediators, such as IL-1β, IL-6, TNFα, IFNγ, and IL-17, determined in colon of inflamed animals (Schmidt et al. 2010). Upon IFNγ stimulation, β5i/LMP7$^{-/-}$ cardiomyocytes and splenocytes had reduced levels of p50, reflecting reduced degradation of the NFκB p105 precursor protein by the proteasome (Opitz et al. 2011). Furthermore, IAV infected β1i/LMP2$^{-/-}$ DCs secreted significantly reduced levels of IFNα, IL-6, IL-1β, and TNFα. This was associated with a delayed and less complete IκBα degradation and impaired NFκB signaling documented in LPS stimulated B cells (Hensley et al. 2010). It is also possible that immunoproteasomes influence the signaling cascade upstream of NFκB activation, like reported by Reis et al. who documented that LPS stimulated β5i/LMP7$^{-/-}$/β2i/MECL-1$^{-/-}$ macrophages generated reduced NO but unaffected TNFα levels in consequence of an impaired TRIF/TRAM signaling (Reis et al. 2011). Although human PBMC pretreated with a β5i/LMP7 specific inhibitor and stimulated either with LPS or anti-CD3/CD28 secreted reduced levels of TNFα, IL-6, IL-23, IFNγ, and IL-2 this experimental setup did not affect NFκB activity in a reporter cell line (Muchamuel et al. 2009). This suggests that β5i/LMP7 also regulates cytokine production via an NFκB–independent pathways

Another possible example for immuoproteasome involvement in signaling transduction is the transcription factor AP-1. In case of iNOS expression it has been reported that enhanced AP-1 DNA binding activity and cJun / cFos mRNA expression inhibited iNOS expression via binding at a silencer domain located in the iNOS promoter region (Pautz et al. 2010). AP-1 is also involved in PTX-3 transcription. Its expression was induced upon cJun binding at an AP-1 binding site in the promoter region of PTX-3, demonstrated in cJun deficient cells upon EGF stimulation (Chang et al. 2015). Additionally, a JNK-specific inhibitor, but not inhibitors against ERKs or p38, blocked PTX-3 expression (Han et al. 2005). Gerber et al. reported that proteasome inhibition induced MAPK activation and cJun-dependent AP-1 activity with subsequent IL-8 induction in monocytes independent of NFκB activation and without additional stimulus (Gerber et al. 2004). Similar results, concerning AP-1 activation could be detected by analyzing β5i/LMP7$^{-/-}$ macrophages. These cells expressed higher levels of cJun, cFos, and ATF-2, which exhibited an enhanced phosphorylated status, even in the absence of stimulation. Furthermore, LPS stimulation or *S. pneumoniae* co-cultivation resulted in an AP-1 activation which was more pronounced in β5i/LMP7$^{-/-}$ cells (see figure 3.22A/B). This effect was confirmed by pretreating macrophages with a proteasome specific inhibitor (see figure 3.22C). Inhibition or alteration of the immunoproteasome may attenuate degradation of cJun and thus prolong its phosphorylated status. It is also possible that AP-1 activation is the consequence of diminished degradation of an up-stream kinase, such as IRAK-1 or MAPKs (JNK, ERK1/2, p38). Because immunoproteasomes have an enhanced ability to degrade oxidized, misfolded, and polyubiquitinated proteins, especially relevant under stress condition such as inflammation (Seifert et al. 2010), it is also possible that AP-1 activation is facilitated by enhanced proteotoxic and oxidative stress due to β5i/LMP7 deficiency. This is in accordance with previous publications. Cuschieri et al. reported a regulatory role of the proteasome in pathogen induced intracellular signaling upstream of AP-1. Proteasome inhibition attenuated IRAK-1 degradation resulting in the maintenance of IRAK-1 phosphorylation and activation. This enhanced IRAK-1 activation was associated with elevated activation of MAPKs (ERK, p38, JNK) which resulted in the activation of AP-1. Thus, LPS stimulated macrophages pretreated with a proteasome inhibitor secreted increased levels of IL-10, unaffected amounts of IL-6, and decreased levels of IL-8 and TNFα. (Cuschieri et al. 2004). Kitamura et al. reported increased phosphorylation of p38 with subsequent IL-6 production upon stimulation, triggered by an accumulation of damaged proteins in cells expressing a non-functional β5i/LMP7 mutant (Kitamura et al. 2011).

Moreover, the activity of transcription factors is influenced by nuclear receptors such as PPARα/γ. They interact with pro-inflammatory transcription factors (like AP-1, NFκB, STAT-1) and thereby modulate their transcriptional activity via a direct protein-protein interaction (Pautz et al. 2010). PPARγ activation represses the induction of iNOS and supports the expression of PTX-3 in

macrophages (Pautz et al. 2010; Majai et al. 2007) and PPARα activation lowers CRP and MBL expression in liver (Blanquart et al. 2003; Rakhshandehroo et al. 2009). Like other transcription factors and nuclear receptors, PPARs are ubiquitinated and rapidly degraded by the proteasome (Genini & Catapano 2006). The involvement of especially immunoproteasomes in regulating PPARα/γ activity has not been elucidated, yet.

TLR triggering, cytokine stimulation, and proteotoxic as well as oxidative stress activates various intracellular signaling pathways that interact and influence each other, finally activating numerous transcription factors. For example, iNOS gene expression is differentially regulated by AP-1, NFκB, Stat1, C/EBP, CREB, GATA, and NF-IL6 (Pautz et al. 2010; Malley et al. 2003). PTX-3 exhibit binding sequences in its promoter region for AP-1, NFκB, SP1, PU-1, and NF-IL6 (He et al. 2007), and CRP displays binding sites for NFκB, C/EBPβ, STAT3, and HNF1α (Cha-Molstad et al. 2000). Pathogen activated signaling pathways are complex and numerous nuclear factors, such as NFκB and AP-1 but also several more, have been demonstrated to play critical roles in the subsequent expression of inflammatory mediators. However, in regard to the complexity of the intracellular signaling, redundancy among signaling cascades, influencing and compensating each other, is likely. This makes it difficult to clarify a selective impact of β5i/LMP7 deficiency on gene regulation.

Conceivably, due to their diverse proteolytic properties different proteasome sub-types presumably influence gene transcription by differentially degrading specific regulatory proteins of endogenous signaling cascades that either inhibit or activate gene transcription. It may be possible that the diversity of proteasome sub-types are important to precisely adjust endogenous cell signaling and activity of transcription factors adapted for cell specific functions.

4.5. Conclusion: β5i/LMP7 deficiency aggravates pneumococcal pneumonia in mice by diminishing expression of opsonizing molecules

The absence of the catalytic immuno-subunit β5i/LMP7 in murine macrophages and liver changed their composition of proteasomes. The altered proteasome constitution, which was not influenced upon pneumococcal infection, modified pathogen induced intracellular signaling pathways resulting in reduced gene transcription of immune modulating molecules, including pentraxins, Ficolin A, and collectins. They either directly opsonize bacteria or promote complement mediated opsonization, facilitating opsophagocytosis of bacteria and their subsequent elimination. The diminished opsonin expression impaired the humoral innate immune response against invading pneumococci resulting in an aggravated systemic dissemination of *S. pneumoniae* in β5i/LMP7$^{-/-}$ mice. The impaired bacterial elimination is accompanied by a more severe case of pneumonia with early mortality in consequence of critical illness during the late phase of disease.

Literature

Aberdein, J.D. et al., 2013. Alveolar macrophages in pulmonary host defence the unrecognized role of apoptosis as a mechanism of intracellular bacterial killing. *Clinical and experimental immunology*, 174(2), pp.193–202.

Agarwal, A.K. et al., 2010. PSMB8 encoding the β5i proteasome subunit is mutated in joint contractures, muscle atrophy, microcytic anemia, and panniculitis-induced lipodystrophy syndrome. *American journal of human genetics*, 87(6), pp.866–72.

Ahl, J. et al., 2013. High incidence of septic shock caused by Streptococcus pneumoniae serotype 3--a retrospective epidemiological study. *BMC infectious diseases*, 13, p.492.

Aki, M. et al., 1994. Interferon-gamma induces different subunit organizations and functional diversity of proteasomes. *Journal of biochemistry*, 115(2), pp.257–69.

Akira, S., Uematsu, S. & Takeuchi, O., 2006. Pathogen recognition and innate immunity. *Cell*, 124(4), pp.783–801.

Ali, F. et al., 2003. Streptococcus pneumoniae-associated human macrophage apoptosis after bacterial internalization via complement and Fcgamma receptors correlates with intracellular bacterial load. *The Journal of infectious diseases*, 188(8), pp.1119–31.

Ali, Y.M. et al., 2012. The lectin pathway of complement activation is a critical component of the innate immune response to pneumococcal infection. *PLoS pathogens*, 8(7), p.e1002793.

Amm, I., Sommer, T. & Wolf, D.H., 2014. Protein quality control and elimination of protein waste: the role of the ubiquitin-proteasome system. *Biochimica et biophysica acta*, 1843(1), pp.182–96.

Anon, 2008. Invasive pneumococcal disease in children 5 years after conjugate vaccine introduction--eight states, 1998-2005. *MMWR. Morbidity and mortality weekly report*, 57(6), pp.144–8.

Ariki, S., Nishitani, C. & Kuroki, Y., 2012. Diverse functions of pulmonary collectins in host defense of the lung. *Journal of biomedicine & biotechnology*, 2012, p.532071.

Arima, K. et al., 2011. Proteasome assembly defect due to a proteasome subunit beta type 8 (PSMB8) mutation causes the autoin fl ammatory disorder, Nakajo-Nishimura syndrome, *Proceedings of the National Academy of Sciences of the United States of America*, 108(36):14914-9.

Arnold, F.W. et al., 2013. Mortality differences among hospitalized patients with community-acquired pneumonia in three world regions: results from the Community-Acquired Pneumonia Organization (CAPO) International Cohort Study. *Respiratory medicine*, 107(7), pp.1101–11.

Bals, R. & Hiemstra, P.S., 2004. Innate immunity in the lung: how epithelial cells fight against respiratory pathogens. *The European respiratory journal*, 23(2), pp.327–33.

Basler, M. et al., 2006. An altered T cell repertoire in MECL-1-deficient mice. *Journal of immunology (Baltimore, Md. : 1950)*, 176(11), pp.6665–72.

Basler, M. et al., 2014. Inhibition of the immunoproteasome ameliorates experimental autoimmune encephalomyelitis. *EMBO molecular medicine*, 6(2), pp.226–38.

Basler, M. et al., 2010. Prevention of experimental colitis by a selective inhibitor of the immunoproteasome. *Journal of immunology (Baltimore, Md. : 1950)*, 185(1), pp.634–41.

Basler, M. et al., 2011. The antiviral immune response in mice devoid of immunoproteasome activity. *Journal of immunology (Baltimore, Md. : 1950)*, 187(11), pp.5548–57.

Basler, M., Kirk, C.J. & Groettrup, M., 2013. The immunoproteasome in antigen processing and other immunological functions. *Current opinion in immunology*, 25(1), pp.74–80.

Baugh, J.M., Viktorova, E.G. & Pilipenko, E. V, 2009. Proteasomes can degrade a significant proportion of cellular proteins independent of ubiquitination. *Journal of molecular biology*, 386(3), pp.814–27.

Bergeron, Y. et al., 1998. Cytokine kinetics and other host factors in response to pneumococcal pulmonary infection in mice. *Infection and immunity*, 66(3), pp.912–22.

Blanquart, C. et al., 2003. Peroxisome proliferator-activated receptors: regulation of transcriptional activities and roles in inflammation. *The Journal of steroid biochemistry and molecular biology*, 85(2-5), pp.267–73.

Bogaert, D., De Groot, R. & Hermans, P.W.M., 2004. Streptococcus pneumoniae colonisation: the key to pneumococcal disease. *The Lancet. Infectious diseases*, 4(3), pp.144–54.

Bottazzi, B. et al., 2010. An integrated view of humoral innate immunity: pentraxins as a paradigm. *Annual review of immunology*, 28, pp.157–83.

Braun, J.S. et al., 1999. Pneumolysin, a protein toxin of Streptococcus pneumoniae, induces nitric oxide production from macrophages. *Infection and immunity*, 67(8), pp.3750–6.

Brown, J.S. et al., 2002. The classical pathway is the dominant complement pathway required for innate immunity to Streptococcus pneumoniae infection in mice. *Proceedings of the National Academy of Sciences of the United States of America*, 99(26), pp.16969–74.

Burgner, D., Rockett, K. & Kwiatkowski, D., 1999. Nitric oxide and infectious diseases. *Archives of disease in childhood*, 81(2), pp.185–8.

Castellheim, A. et al., 2009. Innate immune responses to danger signals in systemic inflammatory response syndrome and sepsis. *Scandinavian journal of immunology*, 69(6), pp.479–91.

Cha-Molstad, H. et al., 2000. The Rel family member P50 mediates cytokine-induced C-reactive protein expression by a novel mechanism. *Journal of immunology (Baltimore, Md. : 1950)*, 165(8), pp.4592–7.

Chang, W.-C. et al., 2015. PTX3 gene activation in EGF-induced head and neck cancer cell metastasis. *Oncotarget*, 6(10), pp.7741–7757.

Chatterjee-Kishore, M. et al., 2000. How Stat1 mediates constitutive gene expression: a complex of unphosphorylated Stat1 and IRF1 supports transcription of the LMP2 gene. *The EMBO journal*, 19(15), pp.4111–22.

Chen, W. et al., 2001. Immunoproteasomes shape immunodominance hierarchies of antiviral CD8(+) T cells at the levels of T cell repertoire and presentation of viral antigens. *The Journal of experimental medicine*, 193(11), pp.1319–26.

Chiou, C.C.C. & Yu, V.L., 2006. Severe pneumococcal pneumonia: new strategies for management. *Current opinion in critical care*, 12(5), pp.470–6.

Chou, B. et al., 2008. Critical contribution of immunoproteasomes in the induction of protective immunity against Trypanosoma cruzi in mice vaccinated with a plasmid encoding a CTL epitope fused to green fluorescence protein. *Microbes and infection / Institut Pasteur*, 10(3), pp.241–50.

Cohen, M.S., 1994. Molecular events in the activation of human neutrophils for microbial killing. *Clinical infectious diseases : an official publication of the Infectious Diseases Society of America*, 18 Suppl 2, pp.S170–9.

Cole, J. et al., 2014. The role of macrophages in the innate immune response to Streptococcus pneumoniae and Staphylococcus aureus: mechanisms and contrasts. *Advances in microbial physiology*, 65, pp.125–202.

Collins, G.A. & Tansey, W.P., 2006. The proteasome: a utility tool for transcription? *Current opinion in genetics & development*, 16(2), pp.197–202.

Crouch, E. & Wright, J.R., 2001. Surfactant proteins a and d and pulmonary host defense. *Annual review of physiology*, 63, pp.521–54.

Cruvinel, W. de M. et al., 2010. Immune system - part I. Fundamentals of innate immunity with emphasis on molecular and cellular mechanisms of inflammatory response. *Revista brasileira de reumatologia*, 50(4), pp.434–61.

Cundell, D., Masure, H.R. & Tuomanen, E.I., 1995. The molecular basis of pneumococcal infection: a hypothesis. *Clinical infectious diseases : an official publication of the Infectious Diseases Society of America*, 21 Suppl 3, pp.S204–11.

Cuschieri, J. et al., 2004. Implications of proteasome inhibition: an enhanced macrophage phenotype. *Cellular immunology*, 227(2), pp.140–7.

Dahlmann, B. et al., 2000. Different proteasome subtypes in a single tissue exhibit different enzymatic properties. *Journal of molecular biology*, 303(5), pp.643–53.

De, M. et al., 2003. Beta 2 subunit propeptides influence cooperative proteasome assembly. *The Journal of biological chemistry*, 278(8), pp.6153–9.

DeMartino, G.N. & Slaughter, C.A., 1999. The proteasome, a novel protease regulated by multiple mechanisms. *The Journal of biological chemistry*, 274(32), pp.22123–6.

Diamond, G., Legarda, D. & Ryan, L.K., 2000. The innate immune response of the respiratory epithelium. *Immunological reviews*, 173, pp.27–38.

Díaz-Hernández, M. et al., 2003. Neuronal induction of the immunoproteasome in Huntington's disease. *The Journal of neuroscience : the official journal of the Society for Neuroscience*, 23(37), pp.11653–61.

Ditzel, L. et al., 1998. Conformational constraints for protein self-cleavage in the proteasome. *Journal of molecular biology*, 279(5), pp.1187–91.

Dockrell, D.H., Whyte, M.K.B. & Mitchell, T.J., 2012. Pneumococcal pneumonia: mechanisms of infection and resolution. *Chest*, 142(2), pp.482–91.

Doni, A. et al., 2012. Interactions of the humoral pattern recognition molecule PTX3 with the complement system. *Immunobiology*, 217(11), pp.1122–8.

Drewry, A.M. et al., 2014. Persistent lymphopenia after diagnosis of sepsis predicts mortality. *Shock (Augusta, Ga.)*, 42(5), pp.383–91.

Ebstein, F. et al., 2012. Emerging roles of immunoproteasomes beyond MHC class I antigen processing. *Cellular and molecular life sciences : CMLS*, 69(15), pp.2543–58.

Eisen, D.P. et al., 2006. Low mannose-binding lectin function is associated with sepsis in adult patients. *FEMS immunology and medical microbiology*, 48(2), pp.274–82.

Fehling, H.J. et al., 1994. MHC class I expression in mice lacking the proteasome subunit LMP-7. *Science (New York, N.Y.)*, 265(5176), pp.1234–7.

Ferrington, D.A. & Gregerson, D.S., 2012. Immunoproteasomes: structure, function, and antigen presentation. *Progress in molecular biology and translational science*, 109, pp.75–112.

Fricke, B. et al., 2007. The proteasome maturation protein POMP facilitates major steps of 20S proteasome formation at the endoplasmic reticulum. *EMBO reports*, 8(12), pp.1170–5.

Gaczynska, M. et al., 1994. Peptidase activities of proteasomes are differentially regulated by the major histocompatibility complex-encoded genes for LMP2 and LMP7. *Proceedings of the National Academy of Sciences of the United States of America*, 91(20), pp.9213–7.

Gadjeva, M., 2014. The complement system. Overview. *Methods in molecular biology (Clifton, N.J.)*, 1100, pp.1–9.

Gallastegui, N. & Groll, M., 2010. The 26S proteasome: assembly and function of a destructive machine. *Trends in biochemical sciences*, 35(11), pp.634–42.

Garcia-Vidal, C. et al., 2010. Pneumococcal pneumonia presenting with septic shock: host- and pathogen-related factors and outcomes. *Thorax*, 65(1), pp.77–81.

Gauthier, J.-F. et al., 2007. Differential contribution of bacterial N-formyl-methionyl-leucyl- phenylalanine and host-derived CXC chemokines to neutrophil infiltration into pulmonary alveoli during murine pneumococcal pneumonia. *Infection and immunity*, 75(11), pp.5361–7.

Genini, D. & Catapano, C. V, 2006. Control of peroxisome proliferator-activated receptor fate by the ubiquitinproteasome system. *Journal of receptor and signal transduction research*, 26(5-6), pp.679–92.

Gerber, A. et al., 2004. Proteasome inhibitors modulate chemokine production in lung epithelial and monocytic cells. *The European respiratory journal*, 24(1), pp.40–8.

Gohlke, S. et al., 2014. Adult human liver contains intermediate-type proteasomes with different enzymatic properties. *Annals of hepatology*, 13(4), pp.429–38.

Griffin, T.A. et al., 1998. Immunoproteasome assembly: cooperative incorporation of interferon gamma (IFN-gamma)-inducible subunits. *The Journal of experimental medicine*, 187(1), pp.97–104.

Groettrup, M. et al., 1997. The subunits MECL-1 and LMP2 are mutually required for incorporation into the 20S proteasome. *Proceedings of the National Academy of Sciences of the United States of America*, 94(17), pp.8970–5.

Groettrup, M., Kirk, C.J. & Basler, M., 2010. Proteasomes in immune cells: more than peptide producers? *Nature reviews. Immunology*, 10(1), pp.73–8.

Groll, M. et al., 1997. Structure of 20S proteasome from yeast at 2.4 A resolution. *Nature*, 386(6624), pp.463–71.

Guillaume, B. et al., 2012. Analysis of the processing of seven human tumor antigens by intermediate proteasomes. *Journal of immunology (Baltimore, Md. : 1950)*, 189(7), pp.3538–47.

Guillaume, B. et al., 2010. Two abundant proteasome subtypes that uniquely process some antigens presented by HLA class I molecules. *Proceedings of the National Academy of Sciences of the United States of America*, 107(43), pp.18599–604.

Hammerschmidt, S. et al., 2005. Illustration of pneumococcal polysaccharide capsule during adherence and invasion of epithelial cells. *Infection and immunity*, 73(8), pp.4653–67.

Han, B. et al., 2005. TNFalpha-induced long pentraxin PTX3 expression in human lung epithelial cells via JNK. *Journal of immunology (Baltimore, Md. : 1950)*, 175(12), pp.8303–11.

Hartshorn, K.L. et al., 1998. Pulmonary surfactant proteins A and D enhance neutrophil uptake of bacteria. *The American journal of physiology*, 274(6 Pt 1), pp.L958–69.

Hayashi, T. & Faustman, D., 2000. Essential role of human leukocyte antigen-encoded proteasome subunits in NF-kappaB activation and prevention of tumor necrosis factor-alpha-induced apoptosis. *The Journal of biological chemistry*, 275(7), pp.5238–47.

He, X., Han, B. & Liu, M., 2007. Long pentraxin 3 in pulmonary infection and acute lung injury. *American journal of physiology. Lung cellular and molecular physiology*, 292(5), pp.L1039–49.

Heink, S. et al., 2005. IFN-gamma-induced immune adaptation of the proteasome system is an accelerated and transient response. *Proceedings of the National Academy of Sciences of the United States of America*, 102(26), pp.9241–6.

Henriques-Normark, B. & Tuomanen, E.I., 2013. The pneumococcus: epidemiology, microbiology, and pathogenesis. *Cold Spring Harbor perspectives in medicine*, 1;3(7). pii: a010215

Hensley, S.E. et al., 2010. Unexpected role for the immunoproteasome subunit LMP2 in antiviral humoral and innate immune responses. *Journal of immunology,* 184:4115-4122

Hershko, A. et al., 1991. Methylated ubiquitin inhibits cyclin degradation in clam embryo extracts. *The Journal of biological chemistry*, 266(25), pp.16376–9.

Hershko, A. & Ciechanover, A., 1998. The ubiquitin system. *Annual review of biochemistry*, 67, pp.425–79.

Hirst, R.A. et al., 2004. The role of pneumolysin in pneumococcal pneumonia and meningitis. *Clinical and experimental immunology*, 138(2), pp.195–201.

Hotchkiss, R.S. et al., 1999. Apoptotic cell death in patients with sepsis, shock, and multiple organ dysfunction. *Critical care medicine*, 27(7), pp.1230–51.

Hotchkiss, R.S. et al., 2009. The sepsis seesaw: tilting toward immunosuppression. *Nature medicine*, 15(5), pp.496–7.

Huber, E.M. et al., 2012. Immuno- and constitutive proteasome crystal structures reveal differences in substrate and inhibitor specificity. *Cell*, 148(4), pp.727–738.

Ichikawa, H.T. et al., 2012. Beneficial effect of novel proteasome inhibitors in murine lupus via dual inhibition of type I interferon and autoantibody-secreting cells. *Arthritis and rheumatism*, 64(2), pp.493–503.

Inforzato, A. et al., 2013. PTX3 as a paradigm for the interaction of pentraxins with the complement system. *Seminars in immunology*, 25(1), pp.79–85.

Joeris, T. et al., 2012. The proteasome system in infection: impact of β5 and LMP7 on composition, maturation and quantity of active proteasome complexes. *PloS one*, 7(6), p.e39827.

Jounblat, R. et al., 2005. The role of surfactant protein D in the colonisation of the respiratory tract and onset of bacteraemia during pneumococcal pneumonia. *Respiratory research*, 6, p.126.

Kadioglu, A. et al., 2000. Host cellular immune response to pneumococcal lung infection in mice. *Infection and immunity*, 68(2), pp.492–501.

Kadioglu, A. et al., 2008. The role of Streptococcus pneumoniae virulence factors in host respiratory colonization and disease. *Nature reviews. Microbiology*, 6(4), pp.288–301.

Kadioglu, A. & Andrew, P.W., 2004. The innate immune response to pneumococcal lung infection: the untold story. *Trends in immunology*, 25(3), pp.143–9.

Van Kaer, L. et al., 1994. Altered peptidase and viral-specific T cell response in LMP2 mutant mice. *Immunity*, 1(7), pp.533–41.

Kaiser, P. & Huang, L., 2005. Global approaches to understanding ubiquitination. *Genome biology*, 6(10), p.233.

Kalim, K.W. et al., 2012. Immunoproteasome subunit LMP7 deficiency and inhibition suppresses Th1 and Th17 but enhances regulatory T cell differentiation. *Journal of immunology (Baltimore, Md. : 1950)*, 189(8), pp.4182–93.

Keller, I.E. et al., 2015. Regulation of immunoproteasome function in the lung. *Scientific reports*, 5, p.10230.

Kerr, A.R. et al., 2004. Nitric oxide exerts distinct effects in local and systemic infections with Streptococcus pneumoniae. *Microbial pathogenesis*, 36(6), pp.303–10.

Kerr, A.R. et al., 2002. Role of inflammatory mediators in resistance and susceptibility to pneumococcal infection. *Infection and immunity*, 70(3), pp.1547–57.

Khan, S. et al., 2001. Immunoproteasomes largely replace constitutive proteasomes during an antiviral and antibacterial immune response in the liver. *Journal of immunology (Baltimore, Md. : 1950)*, 167(12), pp.6859–68.

Kisselev, A.F. & Groettrup, M., 2014. Subunit specific inhibitors of proteasomes and their potential for immunomodulation. *Current opinion in chemical biology*, 23, pp.16–22.

Kitamura, A. et al., 2011. A mutation in the immunoproteasome subunit PSMB8 causes autoinflammation and lipodystrophy in humans. *The Journal of clinical investigation*, 121(10), pp.4150–60.

Klare, N. et al., 2007. Intermediate-type 20 S proteasomes in HeLa cells: “asymmetric” subunit composition, diversity and adaptation. *Journal of molecular biology*, 373(1), pp.1–10.

Knapp, S. et al., 2004. Toll-like receptor 2 plays a role in the early inflammatory response to murine pneumococcal pneumonia but does not contribute to antibacterial defense. *Journal of immunology (Baltimore, Md. : 1950)*, 172(5), pp.3132–8.

Komander, D., 2009. The emerging complexity of protein ubiquitination. *Biochemical Society transactions*, 37(Pt 5), pp.937–53.

Koppe, U., Suttorp, N. & Opitz, B., 2012. Recognition of Streptococcus pneumoniae by the innate immune system. *Cellular microbiology*, 14(4), pp.460–6.

Kremer, M. et al., 2010. Reduced immunoproteasome formation and accumulation of immunoproteasomal precursors in the brains of lymphocytic choriomeningitis virus-infected mice. *Journal of immunology (Baltimore, Md. : 1950)*, 185(9), pp.5549–60.

Krüger, E., Kloetzel, P.M. & Enenkel, C., 2001. 20S proteasome biogenesis. *Biochimie*, 83(3-4), pp.289–93.

Kuronuma, K. et al., 2004. Pulmonary surfactant protein A augments the phagocytosis of Streptococcus pneumoniae by alveolar macrophages through a casein kinase 2-dependent increase of cell surface localization of scavenger receptor A. *The Journal of biological chemistry*, 279(20), pp.21421–30.

Lander, G.C. et al., 2012. Complete subunit architecture of the proteasome regulatory particle. *Nature*, 482(7384), pp.186–91.

Lever, A. & Mackenzie, I., 2007. Sepsis: definition, epidemiology, and diagnosis. *BMJ (Clinical research ed.)*, 335(7625), pp.879–83.

Liu, Y. et al., 2012. Mutations in proteasome subunit β type 8 cause chronic atypical neutrophilic dermatosis with lipodystrophy and elevated temperature with evidence of genetic and phenotypic heterogeneity. *Arthritis and rheumatism*, 64(3), pp.895–907.

Lu, J.H. et al., 2008. The classical and regulatory functions of C1q in immunity and autoimmunity. *Cellular & molecular immunology*, 5(1), pp.9–21.

Lu, Y. et al., 2015. Substrate degradation by the proteasome: A single-molecule kinetic analysis. *Science*, 348(6231), pp.1250834–1250834.

Lv, Y. et al., 2011. LMP2/LMP7 gene variant: a risk factor for intestinal Mycobacterium tuberculosis infection in the Chinese population. *Journal of gastroenterology and hepatology*, 26(7), pp.1145–50.

Lynch, J.P. & Zhanel, G.G., 2009. Streptococcus pneumoniae: epidemiology, risk factors, and strategies for prevention. *Seminars in respiratory and critical care medicine*, 30(2), pp.189–209.

MacMicking, J.D. et al., 1995. Altered responses to bacterial infection and endotoxic shock in mice lacking inducible nitric oxide synthase. *Cell*, 81(4), pp.641–50.

Majai, G. et al., 2007. PPARgamma-dependent regulation of human macrophages in phagocytosis of apoptotic cells. *European journal of immunology*, 37(5), pp.1343–54.

Małek, R. et al. 2007, Role of nuclear factor kappaB in the central nervous system. *Pharmacological reports: PR*, 59(1), pp.25–33.

Malley, R. et al., 2003. Recognition of pneumolysin by Toll-like receptor 4 confers resistance to pneumococcal infection. *Proceedings of the National Academy of Sciences of the United States of America*, 100(4), pp.1966–71.

Mantovani, A. et al., 2008. Pentraxins in innate immunity: from C-reactive protein to the long pentraxin PTX3. *Journal of clinical immunology*, 28(1), pp.1–13.

Markwart, R. et al., 2014. Immunosuppression after sepsis: systemic inflammation and sepsis induce a loss of naïve T-cells but no enduring cell-autonomous defects in T-cell function. *PloS one*, 9(12), p.e115094.

Marriott, H.M. & Dockrell, D.H., 2007. The role of the macrophage in lung disease mediated by bacteria. *Experimental lung research*, 33(10), pp.493–505.

McDermott, A. et al., 2015. Proteasome-associated autoinflammatory syndromes: advances in pathogeneses, clinical presentations, diagnosis, and management. *International journal of dermatology*, 54(2), pp.121–9.

Miller, Z. et al., 2013. Inhibitors of the immunoproteasome: current status and future directions. *Current pharmaceutical design*, 19(22), pp.4140–51.

Mishto, M. et al., 2006. Immunoproteasome and LMP2 polymorphism in aged and Alzheimer's disease brains. *Neurobiology of aging*, 27(1), pp.54–66.

Mishto, M. et al., 2010. Immunoproteasome LMP2 60HH variant alters MBP epitope generation and reduces the risk to develop multiple sclerosis in Italian female population. *PloS one*, 5(2), p.e9287.

Mishto, M. et al., 2014. Proteasome isoforms exhibit only quantitative differences in cleavage and epitope generation. *European Journal of Immunology*, 44(12), pp.3508–3521.

Mitchell, A.M. & Mitchell, T.J., 2010. Streptococcus pneumoniae: virulence factors and variation. *Clinical microbiology and infection : the official publication of the European Society of Clinical Microbiology and Infectious Diseases*, 16(5), pp.411–8.

Mizgerd, J.P. & Skerrett, S.J., 2008. Animal models of human pneumonia. *American journal of physiology. Lung cellular and molecular physiology*, 294(3), pp.L387–98.

Moalli, F. et al., 2011. The therapeutic potential of the humoral pattern recognition molecule PTX3 in chronic lung infection caused by Pseudomonas aeruginosa. *Journal of immunology (Baltimore, Md. : 1950)*, 186(9), pp.5425–34.

Moebius, J. et al., 2010. Immunoproteasomes are essential for survival and expansion of T cells in virus-infected mice. *European journal of immunology*, 40(12), pp.3439–3449.

Mold, C., Rodic-Polic, B. & Du Clos, T.W., 2002. Protection from Streptococcus pneumoniae infection by C-reactive protein and natural antibody requires complement but not Fc gamma receptors. *Journal of immunology (Baltimore, Md. : 1950)*, 168(12), pp.6375–81.

Muchamuel, T. et al., 2009. A selective inhibitor of the immunoproteasome subunit LMP7 blocks cytokine production and attenuates progression of experimental arthritis. *Nature medicine*, 15(7), pp.781–7.

Müller-Redetzky, H.C., Suttorp, N. & Witzenrath, M., 2014. Dynamics of pulmonary endothelial barrier function in acute inflammation: mechanisms and therapeutic perspectives. *Cell and tissue research*, 355(3), pp.657–73.

Newton, K. & Dixit, V.M., 2012. Signaling in innate immunity and inflammation. *Cold Spring Harbor perspectives in biology*, 4(3), pii:a006049

Nüsse, O., 2011. Biochemistry of the phagosome: the challenge to study a transient organelle. *The Scientific World Journal*, 11, pp.2364–81.

Ogunniyi, A.D., Giammarinaro, P. & Paton, J.C., 2002. The genes encoding virulence-associated proteins and the capsule of Streptococcus pneumoniae are upregulated and differentially expressed in vivo. *Microbiology (Reading, England)*, 148(Pt 7), pp.2045–53.

Olfert, E.D. & Godson, D.L., 2000. Humane endpoints for infectious disease animal models. *ILAR journal / National Research Council, Institute of Laboratory Animal Resources*, 41(2), pp.99–104.

Opitz, B. et al., 2010. Innate immune recognition in infectious and noninfectious diseases of the lung. *American journal of respiratory and critical care medicine*, 181(12), pp.1294–309.

Opitz, E. et al., 2011. Impairment of immunoproteasome function by β5i/lmp7 subunit deficiency results in severe enterovirus myocarditis. *PLoS Pathogens*, 7(9), p.e1002233.

Orlowski, M. & Wilk, S., 2000. Catalytic activities of the 20 S proteasome, a multicatalytic proteinase complex. *Archives of biochemistry and biophysics*, 383(1), pp.1–16.

Pautz, A. et al., 2010. Regulation of the expression of inducible nitric oxide synthase. *Nitric oxide : biology and chemistry / official journal of the Nitric Oxide Society*, 23(2), pp.75–93.

Pfaller, M.A. et al., 2012. AWARE Ceftaroline Surveillance Program (2008-2010): trends in resistance patterns among Streptococcus pneumoniae, Haemophilus influenzae, and Moraxella catarrhalis in the United States. *Clinical infectious diseases : an official publication of the Infectious Diseases Society of America*, 55 Suppl 3, pp.S187–93.

Pickart, C.M. & Eddins, M.J., 2004. Ubiquitin: structures, functions, mechanisms. *Biochimica et biophysica acta*, 1695(1-3), pp.55–72.

Van der Poll, T. & Opal, S.M., 2009. Pathogenesis, treatment, and prevention of pneumococcal pneumonia. *Lancet*, 374(9700), pp.1543–56.

Puttaparthi, K., Van Kaer, L. & Elliott, J.L., 2007. Assessing the role of immuno-proteasomes in a mouse model of familial ALS. *Experimental neurology*, 206(1), pp.53–8.

Qureshi, N., Morrison, D.C. & Reis, J., 2012. Proteasome protease mediated regulation of cytokine induction and inflammation. *Biochimica et biophysica acta*, 1823(11), pp.2087–93.

Rakhshandehroo, M. et al., 2009. Comparative analysis of gene regulation by the transcription factor PPARalpha between mouse and human. *PloS one*, 4(8), p.e6796.

Reis, J. et al., 2011. The immunoproteasomes regulate LPS-induced TRIF/TRAM signaling pathway in murine macrophages. *Cell biochemistry and biophysics*, 60(1-2), pp.119–26.

Remington, L.T. & Sligl, W.I., 2014. Community-acquired pneumonia. *Current opinion in pulmonary medicine*, 20(3), pp.215–24.

Robek, M.D. et al., 2007. Role of immunoproteasome catalytic subunits in the immune response to hepatitis B virus. *Journal of virology*, 81(2), pp.483–91.

Rock, K.L. et al., 1994. Inhibitors of the proteasome block the degradation of most cell proteins and the generation of peptides presented on MHC class I molecules. *Cell*, 78(5), pp.761–71.

Rotenberg, Z. et al., 1988. Significance of isolated increases in total lactate dehydrogenase and its isoenzymes in serum of patients with bacterial pneumonia. *Clinical chemistry*, 34(7), pp.1503–5.

Roy, S. et al., 2002. MBL genotype and risk of invasive pneumococcal disease: a case-control study. *Lancet*, 359(9317), pp.1569–73.

Sahara, K. et al., 2014. The mechanism for molecular assembly of the proteasome. *Advances in biological regulation*, 54, pp.51–8.

Said, M.A. et al., 2013. Estimating the burden of pneumococcal pneumonia among adults: a systematic review and meta-analysis of diagnostic techniques. *PloS one*, 8(4), p.e60273.

Sarma, J.V. & Ward, P.A., 2011. The complement system. *Cell and tissue research*, 343(1), pp.227–35.

Schmidt, F. et al., 2006. Comprehensive quantitative proteome analysis of 20S proteasome subtypes from rat liver by isotope coded affinity tag and 2-D gel-based approaches. *Proteomics*, 6(16), pp.4622–32.

Schmidt, N. et al., 2010. Targeting the proteasome: partial inhibition of the proteasome by bortezomib or deletion of the immunosubunit LMP7 attenuates experimental colitis. *Gut*, 59(7), pp.896–906.

Seifert, U. et al., 2010. Immunoproteasomes preserve protein homeostasis upon interferon-induced oxidative stress. *Cell*, 142(4), pp.613–24.

Shishido, S.N. et al., 2012. Humoral innate immune response and disease. *Clinical immunology (Orlando, Fla.)*, 144(2), pp.142–58.

Sibille, C. et al., 1995. LMP2+ proteasomes are required for the presentation of specific antigens to cytotoxic T lymphocytes. *Current biology : CB*, 5(8), pp.923–30.

Sijts, A. et al., 2002. The role of the proteasome activator PA28 in MHC class I antigen processing. *Molecular immunology*, 39(3-4), pp.165–9.

Steel, H.C. et al., 2013. Overview of community-acquired pneumonia and the role of inflammatory mechanisms in the immunopathogenesis of severe pneumococcal disease. *Mediators of inflammation*, 2013, p.490346.

Strehl, B. et al., 2006. Immunoproteasomes are essential for clearance of Listeria monocytogenes in nonlymphoid tissues but not for induction of bacteria-specific CD8+ T cells. *Journal of immunology (Baltimore, Md. : 1950)*, 177(9), pp.6238–44.

Suresh, M. V et al., 2007. Human C-reactive protein protects mice from Streptococcus pneumoniae infection without binding to pneumococcal C-polysaccharide. *Journal of immunology (Baltimore, Md. : 1950)*, 178(2), pp.1158–63.

Suresh, M. V et al., 2006. Role of the property of C-reactive protein to activate the classical pathway of complement in protecting mice from pneumococcal infection. *Journal of immunology (Baltimore, Md. : 1950)*, 176(7), pp.4369–74.

Tanahashi, N. et al., 1997. Molecular properties of the proteasome activator PA28 family proteins and gamma-interferon regulation. *Genes to cells : devoted to molecular & cellular mechanisms*, 2(3), pp.195–211.

Tanaka, K., Mizushima, T. & Saeki, Y., 2012. The proteasome: molecular machinery and pathophysiological roles. *Biological chemistry*, 393(4), pp.217–34.

Tettelin, H. et al., 2001. Complete genome sequence of a virulent isolate of Streptococcus pneumoniae. *Science (New York, N.Y.)*, 293(5529), pp.498–506.

Torres, A. et al., 2013. Risk factors for community-acquired pneumonia in adults in Europe: a literature review. *Thorax*, 68(11), pp.1057–65.

Tu, L. et al., 2009. Critical role for the immunoproteasome subunit LMP7 in the resistance of mice to Toxoplasma gondii infection. *European journal of immunology*, 39(12), pp.3385–94.

Underhill, D.M. & Ozinsky, A., 2002. Phagocytosis of microbes: complexity in action. *Annual review of immunology*, 20, pp.825–52.

Unno, M. et al., 2002. The structure of the mammalian 20S proteasome at 2.75 A resolution. *Structure (London, England : 1993)*, 10(5), pp.609–18.

Vasuri, F. et al., 2010. Studies on immunoproteasome in human liver. Part I: absence in fetuses, presence in normal subjects, and increased levels in chronic active hepatitis and cirrhosis. *Biochemical and biophysical research communications*, 397(2), pp.301–6.

Visekruna, A. et al., 2006. Proteasome-mediated degradation of IkappaBalpha and processing of p105 in Crohn disease and ulcerative colitis. *The Journal of clinical investigation*, 116(12), pp.3195–203.

Voges, D., Zwickl, P. & Baumeister, W., 1999. The 26S proteasome: a molecular machine designed for controlled proteolysis. *Annual review of biochemistry*, 68, pp.1015–68.

Watson, D.A. et al., 1993. A brief history of the pneumococcus in biomedical research: a panoply of scientific discovery. *Clinical infectious diseases : an official publication of the Infectious Diseases Society of America*, 17(5), pp.913–24.

WHO, W.H. statistical report, 2014. *WHO_HIS_HSI_14.1_eng.pdf*, Available at: http://apps.who.int/iris/bitstream/10665/112739/1/WHO_HIS_HSI_14.1_eng.pdf?ua=1&ua=1#page=10&zoom=90,-336,319 [Accessed February 16, 2015].

Yamada, T., 1999. Serum amyloid A (SAA): a concise review of biology, assay methods and clinical usefulness. *Clinical chemistry and laboratory medicine : CCLM / FESCC*, 37(4), pp.381–8.

Zaiss, D.M.W., de Graaf, N. & Sijts, A.J.A.M., 2008. The proteasome immunosubunit multicatalytic endopeptidase complex-like 1 is a T-cell-intrinsic factor influencing homeostatic expansion. *Infection and immunity*, 76(3), pp.1207–13.

Abbreviations

(v/v)	Ratio volume to volume
(w/v)	Ratio weight to volumne
19S	26 Svedberg
26S	19 Svedberg
a1-7	Proteasomal a subunit 1 to 7
AIM2	Part of inflammasome, absent in melanoma 2
ALAT	Alanine transaminase
AMC	7-amino-4-methylcoumarin
AP-1	Activator protein 1
APC	Antigen presenting cell
APS	Ammonium peroxodisulfat
ATF2	Activating transcription factor 2
ATP	Adenosine triphosphate
b1-7	Proteasome b subunit 1 to 7
BAL	Bronchial alveolar lavage
BCA	Bicinchoninic acid protein assay
bi-subunit	Immuno-subunit
BMM	Bone marrow derived macrophages
bp	Base pair
BSA	Bovine serum albumine
C3b	Opsonizing complement factor
CANDLE	Chronic atrophical neutrophilic dermatosis with lipodystrophy and elevated temperature syndrome
CASP	Caspase
CbpA	Choline binding protein A
cDNA	Complementary DANN
cfu	Colony forming unit
CPS	Polysaccharide capsule
CRP	C reactive protein
CTL	Cytotoxic T lymphocyte
CVB3	Coxsackievirus B3
CXCL-1	Chemokine (C-X-C-motif) ligand 1
D39	Streptococcus pneumoniae serotype 2
Da	Dalton, unit equal to g/mol
DC	Dendritic cell
DEAE	Diethylethanolamine
DMSO	Dimethyl sulfoxide
DNA	Desoxyribo nucleic acid
DRFZ	German Rheumatism Research Center Berlin
DTT	Dithiothreitol
DUB	Deubiquitinating enzyme
E1	Ubiquitin activating enzyme
E2	Ubiquitin conjugating enzyme
E3	Ubiquitin ligating enzyme/ ligase
EAE	Experimental autoimmune encephalomyelitis
EDTA	Ethylene diamine tetraacetic acid
ELISA	Enzyme-linked immunosorbent assay
Eno	Enolase
ERK	Extracellular signal-regulated kinase
FACS	Fluorescence associated cell sorting
FCS	Fetal calf serum

FITC	Fluorescein isothiocyanate
G-CSF	Granulocyte colony-stimulating factor
h	Hour
HBV	Hepatitis B Virus
HIV	Human immune-deficiency virus
HPRT1	Hypoxanthine phosphoribosyltransferase 1
HRP	Horse radish peroxidase
Hyl	Hyaluronidase
IAV	Influenza A virus
IFN	Interferon
IgA1	IgA1 protease
IgG	Immunoglobulin G
IkB	I-kappa-B
IKKε	IkB kinase ε
IL-	Interleukin
iNOS	Inducible nitric oxide synthase
IP-10	Interferon gamma-induced protein 10
IRAK	Interleukin-1 receptor-associated kinase
IRF1 / 3	Interferon regulatory factor 1 / 3
JASL	Japanese autoinflammatory syndrome with lipodystrophy syndrome
JMP	Joint contractures, muscle atrophy, microcytic anaemia, and panniculitis-induced lipodystrophy syndrome
JNK	cjun N-terminal kinase
K48	Lysine at amino acid position 48
LCMV	Lymphocytic Choriomeningitis Virus
LDH	Lactate dehydrogenase
Lmp2	Low molecular mass protein 2, subunit beta1i
Lmp7	Low molecular mass protein 7, subunit beta5i
LPS	Lipopolysaccharide
LTA	Lipoteichonic acid
LytA	Autolysin
MACS	Magnetic-activated cell sorting
MAL	MyD88 adapter-like protein
MAPK	Mitogen-activated protein kinase
MASP	Mannon-binding lectin serine protease
MBL	Mannose-binding lectin
MCP-1	Monocyte chemotactic protein 1
m-CSF	Murine macrophage colony-stimulating factor
Mecl-1	Multicatalytic endopeptidase complex subunit 1, subunit beta2i
MEF	Mouse embryonic fibroblast
MHC	Major histocompatibility complex
mIFNg	Murine interferon gamma
min	Minute
MIP-1b	Macrophage inflammatory protein-1b
MKK	Mitogen-activated protein kinase kinase
MOI	Multiplicity of infection
MpH	Macrophage
mRNA	Messenger RNA
MyD88	Myeloid differentiation primary response gene 88
NanA	Neuraminidase
mRNA	Messenger RNA

NanA	Neuraminidase
NFkB	Nuclear factor kappa-light-chain-enhancer of activated B cells
NLR	Nod-like receptor
NNS	Nakajo-Nishimura syndrome
NO	Nitric oxide
NO-2	Nitrite
NOD2	Nucleotide-binding oligomerization domain-containing protein 2
OD_{600}	Optical density at wave length of 600nm
P/S	Penicillin/Streptomycin
PA28	proteasome activator 28
PAC1-4	Proteasome assembling chaperone
PAGE	polyacrylamide gel electrophoresis
PAMP	Pathogen-associated molecular pattern
pavA	Pneumococcal adhesion and virulence
PBMC	Peripheral blood mononuclear cell
PBS	Phosphate buffered saline
PBST	Phosphate buffered saline (with tween-20)
PCR	Polymerase chain reaction
PE	Phycoerythrin
PerCP	Peridinin chlorophyll
Ply	Pneumolysin
PN36	Streptococcus pneumoniae serotype 3
POMP	Proteasome maturation protein
PPARa/g	Peroxiyome proligerator-activated receptor
PRR	Pattern recognition receptor
Psa	Pneumococcal surface antigen A
PSMB8	Proteasome subunit beta type 8 (coding for beta5i)
PspA	Pneumococcal surface protein A
PTX-3	Pentraxin 3
RIP1	Receptor interacting protein 1
RNA	Ribonucleic acid
ROS	Reactive oxygen species
Rpt	Regulatory particle
RT	Reverse transcriptase
RT-PCR	Reverse transcriptase polymerase chain reaction
SAA	Serum amyloid A
SAP	Serum amyloid P
SD	Standard deviation
SDS	Sodiumdodecylsulfoxide
sec	Second
SIRS	Systmic inflammatory response syndrome
SLE	Systemic lupus erythematosus
SP-A	Surfactant protein A
SP-D	Surfactant protein D
STAT 1 / 3	Signal transducer and activator of transcription
STING	Stimulator of interferon genes
TBK1	TANK-binding kinase 1
T-cytotox	Cytotoxic T cell
TEAD	Tris, EDTA, acid, DTT
TEMED	Tetramethylethylenediamine
TGFb	Tissue growth factor
Th	T helper cell
TLR	Toll like receptor
TNF	Tumor necrosis factor

TRAF 3/6	TNF receptor associated factor
Tram	Translocating chain-associated membrane
T-reg	Regulators T cell
Trif	Tir-domain-containing adapter-inducing interferon b
Tris	Tris(hydroxymethyl)-aminomethan
U	Unit
Ub	Ubiquitin
UPS	Ubiquitin-proteasome system
US	United state
UV	Ultra violet
WHO	World Health Organisation
WT	Wild-type

List of figures

List of tables

Danksagung

Als allererstes möchte ich mich bei meinem Betreuer Prof. Dr. Peter-Michael Kloetzel bedanken, der mir ein freies wissenschaftliches Arbeiten an seinem Institut unter ausgezeichneten Bedingungen ermöglichte und mir die Chance gab diese Arbeit anzufertigen. Insbesondere möchte ich mich für seine engagierte Betreuung meiner Arbeit, seine ständige Unterstützung bei der Umsetzung all meiner Ideen und für interessante fachliche Gespräche und Diskussionen bedanken.

Ich bedanke mich bei meiner gesamten Prüfungskommission, insbesondere Prof. Dr. Emanuel Heitlinger und Prof. Dr. Bastian Opitz für ihre Bereitschaft meine Dissertation zu begutachten, und dem damit verbundenen Zeitaufwand.

Ich möchte mich ganz herzlich bei Prof. Dr. Martin Witzenrath bedanken, dass er mich in seiner Arbeitsgruppe aufnahm und es mir ermöglichte meine Tierversuche in seinem Labor durchzuführen. Besonderen Dank gilt Dr. Katrin Reppe, die sich trotz ihres engen Terminplanes stets Zeit nahm, mir mit fachlichem und methodischem Rat zur Seite zu stehen. Danke Katrin, für deine Unterstützung bei der Erstellung des Tierversuchsantrages und deine umfangreiche Einweisung und Betreuung in das tierexperimentelle Arbeiten. Der gesamten AG Witzenrath bin ich zu Dank verpflichtet für Ihre herzige Art und Hilfsbereitschaft, besonders Denise Barthel, Maria Spelling, Sandra Wienhold und Birgitt Gutbier.

Ich bin allen Mitgliedern der AG Kloetzel sehr dankbar, dass sie mich nicht nur mit ihrem fachlichen und methodischen Können unterstützten, sondern dass ich auch in einem freundlichen und kreativen Umfeld arbeiten durfte. Danken möchte ich hier besonders Christin Keller, Elke Bürger, Alexander Kloß, Agathe Niewienda und Andrea Lehmann. Frederic Ebstein und Karin Schmidt bin ich zu höchstem Dank verpflichtet für ihre offen Ohren, ihre Zuversicht und zahlreichen Ideen und Diskussionen.

Des Weiteren sei auch Prof. Dr. Antje Voigt und allen weiteren Gruppenleitern am Institut der Biochemie gedankt für ihre vielen Fragen, Kritik und Ideen in unseren Seminaren, die zum Vorankommen dieser Arbeit beigetragen haben. Dr. Nelli Baal und Prof. Dr. Holger Hackstein (Klinische Immunologie, Justus Liebig Universität Giessen) möchte ich herzlich danken für ihre Hilfe bei der Durchführung der Durchflusszytometrie, Dr. Olivia Kershaw und Prof. Dr. Achim Gruber (Institut für Veterinäre Pathologie, Freie Universität Berlin) für ihre Unterstützung bei der Durchführung und Auswertung der histopathologischen Untersuchungen und Prof. Bastian Opitz (Infektiologie und Pneumologie, Charité Berlin) für das Überlassen muriner Zelllinien.

Außerdem wertschätze ich die Finanzierung meiner Arbeit durch die Deutsche Forschungsgemeinschaft (DFG SFB TR84).

Eidesstattliche Erklärung

Hiermit erkläre ich an Eides statt, dass die vorliegende Dissertation in allen Teilen von mir selbständig und ohne Hilfe Dritter angefertigt wurde. Alle benutzten Hilfsmittel sind vollständig angegeben worden. Es fand keine Zusammenarbeit mit gewerblichen Promotionsberatern statt und die Grundsätze der Humboldt Universität zu Berlin zur Sicherung guter wissenschaftlicher Praxis wurde eingehalten. Die Promotionsordnung der Lebenswissenschaftlichen Fakultät habe ich zu Kenntnis genommen.

Die Dissertation wurde bisher nicht für eine Prüfung oder Promotion oder für einen ähnlichen Zweck zur Beurteilung eingereicht. Ich versichere, dass ich die vorstehenden Angaben nach bestem Wissen vollständig und der Wahrheit entsprechend gemacht habe. Weiterhin erkläre ich, dass ich nicht schon anderweitig einmal die Promotionsabsicht angemeldet oder ein Promotionseröffnungsverfahren beantragt habe.

Felicia Kirschner